HYDROGEOCHEMICAL AND MINERALOGICAL EVALUATION OF GROUNDWATER ARSENIC CONTAMINATION IN MURSHIDABAD DISTRICT, WEST BENGAL, INDIA

by

ANDREW W. NEAL

B.S., GEORGIA COLLEGE AND STATE UNIVERSITY, 2007

A THESIS

submitted in partial fulfillment of the requirements for the degree

MASTER OF SCIENCE

Department of Geology
College of Arts and Sciences

KANSAS STATE UNIVERSITY
Manhattan, Kansas

2010

Approved by:

Major Professor
Saugata Datta

Abstract

More than 75 million people in the Bengal Delta of eastern India and Bangladesh are exposed to drinking water with dangerously high arsenic (As) concentrations; the worst case of environmental poisoning in human history. Despite recognition of dangers posed to chronic exposure to drinking water with elevated As, its biogeochemical cycle is inadequately constrained in groundwater flow systems due to its complex redox chemistry and microbially-mediated transformations. Arsenic concentrations in Bengal Delta sediments are comparable to global averages, but its highly heterogeneous spatial distribution (on scales of meters to kilometers) in sediments and groundwaters is poorly understood. Though many research efforts have targeted understanding this heterogeneity in Bangladesh, less work has been done in eastern India.

Murshidabad (23°56.355'N, 88°16.156'E), an eastern district in West Bengal, India, where groundwaters are highly As-affected (~4000 μg/l), was chosen as our study area. Research objectives were: (1) characterize sediment cores (mineralogically, geochemically) and groundwaters (hydrochemically, isotopically) in areas with contrasting As concentrations—west (low-As) and east (high-As) of river Bhagirathi, a major distributary of Ganges flowing through the heart of Murshidabad; (2) describe and understand the extent of spatial variability, laterally and vertically, of dissolved As concentrations in shallow (< 60 m) aquifers, comparing sediment core chemistry to water chemistry; (3) identify source(s) of aquifer recharge and (4) role(s) of inorganic carbon within the aquifer to understand the bioavailability and mobilization of As from sediments to groundwaters.

Mineralogical differences between high-As (grey) and low-As (orange-brown) sediments, were the presence of greater amounts of micas, Fe- and Mg-rich clays, amphiboles, carbonates, and apatite in high-As sediments; these were virtually absent from low-As sediments. In high-As areas, As was associated with amorphous and poorly-crystalline Fe-oxyhydroxide phases and labile (specifically-sorbed) phases, especially where Fe(II):Fe_T was high in the sediments. High-As groundwaters had high As(III):As_T, iron, bicarbonate, phosphate, and ammonium, and low concentrations of chloride and sulfate. Dry season precipitation was probably the main source of aquifer recharge; lighter values of ^{13}C in dissolved inorganic carbon resulted from oxidation of natural organic matter. This study points to an idea that both microbially-mediated oxidation-reduction and competitive ion-exchange processes occurring in shallow aquifers of Murshidabad drive As mobilization and sequestration by aquifer sediments.

Table of Contents

List of Figures

Acknowledgements

The author expresses his sincerest thanks to everyone who made this work possible in any way, shape or form. First and foremost, thanks to all the people who assisted with field work in Murshidabad, whether it be logistics or sample collection and analysis: Shahjahan and Bhalla for assistance in the field, Sumanta and other drivers for transportation, drilling crews for obtaining aquifer sediment samples, and all the kids from each of the six villages for assisting with well-pumping and carrying supplies. A special thanks to Baren Purkait from the Geological Survey of India for help in the field. Thanks to Rick Socki from NASA–Johnson Space Center for analysis of $\delta^{13}C$ of dissolved organic carbon in water samples; Ratan Dhar from York College of City University of New York for analysis of Fe(II), total Fe and phosphate in sediment samples; Elizabeth Petroske from Kansas Geological Survey for measuring total As and anions in water samples; and Michael DePangher from Spectrum Petrographics, Inc., for thin section preparation. Many thanks to Karen Johannesson and Jade Haug from Tulane University for assistance in the field with sample collection and analysis, and for As speciation and total As concentrations of water samples in the lab.

Numerous people from several departments at Kansas State University whose help is greatly appreciated: Dr. Bimal Paul from Geography for advice, and Thanksgiving dinner; Dr. Jesse Nippert and Troy Ocheltree from Biology for stable isotope analysis of $\delta^{2}H$ and $\delta^{18}O$ in water; Dr. Deon van der Merwe from Diagnostic Medicine/Pathobiology for ICP-MS analysis of sediment digestions; Dr. Mickey Ransom from Agronomy for use of lab facilities; Dr. Debabani Ganguly from Biochemistry for supplies; and Kent Hampton from Entomology for SEM time.

A *huge* appreciation is given to Dr. Ganga Hettiarachchi from Agronomy for discussions and use of her lab facilities for the past two years. Her students were instrumental in accomplishing this work. Special thanks is given to Phillip Defoe for many discussions, along with assistance with XRF, ICP-OES, total digestions, sequential extractions and all-nighters working in the lab; Raju Khatiwada for discussions and an enormous help with the ICP-OES and total digestions; Kathy Lowe for ICP-OES assistance; Vindhya Gudichuttu, Ranju Karna, Chammi Attanayake, Buddhika Galkaduwa, Ashley Raes, and Priscilla Mfombep for vast amounts of help with a variety of tasks.

There are also many people within the Department of Geology whom the author wishes to thank: Dr. George Clark for being himself; Dr. Jack Oviatt and Dr. Allen Archer for use of field equipment; Lori Page-Willyard for administrative assistance; graduate students: Jeff Callicoat, Nick Patch, Chris Flenthrope, Darron DeBoer, Matthew Crawford, O.C. Eke, Bobby Ford, Drew Evans,

Tyler Hill, Charlotte Philip, Amanda Cashman and Robinson Barker. Additional thanks goes to Hal Hockersmith for resolving many technological issues and for helping print posters.

Thanks to K-State NASA Space Grant Consortium, the Geological Society of America Research Award, the Kansas Geological Foundation Scholarship, the American Association of Petroleum Geologists Foundation Grants-in-Aid, Bill Barrett, and Paul and Deana Strunk for significant financial support for two years.

Sincere thanks goes to the members of the author's graduate committee for serving on the committee: Dr. Sambhudas Chaudhuri for countless research-related and philosophical discussions and guidance, and Dr. Matthew Brueseke for overall helpfulness, optical mineralogy instruction, petrographic microscope and camera use, and leading some fantastic field trips.

And last, but definitely not least, the author thanks, with the greatest appreciation, his advisor, Dr. Saugata Datta, for the immense number of opportunities and funding which he has provided during the past 2+ years, along with never-ending enthusiasm, encouragement, and valuable time given for innumerable research discussions. Thank you.

Chapter 1 - Introduction

Arsenic (As) is a naturally-occurring element that is extremely toxic to humans at high doses. It occurs in various forms in many environments: as As-bearing minerals within soils, sediments, and rocks, industrial effluents, air particulate matter, and groundwater. The occurrence of elevated levels of dissolved As in groundwater used for human consumption has been a major public health concern in the past several decades in many regions of the world (Smedley and Kinniburgh, 2002; Mukherjee et al., 2009b and references therein). Chronic exposure to drinking water contaminated with As has been linked to severe medical conditions such as melanosis, hyperkeratosis, skin cancer, bladder cancer, lung cancer, hypertension, and many other adverse health effects (Hopenhayn, 2006; Chen et al., 2009; Smith et al. 2009; Parvez et al., 2010). Due to the toxicity of As, the World Health Organization and the United States Environmental Protection Agency set the maximum contaminant level for As in drinking water at 10 μg/l in 1993 and 2001, respectively (Yu et al., 2003).

Arsenic Geochemistry

Arsenic is a metalloid in group 5 of the periodic table, and 47th in abundance of the 90 naturally occurring elements (Plant et al., 2003). It can exist in –III, -I, 0, III, and V oxidation states. Arsenic is a trace metal that occurs as a major constituent in more than 200 minerals (Smedley and Kinniburgh, 2002), including (with % of total natural arsenic minerals) arsenates (60%), sulfides and sulfosalts (20%; enargite, cobaltite, niccolite, arsenolite and claudetite), and arsenides, arsenites, oxides, alloys, and polymorphs of elemental arsenic (20%) (Plant et al., 2003). The most abundant As mineral is arsenopyrite (FeAsS), which forms in medium to high temperature hydrothermal veins (Smedley and Kinniburgh, 2002). Other common As-bearing minerals are arsenian ('As-rich') pyrite ($Fe(S,As)_2$), realgar (AsS), scorodite ($FeAsO_4 \cdot 2H_2O$) and orpiment (As_2S_3) (which is probably the most abundant source of As in ore zones [Mason and Berry, 1978; Cullen and Reimer, 1989; Nordstrom, 2000]).

Arsenic is strongly sorbed to carbonates (Mukherjee et al., 2009b and references therein), oxides of iron, aluminum and manganese, and some clays, leading to As-enrichment in ferromanganese nodules and manganiferous deposits (Plant et al., 2003). The most common Fe oxides found in soils and sediments with which As associates are hematite (Fe_2O_3), goethite (FeOOH), ferrihydrite ($Fe(OH)_3$), magnetite (Fe_3O_4), Schwertmannite ($Fe_8O_8(OH)_6(SO)_4 \cdot nH_2O$), and

green rust (Langmuir, 1997), which are all weathering products of Fe-bearing primary and secondary minerals.

Generally, dissolved As in groundwater exists primarily in its inorganic form as oxyanions of arsenite [As(III): $H_3AsO_3^0$, $H_2AsO_3^-$, $HAsO_3^{2-}$, AsO_3^{3-}] or arsenate [As(V): $H_3AsO_4^0$, $H_2AsO_4^-$, $HAsO_4^{2-}$, AsO_4^{3-}], depending on redox conditions. Concentrations of As in natural waters vary by more than four orders of magnitude, and depending on the source of the As and the local geochemical conditions (Meng et al., 2000; Smedley and Kinniburgh, 2002; Plant et al., 2003). Because As exhibits a relatively slow redox transformation, As(III) and As(V) often occur in the same redox environment. Therefore, ratios of As(III)/As(V) can vary considerably (Mukherjee et al., 2009b). The ratios can also depend upon abundance of organic carbon and microbial activity (Smedley and Kinniburgh, 2002). At circumneutral pH, As(III) exists as $H_3AsO_3^0$, an uncharged molecule, so its mobility is enhanced, whereas an As(V) anion is more likely to sorb strongly to mineral surfaces.

Arsenic is unique among other oxyanion-forming elements in that its mobilization can be controlled by both oxidizing and reducing conditions at pH values typical of most groundwaters (pH 6.5 to 8.5) (Smedley and Kinniburgh, 2002). The solubility of most trace metal cations at near-neutral pH is limited by precipitation as, or coprecipitation with, an oxide, hydroxide, carbonate or phosphate mineral, or by their strong adsorption to hydrous metal oxides, clays, and organic matter. Arsenate is different in that it tends to be less strongly sorbed as pH increases (Dzombak and Morel, 1990). The oxidation state of As influences many of its properties such as adsorption to soil minerals, solubility in soil, and toxicity to plants and animals.

Arsenic can be removed from groundwater by several natural processes. In the presence of organic matter, ferrous Fe and sulfide can precipitate (or co-precipitate with As) to form pyrite, onto which As(III) can sorb strongly via inner-sphere complexation (Bostick and Fendorf, 2003). Sorption of As(V) on clay minerals is a pH-driven process that can occur. The degree of sorption of As(V) depends on clay mineralogy, surface area, surface charge, and availability of sorption sites. The maximum amount of sorption of As(III) and similar elements on clay minerals occurs at pH 7.5-9.5 (Clauer and Chaudhuri, 1995; Lin and Puls, 2000). Arsenic mobility in groundwater can also be affected by presence of carbonate phases (e.g. As(III) can be associated in the calcite crystal lattice or surface adsorbed at high pH) (Mukherjee et al., 2009b and references therein).

On the other hand, As may be mobilized from the solid phase into groundwater via a number of processes. First, competitive anion exchange is a process by which arsenic oxyanions ‘compete’

with more abundant similar anions like phosphate (PO_4^{3-}, HPO_4^{2-}, etc.), sulfate (SO_4^{2-}), carbonate (CO_3^{2-}), bicarbonate (HCO_3^-), and chloride (Cl^-) for sorption sites on metal oxyhydroxides and clay minerals. Phosphate has been shown to have the highest competitive exchange with arsenic, followed by CO_3^{2-} and HCO_3^-, SO_4^{2-}, and Cl^- (Mukherjee et al., 2009b and references therein). Also, changes in pH can also affect As mobility. Desorption of As from oxyhydroxides can occur with an increase in pH because As(V) tends to be more strongly sorbed on oxyhydroxides at circumneutral to acidic pH, and mineral surfaces tend to become increasingly negatively charged at alkaline pH (O'Shea, 2006). Secondly, natural organic matter (NOM), due to its high surface area and affinity for forming complexes with As, can significantly enhance As mobility in water by forming water-soluble complexes with arsenic. This inhibits As sorption on mineral surfaces, and displaces already sorbed arsenic (Mukherjee et al., 2009b). NOM oxidation, coupled with reduction of dissolved O_2 (which produces dissolved inorganic carbon), can facilitate microbial reactions that mobilize As from the solid phase into the aqueous phase (Oremland and Stolz, 2003). This concomitantly releases As phases that have formed complexes with NOM (Chapelle, 2001). Finally, As can be liberated via oxidation of iron sulfides (i.e. pyrite) when they come into contact with oxygenated water or the atmosphere.

Global Occurrence of Arsenic

Arsenic is found in many different forms throughout the world on every continent. Arsenic concentrations in the environment can be enriched by mining and smelting operations, geothermal and volcanic activity, combustion of arsenical coals, release of production waters following petroleum recovery, and animal feed additives. Arsenic is found in river waters influenced by mining activities (e.g. Thailand, Ghana, Canada) and geothermal waters (e.g. western US, New Zealand). Arsenic levels in groundwater can be affected by smelting and geothermal activity, which are known to contain up to 10,000 μg/l As (Welch et al., 1988) and 50,000 μg/l As, respectively (Smedley and Kinniburgh, 2002 and references therein).

The first cases of mass As poisoning from drinking As-laden groundwater came into the limelight roughly a half century ago in Taiwan (Blackfoot Disease) (Smedley and Kinniburgh, 2002 and references therein) and Chile and Uruguay (Bundschuh et al. 2004, 2008, 2009, Garcia and Bundschuh, 2006). A multitude of cases of mass poisoning from As-contaminated drinking water have since been reported from around the globe in places like Australia, New Zealand, Pakistan, Iran, Hungary, Romania, Ghana, and portions of the northeastern and western United States (Appelo et al.,

1996; Welch et al., 2000; Smedley et al., 2005; Ravenscroft et al., 2005; Naidu et al., 2006, Charlet et al., 2007; Fig. 1). Other areas of naturally occurring elevated As concentrations in groundwater include Argentina (Nicolli et al., 1989; Hopenhayn-Rich et al., 1996), Mexico (Armienta and Segovia, 2008), Inner Mongolia (Luo et al., 1997), and parts of China (Lin et al., 2002), but by far the most significant As contamination is happening in south and southeast Asia (BGS and DPHE, 2001).

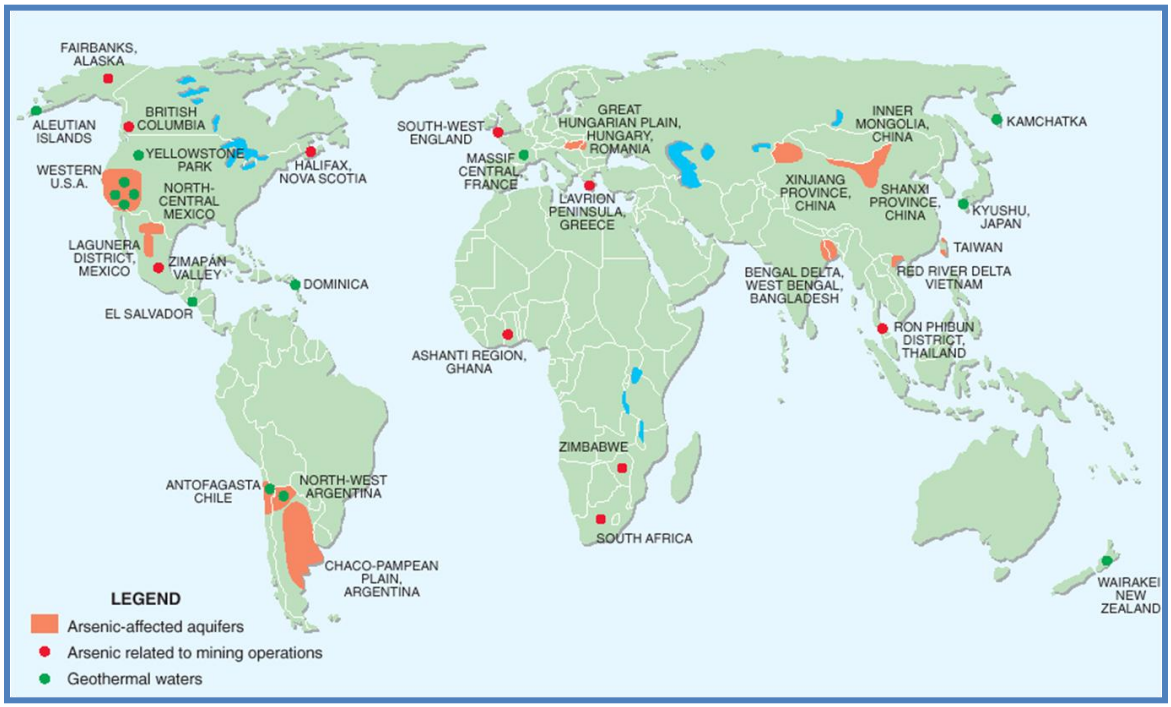

Figure 1: Distribution of documented world problems with As in groundwater in major aquifers as well as areas of water and environmental problems related to mining and geothermal sources (Smedley and Kinniburgh, 2002).

Arsenic in South and Southeast Asia

Major portions of south and southeast Asia are severely affected by As contamination in groundwater. The problem is widespread in places like Taiwan, Vietnam, Cambodia, Laos, Myanmar, Thailand, Nepal, India and Bangladesh, and is worsened due to the population density in this region. These occurrences of As are mainly confined to major river valleys and alluvial-deltaic areas such as the Red River Delta in Vietnam, Mekong River Delta in Cambodia, Ron Phibun District in Thailand, Irrawaddy Delta in Myanmar, and the Bengal Delta in Bangladesh and eastern India (BGS and DPHE, 2001). The contaminated aquifers are mostly comprised of Quaternary

alluvial-deltaic sediment deposits in floodplains and delta plains of the major Himalayan rivers (Smedley and Kinniburgh, 2002) and are characterized by reducing conditions associated with high dissolved ferrous iron concentrations (Nordstrom, 2002; Saunders et al., 2005 and references therein). The majority of contaminated wells in this region occurs mainly in shallow (< ~80 m below ground level) aquifers, with As concentrations generally being much lower in deeper wells (Mukherjee et al., 2008). These Quaternary sediments are believed to contain As that is mobilized into groundwater under reducing conditions by microbial activity on in-situ minerals, facilitated by presence of high amounts of organic matter, especially in the Bengal Basin (Harvey et al., 2002).

Geology of the Bengal Basin and its Relation to Arsenic Occurrence

Arsenic pollution in the Indian context occurs predominantly in the alluvial deposits of major rivers flowing south and east from the Himalayas and the Tibetan plateau. The most important Himalayan river system is the Ganges-Brahmaputra-Meghna (GBM). The Bengal Basin occupies most of Bangladesh and West Bengal, India, and is roughly equivalent to the delta of the GBM rivers (Morgan and McIntire, 1959). Bounded by the Indian craton to the west, the Shillong Plateau to the north, and the Indo-Burman range to the east, the Bengal Basin is filled by kilometers of alluvial sediments that form one of the most productive aquifers of the world. The distribution of arsenic in the Bengal Basin is closely related to its Quaternary history. The greatest differences in the aquifer properties relate to the age of the sediment, which was controlled by fluvial incision during the Last Glacial Maximum (LGM) (Ravenscroft, 2003), whereby the Holocene channel-fill sequences are separated by Pleistocene terraces known as Barind and Madhupur Tracts. These older aquifers are brown, intensely-weathered sands, with reduced permeability (20-30 m/day), but contain groundwaters of excellent quality, low in iron and total dissolved solids and with As mostly below detection limits (Ravenscroft, 2003). The Holocene aquifers are grey, highly permeable (30-50 m/day) sands containing water of variable quality, characterized by high iron, Mn and As concentrations.

Initial formation of the Ganges-Brahmaputra delta occurred around 11 ka, when rising sea level led to back-flooding of lowstand surface and the trapping of riverine sediments, an event that is clearly marked by the transition from clean alluvial sands or Pleistocene laterites to overlying muds containing wood and estuarine/marine shells (Goodbred et al., 2003). Seasonal discharge and large sediment loads of these rivers favor channel migration and avulsion, and thus the lateral erosion of interchannel floodplain units. This was evident especially during the early Holocene with the

enormous sediment loads from the strengthening of the monsoon where, after slowing of sea-level rise, migration of these rivers was rapid, resulting in reworking of floodplain units before they could be buried (Goodbred et al., 2003 and references therein).

The older (Pleistocene) bright-orange alluvial sediments of the Madhupur and Barind Tracts in the north and west normally conduct low-As groundwater, but the young (Holocene) grey alluvial and deltaic deposits in West Bengal and Bangladesh are the sediments mostly affected by As (BGS and DPHE, 2001). Some of the thicker Holocene deposits may reflect infills of larger river channels formed during the previous glacial low-stand in sea level (van Geen et al., 2003), where a high percentage of contaminated wells occur at depths between 28 and 45 m (McArthur et al., 2001).

The source of As in this environment is believed to originate in As-rich lithologies of the Himalayas, which have been eroded, transported and deposited as alluvial-deltaic sediments. Because this area is situated in a fluvio-deltaic system originating from eroded high-grade granulites and Gondwana deposits, aquifer sediments should consist of a wide variety of reworked minerals, dominated by quartz and feldspar. Nickson et al. (2000) proposed that the As originated from coal seams of the Rajmahal basin which are situated on top of basaltic rocks, isolated outcrops of sulfide containing up to 0.8% As in the Darjeeling Himalaya, and/or the Gondwana coal belt. Weathering of these minerals produces As-rich secondary iron oxyhydroxides (e.g. FeOOH), which can also form coatings on other minerals grains (Ravenscroft et al., 2005), by scavenging As from river water during their transport as part of the normal river sediment load (BGS and DPHE, 2001). These sediments are then deposited and buried throughout the region within the active floodplains. Natural variations in the amount of iron oxyhydroxides at the time of sediment burial may be a key factor in controlling distribution of high As groundwaters (BGS and DPHE, 2001).

Chapter 2 - Background

The installation of millions of tubewells in the Bengal Basin beginning in the early 1970s to accommodate increased demand for irrigation has led to one of the worst cases of mass poisoning in human history (Smith et al., 2000). Tubewells were installed with the aid of World Bank and United Nations Children's Fund (UNICEF), along with the Indian and Bangladeshi governments, not only for irrigation waters, but also in an attempt to alleviate the suffering from chronic illness, disease, and infant mortality due to utilization of pathogen-laden surface waters as a drinking water source.

In the late 1970s and early 1980s, reports of skin lesions, keratosis, and various cancers began to surface in hospitals and doctors' offices throughout the region (PHED, 1991). Arsenic concentrations exceeding the national Indian standard of 50 μg/l were first discovered in 1978 in several wells in North 24 Parganas district of West Bengal (Guha Mazumder et al., 1998), followed by identification of arsenicosis in 1984 (Garai et al., 1984; Mukherjee et al., 2008). Shortly thereafter, As was found in groundwaters from shallow tubewells in many other parts of West Bengal. In 1993, Bangladesh, was found to contain As concentrations exceeding the WHO guideline of 10 μg/l (Swartz et al., 2004).

Arsenic is found throughout the entire Bengal Basin, where more than 75 million people in this region are believed to be exposed to drinking water with As concentrations above the national drinking water standard for India and Bangladesh. Arsenic concentrations in West Bengal range from < 1 μg/l to ~4600 μg/l (BGS and DPHE, 2001; Datta et al., 2010a,b; Neal et al., 2009, 2010a,b,c). Currently, some of the most-affected districts in West Bengal are Malda, Murshidabad, Nadia, and North and South 24 Parganas.

Awareness of the problem with As in drinking water and its extent throughout the Bengal Basin grew rapidly (and is still growing), raising many questions. Even today (Chapman Conference, 2009) multiple questions remain partially unanswered: Where was the source of the arsenic? Why was there As in the groundwater? How did it get into the groundwater? How could one tell if their well water contained arsenic? Could the As be removed from the groundwater? How much would it cost to remove As from the groundwater or obtain water from a clean source? Many studies have since been carried out on a myriad of fronts for the Bengal Basin As problem, from the physical health aspect to socio-economic impacts to hydrological and geochemical processes partially responsible for the problem, to remediation efforts and finding alternative water sources.

For the past decade, several studies by various governmental and non-governmental agencies and researchers have been carried out to try to understand the causes and effects of As contamination in the Bengal Basin. From these studies a better understanding of the physical, chemical and biological interactions, and human impacts on their relationships, at the surface and within the subsurface at the sediment-water interface was achieved. Some of the seminal works in this area pertains to work in Bangladesh, India, and then in Cambodia, Vietnam, such as (Dhar et al., 1997, 2008; Nickson et al., 1998, 2000; BGS and DPHE, 2001; McArthur et al., 2001, 2004, 2008, 2010; Harvey et al., 2002, 2005, 2006; Dowling et al., 2002; Pal et al., 2002; van Geen et al., 2003, 2004, 2006, 2008a,b,c; Tareq et al., 2003; Goodbred et al., 2003; Stüben et al., 2003; Zheng et al., 2004, 2005; Horneman et al., 2004; Ravenscroft, 2003; Ravenscroft et al., 2005; Polizzotto et al., 2005, 2006, 2008; Ghosh et al., 2006; Charlet and Polya, 2006; Mukherjee et al., 2007a,b, 2008, 2009a,b; Stute et al., 2007; Charlet et al., 2007; Nath et al., 2008, 2009; von Brömssen et al., 2008; Seddique et al., 2008; Michael et al., 2009; Datta et al., 2009; Sinha et al., 2009; Hoque et al., 2009; Naidu et al., 2009; Itai et al., 2010; Neumann et al., 2010; Burgess et al., 2010; Fendorf et al., 2010; Burnol and Charlet, 2010; Reza et al., 2010; Baig et al., 2010; etc.).

One of the earliest publications was from Dhar et al. (1997) who found that ~38% of the 3400+ wells surveyed in Bangladesh contained As above the Indian and Bangladeshi standard of 50 μg/l. At least 58% of the people surveyed (including children) were identified to have arsenical skin lesions such as melanosis, leucomelanosis, keratosis, hyperkeratosis, gangrene and skin cancer (Dhar et al., 1997). It was suggested that chronic intake of ~10 μg/kg/day (of As) or higher may result in dermatological and other signs of arsenical toxicity (Dhar et al., 1997 and references therein).

Dissolution of As-rich FeOOH under reducing condition in the aquifer is the leading cause of As mobilization into groundwater (Nickson et al., 1998; McArthur et al., 2001, BGS and DPHE, 2001). The redox boundary for ferric/ferrous transition is close to the arsenate/arsenite boundary for neutral pH and thus much of the arsenic occurring in groundwater is in the form of (As(III)) (Dowling, et al., 2002). Concentrations of Fe and As co-vary in sediments but do not co-vary in solution, which may be due to removal of Fe from solution into vivianite ($Fe^{2+}_3(PO_4)_2 \cdot 8H_2O$), siderite ($Fe^{2+}/Fe^{3+}CO_3$), or mixed-valent oxides/hydroxides, and/or carbonates (McArthur et al., 2001). This may be partially explained by reduction of (As-bearing) Mn-oxides occuring slightly before reduction of Fe-oxides, releasing the sorbed As, which in the presence of Fe-oxyhydroxides can be re-absorbed as As(V). Since As(III) is less strongly sorbed to Fe-phases, an increase in redox

condition will reduce As(V) to As(III), resulting in release of As from the solid phase to the groundwater (Stüben et al., 2003).

Arsenic occurring within FeOOH is microbially reduced and releases its sorbed As into groundwater, a process that is driven by microbial metabolism of buried peat deposits (McArthur et al., 2001; Zheng et al., 2004). This is demonstrated by a strong correlation between levels of dissolved As, Fe, NH_4^+, and CH_4, suggesting a source of organic carbon (which can be present up to 6 wt% in aquifers [Ravenscroft et al., 2005]) is essential to the overall release of arsenic.

Pyrite was believed to be a sink, not a source, for arsenic (McArthur et al., 2001). The inverse relationship of dissolved sulfate with As in natural groundwater and the presence of acid volatile sulfide (AVS) in the sediments near the dissolved As peak suggests that oxidative dissolution of pyrite has not liberated arsenic (Harvey et al., 2002 and references therein). Zheng et al. (2004) confirmed that As can remain mobile under sulfate-reducing conditions, suggesting that authigenic sulfide precipitation does not necessarily constitute a significant sink for As in the groundwaters. So the idea was discounted that As in groundwater was derived from oxidation of As-rich pyrites in aquifer sediments as atmospheric oxygen enters the aquifer after drawdown of water table due to extraction (Das et al, 1995; Saha et al., 1995) since As (and dissolved Fe and bicarbonate) concentrations increased with depth in wells.

McArthur et al. (2001) also concluded that competitive ion exchange of fertilizer phosphate (Dowling et al., 2002) is not the major cause of As pollution of groundwater in the Bengal Basin., rather dissolved P comes mainly from FeOOH as it is reductively dissolved, with more or less subordinate amounts contributed from anthropogenic sources. Also, wells fairly distant (4 to 10 km) from agricultural areas have PO_4 concentrations higher than many wells close to intensive agricultural areas (Tareq et al., 2003).

McArthur et al. (2008) proposed that an impermeable clay paleosol (Last Glacial Maximum paleosol (LGMP)), which now caps the land surface exposed during the last lowstand of sea level, affects groundwater flow and controls location and distribution of arsenic pollution in shallow aquifers of West Bengal (and possibly globally). The presence of the LGMP defines paleointerfluvial areas (which beneath it are unpolluted zones of the aquifer), and its absence indicates paleochannels, or As-polluted zones of the aquifer. It was predicted that the LGMP prevents downward migration of As and organic matter, which is a driver of As-pollution via reductive dissolution of As-bearing iron oxyhydroxides (McArthur et al., 2008 and references therein). Where groundwater flow is horizontal,

As is carried from paleochannels toward paleointerfluvial aquifers, along a path in which sequestration (sorption) of As reduces risk of contamination.

An eight year well monitoring study by McArthur et al. (2010) showed that As concentrations are decreasing in some wells in the shallow (14 to 55 m depth) aquifers of the Bengal Basin and increasing in others. McArthur attributes much of the spatial heterogeneity of As-polluted water to distribution of paleochannels, paleointerfluves and concentrated local groundwater flow along the margins of these features, under the influence of irrigation pumping. In paleo-channel settings, As-pollution induced by pumping can be restored to the initial low-As condition upon cessation of pumping for at least one year (McArthur et al., 2010).

Along these same lines, similar separate studies by Weinman et al. (2008) and Hoque et al. (2009) examined spatial variation in groundwater in southeast Bangladesh at very shallow (< 15 m) depths in alluvial aquifers in an effort to link near-surface (< 3 m depth) sediment deposits/attributes to dissolved As distribution in tubewells. Finer-grained materials on the surface can act as barriers to prevent infiltration of oxygenated water, thus controlling groundwater As mobilization in these very shallow aquifers. Arsenic concentrations were very low in aquifers having permeable, coarse sandy materials or relatively thin silt/clay layer at the surface (Hoque et al., 2009). Additionally, Weinman et al. (2008) found that artificial filling of villages for flood protection can mimic the natural fine-grained stratigraphy commonly associated with high concentrations of arsenic.

Dissolved As concentrations throughout the Bengal Basin are extremely laterally patchy over small scales, with high As concentrations being found within tens of meters of low As concentrations in many cases (Harvey et al., 2005 and references therein). If groundwater flow is across concentration gradients, then As can be transported from areas of high concentration to areas of low concentration, and vice versa. This spatial 'patchiness' of dissolved As concentrations may correspond to the spatial pattern of groundwater flow paths (Harvey et al., 2005), which may be one explanation of the spatial variability of dissolved As concentrations in the subsurface.

A study conducted by van Geen et al. (2003) in Bangladesh found that in a 25 km^2 area more than 75% of wells which are between 15 and 30 m depth exceeded the Bangladesh standard of 50 μg/l, and then declined gradually to less than 10% at 90 m. These workers stated that although orange-brown sediment is consistently associated with low As-bearing groundwater, a grey sediment color does not necessarily indicate elevated dissolved As concentrations. Zheng et al. (2005) found that the highest amounts of P-extractable As in grey sediments are associated with high $Fe(II)/Fe_T$ ratios, which usually increase with depth (Horneman et al., 2004), suggesting that mobilizable As is

bound to surfaces rather than within the crystalline structure. Deeper, low As (< 5 μg/l), Pleistocene aquifer sands had leachable Fe(II)/Fe_T ratios that averaged ~0.2 (Horneman et al., 2004). In Bangladesh, van Geen et al. (2008a) found a striking relationship between dissolved As concentrations in shallow reducing groundwater and P-mobilizable As in the solid phase, a constant ratio of ~250 μg/l dissolved As per 1 mg/kg P-mobilizable As, and proposed the distribution of groundwater As in shallow aquifers of the Bengal Basin may chiefly reflect the different flushing histories in the region during the last few thousand years.

Incongruent dissolution during reduction of arsenic-bearing Fe(III) to Fe(II) phases or mixed Fe(II)/Fe(III) phases releases As into the groundwater, but Fe is often retained in the solid phases (i.e. vivianite, siderite, magnetite, etc.) (Horneman et al., 2004). This may be a reason why elevated concentrations of dissolved Fe and As are not always found together, and it also supports the idea that reduction of Fe hydroxides is a necessary but not a sufficient condition for elevated As concentrations in groundwater in Holocene aquifers (Horneman et al., 2004; Zheng et al., 2004; van Geen et al., 2006, 2008a). Incubation studies of grey aquifer sands from Bangladesh by Radloff et al. (2007) showed that Fe release during the incubations did not occur concurrently further corroborating the notion of a non-correlation between As and Fe concentrations. Results from incubation studies also revealed that spatial distribution of dissolved As and As release rates are not necessarily linked.

Polizzotto et al. (2005, 2006) suggested that As may be released in the near surface through cyclic, seasonal redox conditions, then subsequently transported to depth, where As concentrations in the groundwater increase with depth to a maximum at ~30 m. Small framboidal pyrite (≤ 20 μm) was observed in surficial (< 9 m) Holocene sediments (Polizzotto et al., 2005), partially supporting the pyrite oxidation hypothesis, by proposing that recently deposited sediments with As(V)-bearing ferric (hydr)oxides undergo reduction during ensuing seasonal addition of organic carbon and flood waters. The solid-phase As is deposited in association with detrital sulfides and ferric (hydr)oxides, which dissolve with increasing depth as sediments are buried to the depths of the grey Holocene aquifer sediments (Horneman et al., 2004; Polizzotto et al., 2005). During the dry season, sulfides are oxidized and As is redistributed into ferric (hydr)oxides (Polizzotto et al., 2005, 2006), thus cyclic redox conditions are perpetuated into the next rainy season. Polizzotto et al. (2006) suggested that Fe(III) (hydr)oxides are yet to be detected in sediments from the Holocene aquifer at depths where dissolved As concentrations are highest, however, in general, solid-phases remain incompletely characterized or even identified. Column experiments showed that biotic-stimulated reductive

dissolution of As-bearing ferrihydrite can promote As sequestration rather than desorption under conditions similar to those found in the Holocene aquifer of the Bengal Basin (Kocar et al., 2006).

From a study of an As "hotspot" in Chakdaha block in Nadia district which is just south of Murshidabad, Charlet et al. (2007) reported that even though Fe dissolution did play an important role in the release of As, selective dissolution extractions indicated that adsorption of As on carbonates and micas may also be a vital component of As cycling in the sediment. Aquifer mineralogy in this study was characterized by fairly homogeneous grey, fine to medium-grained sand made of Fe(II)/Fe(III) oxide-coated quartz particles, feldspars, micas, and carbonates. Finer particles consisted of illite, magnetite and illmenite. Selective As extraction studies showed two major sinks for As: amorphous Fe(III) oxide (34% ± 8% of total extracted As) and acid volatile sulfides and/or carbonates (19% ± 7% of total As), both on which As was adsorbed or co-precipitated, in addition to micas (Charlet et al., 2007). HCO_3^- and PO_4^{3-} were the dominant anions in the aquifer, which compete with As species for adsorption sites at mineral surfaces, thus releasing As into groundwater.

In West Bengal, Nath et al. (2009) found that concomitant occurrence of high As and high Fe in groundwater, along with high pCO_2, results from reductive dissolution of Fe-oxyhydroxides that mobilizes As, and siderite controls the Fe concentration. Seddique et al. (2008) claimed the spatial variability of As-enriched groundwater resulted from the weathering of heterogeneously distributed biotite, while micas were virtually absent in these high-As groundwater areas studied by Nath et al. (2009). The As enrichment in groundwater was explained by release of As through desorption from the solid phase in the silty-clay fraction of the sediments. Sorption experiments showed that organic matter-rich silty sediments play a major role in maintaining a reducing condition in the subsurface (Nath et al., 2009), thereby, to some degree, controlling As mobility.

Most As-related studies in the GBM delta focused on processes that release As into the shallow aquifers. Datta et al. (2009), however, investigated the fate of As during groundwater discharge and found that high As concentrations in sediment result from As-rich groundwater discharging to the Meghna River (Bangladesh) through a more oxidizing environment. Here a significant portion of dissolved As sorbs to Fe-bearing minerals (i.e. biotite, hornblende, goethite, magnetite, vivianite and clays (chlorite, illite, smectite)), forming a natural reactive barrier (NRB). The NRB, when recycling and reworking of its sediments occurs in an active fluvial-deltaic environment such as the GBM Delta, can provide a potential source of As to further contaminate the groundwater. Results presented from this study suggest that there is a systematic process that is

driven by seasonally active hydrological and biogeochemical interactions between discharging anoxic groundwater and more oxic river water (Datta et al., 2009).

Sequential extractions of sediments from the Chapai-Nawabganj District of northwestern Bangladesh by Reza et al. (2010) revealed that fine-grained Mn and Fe hydroxides and organic matter are the major leachable solids carrying arsenic. Statistical analysis from this work clearly shows that As is tightly associated with Fe and Mn in sediments, but As is better correlated with Mn in groundwater. This may be due to reductive dissolution of MnOOH and FeOOH, where possible precipitation of dissolved Fe as siderite under reducing conditions may account for the poor correlation between Fe and As in solution (Reza et al., 2010).

Mukherjee et al. (2008) compared hydrogeochemistry in the western and eastern margins of the Bengal Basin and concluded that presence of As in groundwater in different parts of the basin cannot be explained simply by mobilization mechanisms, rather it may be a function of retention (and potential re-mobilzation) mechanisms. This study also indicated that simultaneous redox processes occur at different depths, suggesting an environment with overlapping redox zones.

Mukherjee et al. (2007a) demonstrated by using a hydrostratigraphic model the presence of a continuous, semi-confined sand aquifer underlain by a thick clay aquitard in areas of West Bengal. Michael et al. (2009) suggested that at the onset of extensive groundwater extraction for irrigation, anthropogenic activities became dominant over natural hydrogeologic forces. Groundwater withdrawal significantly altered the shallow groundwater flow system. Flow paths became more vertical and had more-local recharge locations (and inflow from rivers) compared to the larger scale, more-horizontal flow paths under predevelopment conditions.

Evaluation of $\delta^{18}O$ and $\delta^{2}H$ of waters shows that local precipitation falls along the Global Meteoric Water Line (GMWL) ($\delta^{2}H=8\delta^{18}O+10$ (Craig, 1961)) (Stute et al., 2007) and the Local Meteoric Water Line (LMWL) ($\delta^{2}H=7.2\delta^{18}O+7.7$ (Mukherjee et al., 2007b)). Monsoonal precipitation was more depleted than dry-season precipitation in Gangetic West Bengal (Mukherjee, et al., 2007b) Plots of stable isotopes of hydrogen and oxygen for water samples revealed that the Bhagirathi River was very depleted ($\delta^{2}H$ ~ -55‰ and $\delta^{18}O$ ~ -8.0‰) and groundwaters all plotted along the Global Meteoric Water Line, indicating precipitation as the main recharge source for groundwaters (Stüben et al., 2003). However, Lawson et al. (2008) argued that (evaporated) surface waters (i.e. ponds or re-infiltrating irrigation water) contribute a fair amount of recharge to the groundwater. Neumann et al. (2010) recently suggested that recharge from these ponds contains degradable organic carbon that, along with groundwater flow drawn by irrigation pumping,

transports pond water to the depth where dissolved As concentrations are greatest. Pond-derived recharge carries biologically degradable organic carbon into the aquifer, which can catalyze several biogeochemical pathways that may mobilize As into groundwater, such as magnetite reduction, arsenic desorption, biotite weathering, and apatite dissolution (via microbial mineral weathering (Mailloux et al., 2009)), which may be occurring individually or simultaneously at a given location (Neumann et al., 2010). Even though rice fields are one of the largest sources of water to the aquifer, they do not seem to contribute recharge that can mobilize arsenic (Neumann et al., 2010).

Deeper waters from Pleistocene aquifers are relatively As free, and ^{3}H dating (along with small amounts of O_2) of some groundwaters revealed recent contact with the atmosphere, i.e. young groundwater (Zheng et al., 2004). Isotopic signatures of deep groundwater closely reflect those of meteoric water (Lawson et al., 2008). However, widespread irrigation pumping of the deep aquifer in the Bengal Basin may eliminate deep groundwater as an As-free resource within a few decades (Burgess et al., 2010).

Chapter 3 - Objectives and Hypotheses

Objectives

The emphasis of this study was to compare the geochemistry and mineralogy of aquifer sediments with hydrochemistry and stable isotopes (O, H, C) of groundwaters and surface waters in contrasting groundwater As-bearing environments within Murshidabad district of West Bengal, India. This work focused on four high-As zones east of the river Bhagirathi and two low-As zones west of Bhagirathi. The main objective was divided into four different sub-objectives:

1. Characterize aquifer sediments by identifying major and accessory minerals present to determine the presence of any conspicuous/favorable minerals with which As could be associated and then subsequently mobilized into groundwater under changing redox conditions; and to test which mechanism(s) of As mobilization that have been proposed by many researchers to mobilize As into groundwater is most favorable in these sampling sites (pyrite oxidation; competitive ion exchange; reductive dissolution of Fe (oxy)(hydr)oxides)
2. Describe on the scale of meters to tens of meters, the spatial variability of dissolved As concentrations in groundwaters in each sampling area.
3. Identify the source(s) of groundwater recharge in the local aquifers through analysis of stable isotopes of hydrogen and oxygen and the role of recharge mechanism in controlling mobility of As in subsurface aquifers.
4. Determine the relative contribution of carbon to As mobilization via analysis of ^{13}C isotopes of dissolved inorganic carbon (DIC) in water samples.

Hypotheses

Because the study area is situated in a fluvio-deltaic system originating from eroded high-grade granulites and Gondwana deposits, aquifer sediments should consist of a wide variety of reworked minerals, dominated by quartz and feldspar. (A) Pyrite oxidation at well depths in the Holocene aquifer is improbable due to presence of reducing conditions but may occur near the surface where atmospheric contact can release As, and then As can be transported to depth. (B) Competitive ion exchange may be occurring in areas where high phosphates are detected in the waters/sediments in conjunction with high dissolved As. Phosphate displaces As from the sediments, thus releasing the As into the groundwater. (C) A more likely scenario is reductive dissolution of Fe (and possibly Mn) (oxy)(hydr)oxides, and this will be more convincing with evidence such as high

Fe(II):Fe_T and As(III):As_T in sediments (and waters), along with elevated levels of NH_4^+, Fe and HCO_3^- (and low levels of Cl^-, SO_4^{2-}, NO_3^-, and NO_2^-) in the groundwaters.

Precipitation is the most likely groundwater recharge mechanism in this study. Ponds (large surface water reservoirs) are likely *not* a major contributor to recharge of groundwater because the base of these ponds tend to silt in fairly quickly, acting as a sealing agent.

Previous studies have proposed that carbon plays a major role in As mobilization (Harvey et al., 2002, 2005; Neumann et al., 2010) and it is known that certain values of ^{13}C of DIC can be used as tracers to indicate interaction with atmospheric CO_2 or a carbonate and/or organic-rich component. The hypothesis here is that groundwaters with high dissolved As should have ^{13}C values indicating a carbonate and/or organic-rich component, which aids in the As mobilization process(es).

Chapter 4 - Methods and Materials

Study Area Description

The study area is located in Murshidabad (pop. ~5.8 million; area: 5,324 km^2), one of 18 districts in the state of West Bengal, India, along its border with Bangladesh, and is part of a vast alluvial plain created by the Ganges-Brahmaputra-Meghna (GBM) river system (Fig. 2). The Ganges drainage basin is ~1,060,000 km^2 and includes large tracts of high-grade metamorphic terrains of the Himalayan belt as well as Precambrian basement of the Indian craton (Garzanti et al., 2010 and references therein). It carries an annual sediment load of ~16 x 10^{16} tons $year^{-1}$ (Subramanian, 1996) down through northern and eastern India and Bangladesh toward the Bay of Bengal, forming the largest fluvio-deltaic system on earth. The Ganges enters West Bengal in Malda district, and flows south into Murshidabad district where it turns and flows southeastward into Bangladesh. Just south of the northern border of Murshidabad, Ganges splits to form the river Bhagirathi, a distributary of the Ganges, that meanders south (~120 km) through the study area, through the mega-city of Kolkata (approximately 200 km from the study site), and finally into the Bay of Bengal.

The study area is relatively flat, formed by upward-fining sedimentary sequences deposited in older river valleys that formed during Pleistocene low-stand(s) of sea level. The whole region is dissected by numerous rivers and smaller streams, along with man-made canals and countless ponds. East of Bhagirathi in the active floodplains is evidence of a series of ancient oxbow lakes and paleo-meanders. Nearly all villages are built on top of natural or artificial levees to protect them from monsoonal flooding during the late summer months (June-October), which is when the majority of 1500+ mm of annual rainfall occurs. The study area is situated near the Tropic of Cancer, so the local climate is tropical with high humidity and maximum summer temperatures in excess of 40°C.

Within Murshidabad are 26 blocks (smaller administrative units) of which six were chosen for sampling in this study (Fig. 2). Sites ranged in size from ~0.5 to ~1 km^2, and covered a total area of about 3 km^2. Each site was chosen based either on previous work done by Sur et al. (2006), where areas of elevated (as well as low) As concentrations in groundwater had been pin-pointed, or by communication with locals knowledgeable of specific areas with high-As groundwaters. Nabagram (Binodpur: 24°11.850'N 88°13.569'E) and Kandi (Hizole: 23°58.585'N 88°6.815'E) blocks were located west of river Bhagirathi in the older Pleistocene terraces, while Beldanga (Makrampur: 23°56.355'N 88°16.156'E), Hariharpara (Koshalpur, Bahariparamore: 24°3.658'N 88°21.544'E),

Jalangi (Baramasia: 24°12.656'N 88°41.385'E), and Naoda (Rejlapara, Raipur: 23°54.093'N 88°28.068'E) blocks were situated east of Bhagirathi in the younger Holocene flooplains.

Sample Collection

Water Sampling

During the course of two field trips (June 2009, January 2010), groundwaters from tubewells (Fig. 3) and irrigation wells (shallow aquifer < 60 m and deep aquifer > 60 m), and surface waters from ponds, rivers, and canals were collected in and around villages. Tubewell waters (n=75) were collected from wells ranging in depth from 8.5 to 40 m. Irrigation waters (n=8) were collected from electric pump wells ranging from 25 to 138 m in depth, usually in rice fields on the flanks of villages. Well waters were collected only after a minimum of 5-10 minutes of pumping to purge the well casing several times (van Geen et al., 2003). Surface waters were collected from lower depths of ponds (n=11) adjacent to sampled tubewells. Some canal waters from them was also collected (n=2). Additionally, river water samples were collected from Bhagirathi (n=4) and Ganges (n=1).

Before heading to the field sites, each sample bottle was pre-washed following a specific protocol. Each bottle was rinsed three times with tap water, rinsed three times with de-ionized water, soaked in RBS (detergent) overnight, rinsed three times again with de-ionized water, soaked in an acid bath (10% Trace Metal grade HCl) overnight, rinsed with de-ionized water three times, and air-dried on Kim-wipes.

All samples were collected in duplicate, and some in triplicate (January 2010) after rinsing the bottles three times with the water to be collected—one in a white Fisherbrand® 500 ml Nalgene® high-density polyethylene narrow-mouth bottle (Cat. No. 2006-0016) (unfiltered, unacidified) and the other (sometimes 2 each) in an amber 125 ml Nalgene® high-density polyethylene narrow-mouth bottles (Cat. No. 2004-0004) (one unfiltered, unacidified; one filtered, acidified to prevent precipitation of dissolved iron as well as adsorption of trace metals onto the container surface [Tareq et al., 2003]). Sample bottles were filled to the top leaving no head space in the bottle. Filtered, unacidified samples were collected in plastic 50 ml centrifuge tubes (Fisherbrand® Disposable Centrifuge Tube, Sterile, Polypropylene, 50 ml; Cat. No. 06-443-20). The 125 ml amber-colored bottles (if acidified) were acidified with 1% HNO_3 (Fisherbrand®) in order to prevent precipitation during the preservation time between collection and analysis. Acidification was done in the field (January 2010) and in the lab (June 2009) directly after returning to the US.

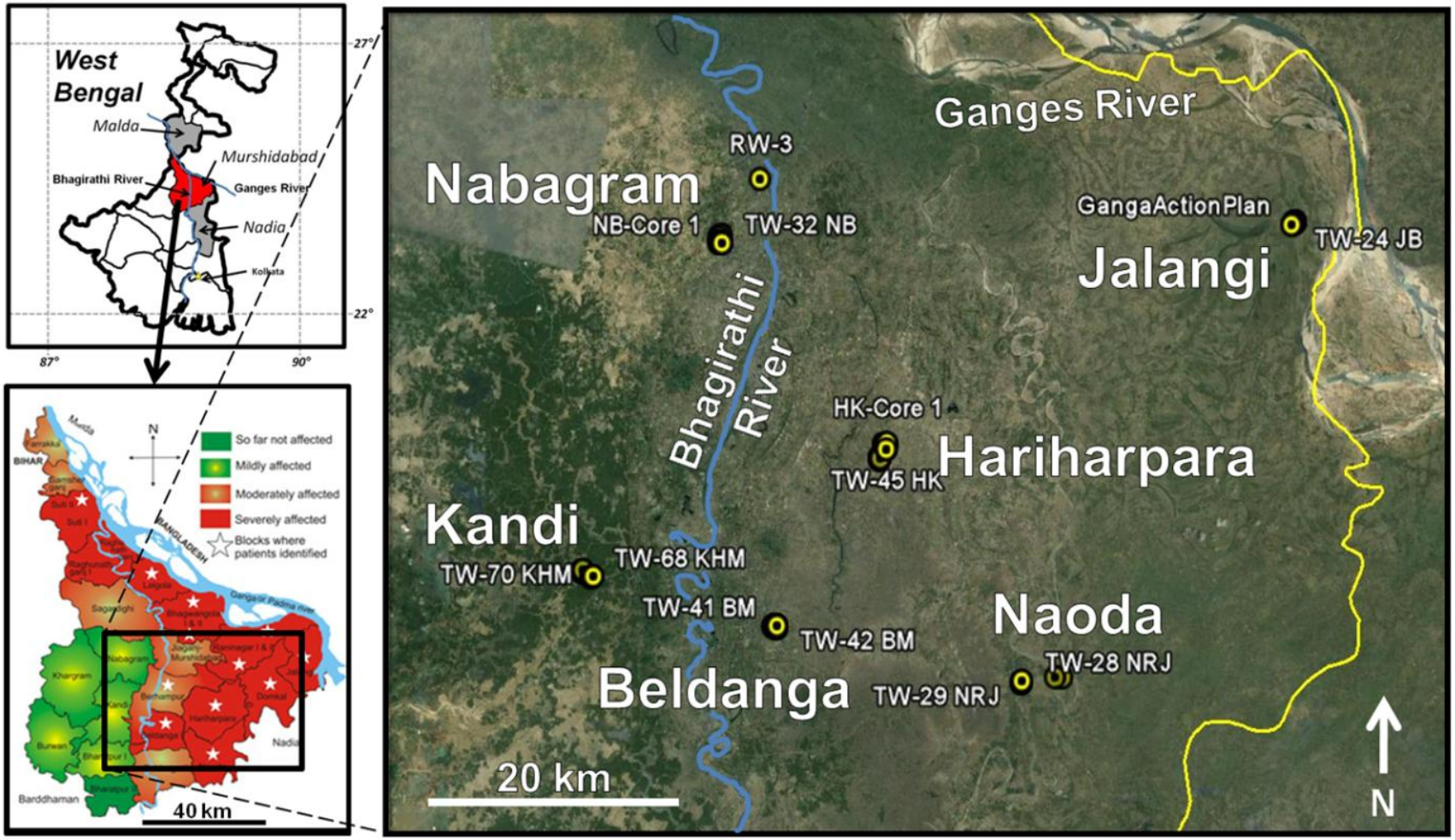

Figure 2: Map showing location of Murshidabad district in relation to West Bengal and river Bhagirathi (top left) and location of study area within Murshidabad (bottom left) (http://www.soesju.org/arsenic/wb.htm). Sampling locations are shown in Google Earth image (right). Two low-As areas (Nabagram, Kandi) west of river Bhagirathi (blue line) and four high-As areas (Beldanga, Hariharpara, Jalangi, Naoda) east of Bhagirathi were sampled in this study. Yellow line indicates international border between India and Bangladsh.

Figure 3: Typical hand-pump tubewell of the hundreds of thousands found throughout this region in India.

Filtering was done using disposable plastic syringes (25 ml) pushing the water through a 0.45 μm polypropylene filter (Whatman syringe filter, 25 mm GD/X Disposable Filter Device, PP Filter Membrane with Polypropylene Housing, Cat. No. 6878-2504) into respective sample bottles. Fifteen water samples (14 tubewell, 1 irrigation) were collected in large jugs during June 2009 for separation of inorganic arsenic species procedures done in the field immediately upon sample collection.

Also, during the January 2010 trip, 27 samples (24 tubewell, three irrigation) were collected for dissolved inorganic carbon (DIC) analysis. These 27 samples were collected in 20 ml glass vials (National Scientific Vials, Headspace 20 mm Crimp; Cat. No. C4020-20) and sealed with a rubber stopper (National Scientific Headspace Septa, Teflon/Rubber; Cat. No. C4020-34) and a crimp top (National Scientific 20 mm Tear Off Seal; Cat. No. C4020-5A), with a hand-crimper (Wheaton Aluminum Seal Hand Crimper; Cat. No. 06-406-21). The glass vials were previously treated with an

$HgCl_2$ (Acros Ogranics, Mercury(II) Chloride, 99.5%; Cat. No. 7487-94-7) solution and heated on a hot plate (Corning Remote Hotplate) in the lab (KSU-Geology) so to form a thin precipitate covering on the inside bottom of the vial to remove organic carbon from the sample (Zheng et al., 2005).

Each sample bottle was labeled with the type of sample (i.e. tubewell (TW), pond water (PW), etc.), sample number, location (block-thana, ex: Beldanga-Makrampur = BM), and date. Coordinates were taken at each sampling location with hand-held GPS (Garmin eTrex Vista HCx). Sample ID, coordinates and other relevant information (i.e. well depth, date of well installation, owners name, number of members in household, symptoms of arsenic poisoning, etc.) were recorded manually in field notebooks. For each respective type of water sample bottle the following analyses were performed (when applicable):

1. 500 ml white Nalgene® bottles (unfiltered, unacidified) – total As, anions, conductivity, total dissolved solids, dissolved oxygen, pH
2. 125 ml amber Nalgene® bottles (unfiltered, unacidified) – stable isotopes ($\delta^{18}O$ and $\delta^{2}H$)
3. 125 ml amber Nalgene® bottles (filtered, acidified) – cations
4. 20 ml glass vials – $\delta^{13}C$ of dissolved inorganic carbon (DIC)

Sediment Sampling

Surficial sediments (0 to 2 m depth)

In this study, both surface and subsurface samples were collected from each block where water sampling was done. Surface samples were collected in plastic liners (~60 cm x ~2.2 cm) placed in a coring sleeve attached to a T-handle (Fig 4). The coring device was pressed down into the ground, collecting sediments in the liner. When the corer was fully inserted (~60 cm), it was carefully removed from the ground, taking care not to lose any sample. The top of the corer had a threaded cap which could be unscrewed to expose ~2 cm of the liner. The liner was then cautiously pulled out from corer, and a blue plastic cap was placed over the end of the liner and taped shut with black electrical tape. Once the blue cap was secured on the top end of the liner, the remaining portion of the liner was removed from the core. The liner was flushed with high-purity N_2 gas, and a red plastic cap (red) was quickly placed over the lower end and sealed with electrical tape. The core liner was labeled with location (same format as water samples), sample number, and depth interval, then placed in the shade (or coolest place possible). If soil/sediment conditions were permissible, with the addition of a 1 m extension between the T-handle and corer, a second (sometimes third) successive

core was taken from just below where the surface core was taken. Occasionally, these surface cores were taken near high-As wells, but typically were collected above where a borehole would be made (near a well that was known to have high dissolved arsenic concentrations in the groundwater) to collect the deeper subsurface sediments. Five surface cores were also taken just at the edge of river Bhagirathi (4 locations) and river Ganges (1 location).

Figure 4: T-handle corer with plastic liner insert being employed to collect surficial (0-2 m) sediments near a tubewell in Hariharpara with significantly elevated concentrations of dissolved As.

Subsurface (shallow to deep aquifer sediments)

Subsurface sediments were collected from shallow (2 to < 15 m), intermediate (15 to < 25 m), and deep (25 to ~40 m) cores in each block (Nabagram-2, Kandi-1, Beldanga-3, Hariharpara-2, Jalangi-1, Naoda-1) via local drilling method (Fig 5). The drilling rig consisted of bamboo poles lashed together with rope and a lever system connected by a chain to drilling pipe. As the pipe was driven deeper into the ground, the sediment would move up through the inside of the pipe and out the top once there was enough sediment to fill the entire length of the pipe.

The drilling technique used is sometimes called the "hand percussion" or "hand-flapping" method. The way this procedure worked was a driller (or two) would stand behind the drilling structure pulling down on the bamboo lever, which raised the other side that was attached to the pipe by chain. When the driller would raise his end of the lever, the other end would go down with the weight of the pipe and the force of gravity. Another driller would sit (or stand, depending on the amount of pipe above the surface at the time) on the bamboo cross-member of the rig and place the ball of his hand tightly over the top end of the pipe as the pipe was being lifted. This process created a vacuum or circulation of water and sediments through the pipe. The driller would then lift part of his hand from the pipe to release the vacuum and allow water and sediment to escape from the top as the pipe was again lowered into the ground. This process was repeated over and over in a rhythm that kept the circulation continuing. Once about ¾ of the pipe was below the surface, another 3 m pipe would be attached by screwing it onto the pipe already in the borehole. The same process continued until maximum attainable depth was reached. For instance, if the sediment was sandy, drilling became more difficult at deeper depths due to sand caving in on the hole, or if there was a thick clay layer, drilling was much more difficult as well. Boreholes were drilled to 30 m depth in Kandi, 33 m in Nabagram, and ~40 to ~43 m depth in Beldanga, Hariharpara, Naoda, and Jalangi..

Sediment was collected at regular depth intervals (usually ~3 m) and at noticeable changes in lithology (i.e. grain size, color, etc.) in each borehole. Vinyl gloves (Fisherbrand® Powder-Free, Latex-Free, Vinyl Exam Gloves; Cat. No. 19-041-190C) were worn when collecting each sample and transferring sediment either directly from the pipe (more consolidated sediments, i.e. silt, clay) or from a small, clean pale that captured the looser sediments as they discharged from the top of the drilling pipe. Samples were immediately placed in an O_2-impermeable Remel® bag (Mitsubishi Gas Company, Remel®, Cat No. 2019-11-02), along with an O_2 absorber pouch (Mitsubishi Gas Company, AnaeroPouch® Anaero; Cat. No. 23-246-379) (Fig. 6). The bag was immediately flushed with N_2 gas (to prevent oxidation of anaerobic sediments) in the field and sealed. Duct tape was

added to some sample bags for extra security in the sealing them. Sample bags were labeled according to location (as water samples were) along with a sample number, depth (in feet), and the date of collection. They were stored as cool as possible while in the field.

For each respective type of sediment sample, the following analyses were performed:

1. Surface core samples – petrographic analysis (thin sections)
2. Subsurface (shallow to deep) core samples – petrographic analysis (thin sections), X-Ray Fluorescence (XRF), Scanning Electron Microscopy (SEM) with energy dispersive x-ray spectrum (EDS), Fe(II), total Fe and phosphate, total digestion, sequential extractions

Sample Transport

All samples (water and sediment) were shipped via DHL to Kansas State University (KSU), Manhattan, Kansas, USA, immediately after returning from the field. Upon receipt of the sample shipments, samples were stored in refrigerators (core liners in freezer) in KSU-Geology Department until further analyses were performed in the lab.

Figure 5: Local drilling method used to collect shallow to deep (< 45 m) sediments in Beldanga.

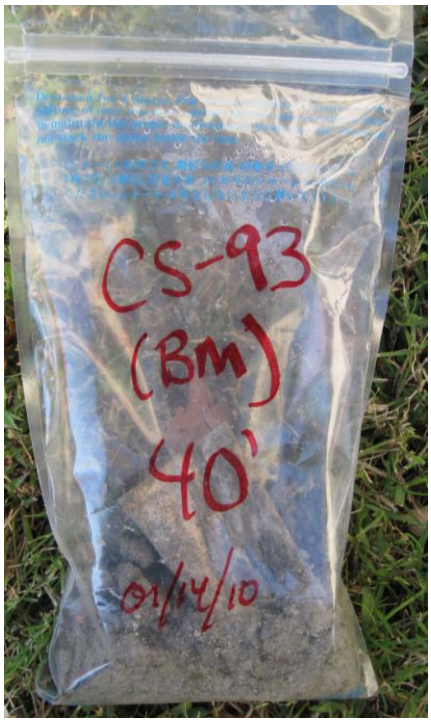

Figure 6: Subsurface (aquifer) core sediment from 40 feet (~12 m) depth in Beldanga placed in an O_2-impermeable Remel® bag with Anaero® O_2 absorber, flushed with N_2 gas, and sealed.

Analyses

Field Analyses

HACH® Hydrolab® for water parameters

Temperature (°C), pH, conductivity (µS/cm), total dissolved solids (TDS) (mg/l), dissolved oxygen (DO) (mg/l) and oxidative redox potential (ORP) (mV) of 33 water samples were measured in the field (January 2010) using a HACH® Hydromet Hydrolab® MS5® Water Quality Multiprobe (Cat. No. 003078HY) with a flow through cell (Fig. 7). The Hydrolab® was connected to a hand-held PDA (Trimble® Recon® handheld 400 64/256 Yellow BT/802; Cat. No. 69670) for instantaneous display of values for each measurement. The Hydrolab® was calibrated for pH (using pH buffers of 4 and 7) and conductivity (standards of 0.500 mS/cm [Cat. No. 013770HY] and 47.6 mS/cm [Cat. No. 013650HY]) on the same day field work began.

These analyses were performed mainly on tubewell waters, and irrigation waters (where possible) by placing a bucket under the spigot and allowing the bucket to fill with water. Wells were pumped for ~8 to 10 minutes in the same manner mentioned above for water sample collection, and water was allowed to flow over the top of the bucket with continuous pumping. Sensors of the Hydrolab were placed in the bucket. Pumping continued until values for each measurement were stabilized (or showed little change within 30-60 seconds). All values were saved in the memory of the Trimble® unit and were also recorded in the field notebook for future reference.

Arsenic Speciation of waters

Arsenic species were separated in the field using an anion-exchange chromatography method (BioRad AG 1 x 8; 50-100 mesh, acetate form) developed previously (i.e., Ficklin, 1983), and shown to work well for groundwaters (Wilkie and Hering, 1998; Haque and Johannesson, 2006; Haque et al., 2008) (Fig 8). Filtered groundwater samples (via 0.45 µm polyether sulfone membrane (Cat. No. 09-927-43B)) were first acidified (ultra-pure HNO_3) to pH ~3.5 prior to passing through the anion-exchange columns. Arsenite, which occurs as $H_3AsO_3^o$, passed through the column and is collected in pre-cleaned, amber HDPE bottles, whereas As(V) was retained on the column owing to its occurrence as $H_2AsO_4^-$ (Wilkie and Hering, 1998).

Field Test Kits for water chemistry

Several field test kits and water quality probes were used in the field for determining in-situ aqueous parameters during both field trips. For samples collected during June 2009, conductivity (Mettler Toledo SevenGo™ Conductivity Meter SG3 with MT InLab® 731 Conductivity Sensor; Cat. No. 51344120) and TDS were measured for the 50 water samples after being calibrated with their respective reference standards (conductivity: 12.8 mS/cm, 1413 µS/cm). DO was measured for the 50 water samples in the lab using a Mettler Toledo SevenGo™ Pro Dissolved Oxygen Meter SG6 (Cat. No. 01-910-531).

Phosphate concentrations were analyzed using CHEMets® Kit (Phosphate, K-8510). The sample cup was filled to the 25 ml mark with the sample water, and 2 drops of A-8500 Activator Solution were added. The cup was capped and shaken well. A CHEMet ampoule was placed in the sample cup, and the sample was stirred briefly with the tip of the ampoule. Then the tip of the ampoule was immediately snapped by pressing the ampoule against the side of the cup, causing the ampoule to fill, and leaving a small bubble to facilitate mixing. The contents of the ampoule were mixed by inverting the ampoule several times, allowing the bubble to travel from end to end. The ampoule was dried and given 2 minutes for color development. The comparator was held in a nearly horizontal position under a bright light (in this case, sunlight), and the ampoule was placed between the color standards and moved from left to right, until the best color match was found.

Alkalinity was measured for each of the 50 samples using a HACH® Alkalinity Test Kit (10-4000 mg/l, Model AL-DT; Cat. No. 20637-00) digital titration method. For each sample, ~20 ml of water sample was used. The 20 ml sample was added to a 100 ml graduated cylinder, and one Phenolphthalein Indicator Powder Pillow (Cat. No. 942-99) was added to the sample, swirling the cylinder to mix the contents. The solution did not turn pink for any of the samples, so it was concluded that no value for $CaCO_3$-P alkalinity was important for these samples. Then a Bromcresol Green-methyl Red Indicator Powder Pillow (Cat. No. 943-99) was added to the sample and swirled to mix. A digital titration cartridge of 1.6 N H_2SO_4 (Cat. No. 14389-01) with a delivery tube was attached to the HACH® digital titrator and inserted in the 20 ml water sample. Titration of the sulfuric acid into the sample proceeded until a light greenish blue-grey (pH 5.1) a light violet-grey (pH 4.8) or a light pink (pH 4.5) color (depending on composition) was achieved. The total number of digits displayed on the titrator was recorded and multiplied by 5 (the respective digit multiplier for a 20 ml sample) to obtain the amount (mg/l) as HCO_3^--Total Alkalinity. The resulting liquid was discarded. Before the next sample was analyzed for alkalinity, the graduated cylinder and the

delivery tube were rinsed 3 times with de-ionized water and 3 times with water from the next sample to be analyzed to maintain precision and consistency.

Alkalinity, ammonia, and phosphate values were determined for 33 tubewell and two irrigation water samples (January 2010). Arsenic was measured for a select few tubewell waters to quickly evaluate arsenic levels and help determine drilling locations for collecting sediment core samples.

Alkalinity was determined for 33 tubewell and two irrigation well water samples as described above.

Ammonia was determined for 33 tubewell and two irrigation well water samples using CHEMets® Kit (Ammonia, K-1410). Five drops of A-1402 Stabilizer Solution were added to a 30 ml sample cup. The sample cup was filled to the 25 ml mark with the sample, and 2 drops of A-1401 Catalyzer Solution were added. The sample was stirred with the tip of a self-filling ampoule for colorimetric analysis (R-1401). Two drops of A-1400 Activator Solution were added to the sample and stirred briefly with the tip of the ampoule. Then the tip of the ampoule was immediately snapped by pressing the ampoule against the side of the cup, causing the ampoule to fill, and leaving a small bubble to facilitate mixing. The contents of the ampoule were mixed by inverting the ampoule several times, allowing the bubble to travel from end to end. The ampoule was dried and given 15 minutes for color development. The comparator was held in a nearly horizontal position under a bright light (in this case, sunlight), and the ampoule was placed between the color standards and moved from left to right, until the best color match was found. Sometimes the sample was the same color as a reference standard, but other times it was between two color standards, so an estimate was made. After analysis of each sample, the liquid was discarded, and the sample cup was rinsed 3 times with de-ionized water and then 3 times with the next sample.

A HACH® Arsenic Test Kit (Cat. No. 2800000) was used for an in-situ estimate of arsenic values for 18 tubewell waters (van Geen et al., 2003, 2004, 2005a,b) to help determine where sites for sediment samples should be located for coring. An Arsenic Test Strip (Cat. No. 28001-00) was inserted into the reaction bottle cap so that the pad completely covered the small opening, and the flap was closed and pressed to secure it. The reaction bottle (Cat. No. 2800200) was filled to the fill line (50 ml). An Arsenic Reagent #1 (Na_2HPO_4) powder pillow (Cat. No. 27978-99) was added to the sample and swirled to mix so that most of the powder dissolved. Then an Arsenic Reagent #2 ($2KHSO_5 \cdot KHSO_4 \cdot K_2SO_4$) powder pillow (Cat. No. 27977-99) was added to the sample and swirled to mix. Three minutes passed before adding an Arsenic Reagent #3 ($C_{10}H_{14}N_2Na_2O_8 \cdot 2H_2O$) powder

pillow (Cat. No. 27979-99) to the sample. The sample was swirled to mix and given two minutes, then swirled again. One scoop of Arsenic Reagent #4 (H_2NSO_3H) powder (Cat. No. 454-29) was added to the sample and swirled to mix to dissolve most of the powder. An Arsenic Reagent #5 (Zn powder) powder pillow (Cat. No. 27981-99) was added to the sample. The cap was immediately attached, and the bottle was swirled carefully to mix the reagents. Approximately 35 minutes were allowed for reaction time. Each sample was swirled twice during the reaction period. After the ~35 minutes reaction time was completed, the test strip was removed and the developed color on it was immediately compared to the chart on the test strip bottle to give an estimate of the arsenic value (μg/l) of the water. Upon completion of the analysis and prior to the next analysis, the reaction bottle was rinsed 3 times with de-ionized water and then again 3 times with the next sample.

Arsenic field test kits have been proven as reliable means to measure As quantitatively in the field (van Geen et al., 2005a,b, 2006; Jakariya et al., 2007; Sankararamakrishnan et al., 2008; van Geen 2008c; Dhar et al., 2008; Rahman et al., 2009). Studies by van Geen et al. (2003) found that after comparing field and laboratory measurements of As in Araihazar, Bangladesh, the HACH® Arsenic Test Kit correctly determined 88% of 799 wells greater than the local standard of 50 μg/l, and that inconsistencies in the 50 to 100 μg/l range could be avoided by doubling the reaction time. Based on these results from previous work, the HACH® Arsenic Test Kit was used in this study.

Phosphate values were determined for 33 tubewell and 2 irrigation well water samples using a HACH® Phosphate, Ortho Test Kit (0-50 mg/l Model PO-19; Cat. No. 2248-00), via colorimetric method. This procedure began by filling the two tubes in the kit to the first (5 ml) line with sample water and inserting one of the tubes into the left opening of the comparator. One PhosVer® 3 Phosphate Reagent Powder Pillow ($C_6H_8O_6$, $K_2S_2O_7$, $Na_2MoO_4•_2H_2O$) (Cat. No. 2209-99) was added to the second tube and swirled to mix. The second tube was then inserted into the right opening of the comparator. The comparator was held so that bright sunlight was directly behind the tubes. The color disc was rotated until the colors in the front windows matched. The reading in the scale window was divided by 10 to obtain mg/l phosphate. As with the other field kit procedures, the water was discarded and the tubes rinsed 3 times with de-ionized water and then 3 times again with the next sample before analysis.

Sediment characteristics

Observations of general physical characteristics of sediment samples (e.g. sediment color (wet), grain size(s) (general feel in hand, e.g. sandy, silty, clayey, etc.), depths of sediments, visible

mineral content [with aid of hand lens], presence or absence of visible plant/organic matter, etc.) were made in the field at time of collection and recorded in a field notebook and sometimes on the sample bag itself.

Figure 7: HACH® Hydrolab® MiniSonde with hand-held Trimble® unit, along with other field equipment in Beldanga.

Figure 8: As(III) being separated from As(V) in groundwater samples via anion-exchange columns in Beldanga.

Lab Analyses

Water Analyses

Total Arsenic and Arsenic Speciation in waters

From the speciation procedures done in the field, As(III) was quantified in the eluted fractions and total dissolved As was measured on separate aliquots by high-resolution (magnetic sector) inductively coupled plasma mass spectrometry (HR-ICP-MS [detection limit for As < 1 ppt]; Haque et al., 2008; Datta et al., 2009; 2010a,b; Neal et al., 2009, 2010a,b,c) in the Department of Earth and Environmental Sciences at Tulane University in New Orleans, Louisiana. Arsenate was then determined by difference between total dissolved As and As(III) for each of the 15 samples. A second batch of water samples (n=21) was analyzed for total As concentration in the HR-ICP-MS. Total As was measured in an additional 20 groundwater and surface water samples at Kansas Geological Survey (KGS) at the University of Kansas in Lawrence, Kansas, with an inductively coupled plasma – optical emission spectrometer (ICP-OES).

Anions in waters

Major anions (Cl^-, SO_4^{2-}, NO_2^-, NO_3^-) for all 50 water samples collected during June 2009 were measured at the KGS using an Ion Chromatograph (IC) (Dionex IC-3000). Five standards were prepared using 0.2 μm filtered de-ionized distilled water and stock standard solutions of 1000 mg/l. The standards for each element were made for the following (in mg/l, (NO_2^- in μg/l)): Cl^- [5, 10, 40, 60, 100]; NO_2^- [0.1, 0.2, 0.4, 0.8, 1.0]; NO_3^- [1.0, 2.5, 5, 15, 25]; SO_4^{2-} [5, 10, 40, 60, 100]. Samples were prepared by filtering through 0.2 μm filters (Cat. No. 09-927-26C), and approximately 2.5 ml of sample was added to IC vials which were then loaded into the autosampler. The five standards, along with a blank, were run for calibration of the machine. Then the 50 water samples were analyzed for their respective anion concentrations.

Alkalinity (bicarbonate) was measured for the same 50 water samples (39 tubewells, 3 irrigation wells, 3 ponds, 5 rivers) by HACH® Alkalinity Test Kit (~5 weeks after collection in the field) using same method as described above in 'Field Analyses' section. Phosphate was measured for the same 50 water samples using a HACH® Phosphate, Ortho Test Kit, following the same method as describe above.

Cations in waters

Major cations (Fe, Mg, Ca, K) for 20 water samples collected during June 2009 were measured in the Department of Agronomy at Kansas State University using ICP-OES (Varian 720-ES ICP Optical Emission Spectrometer). Four multi-element standards were prepared with concentrations of 25, 50, 75, and 100 mg/l of each element, made from stock solutions each with a concentration of 1000 µg/ml for each of the four elements. The most common line with least interference was chosen for each element (Fe: 259.940 nm; Mg: 279.078 nm; Ca: 315.887 nm; K: 766.491). Sub-samples were taken from the 125 ml HDPE bottles that had previously been acidified in the field with 1% HNO_3 and placed in 90 x 13 mm ICP vials in a sample-holder rack. The instrument was calibrated with the standards and the samples were analyzed for Fe, Mg, Ca, and K concentrations (mg/l).

δ^2H and $\delta^{18}O$ of water samples of Murshidabad

Stable isotope values of δ^2H and $\delta^{18}O$ for 75 water samples were measured using stable isotope mass spectrometry (SIMS) (Picarro G1301) in the Stable Isotope Mass Spectrometry Lab in the Department of Biology at Kansas State University. The precision of the Picarro G1301 was ~50 ppmv. After filtering through a 0.2 µm filter, approximately 2 µg of sample was injected into the Picarro water analyzer for determination of δ^2H and $\delta^{18}O$. Inside the Picarro analyzer, the injected water sample was converted to vapor and carried by a N_2 carrier stream to the analyzer where the relative abundance of heavy and light isotopes was measured. Due to the adsorptive nature of water, there is a slight memory effect between samples as water molecules from one injection linger on the surface of the analyzers internal plumbing. To remove the memory effect, a total of 6 injections were made into the analyzer per sample. The data from the first three were removed from the analysis (due to memory effect), and the last three were averaged (as recommended in the Picarro instrument user's manual). The average value represents a 'raw' data point that is then corrected to three secondary standards (Evian bottled water [δ^2H = -78.07‰ and $\delta^{18}O$ = -10.01‰], KSU de-ionized water [δ^2H = -40.72‰ and $\delta^{18}O$ = -5.30‰], and KSU de-ionized enriched water [δ^2H = -8.36‰ and $\delta^{18}O$ = 4.03‰]) that are analyzed along with each batch of samples. The standards have been calibrated to National Institute of Standards and Technology (NIST) accepted standards (Greenland Ice Sheet Precipitation (GISP: δ^2H = -189.5‰ and $\delta^{18}O$ = -24.78‰), Standard Light Arctic Precipitation (SLAP: δ^2H = -428.0‰ and $\delta^{18}O$ = -55.5‰), and Vienna Standard Mean Ocean Water (VSMOW: δ^2H = 0‰ and $\delta^{18}O$ = 0‰)) (Coplen, 1994). The δ^2H and $\delta^{18}O$ values of the standards

span the entire range of expected isotope values for the samples submitted. In order for correction of drift in the analyzer during a batch of samples, a working standard of known isotope ratios was analyzed every four samples. Finally, the raw isotope data was corrected to the three standards analyzed with the measured water samples.

δ^{13}C-DIC of water samples

Values for $\delta^{13}C$ from bicarbonate were measured for 24 water samples (Beldanga: n=5; Hariharpara: n=6; Nabagram: n=9; Kandi: n=4) at the National Aeronautics and Space Administration (NASA) Johnson Space Center (JSC) in Houston, Texas. The $\delta^{13}C$ from bicarbonate was extracted and analyzed via Thermo® Finnigan™ GasBench-II coupled with a MAT-253 mass spectrometer operating in continuous flow mode.

Glass Exetainers® were filled with 30 to 60 µl of 100% H_3PO_4, taking care that acid was delivered to the bottom of the exetainer®, and capped. All exetainers® were placed into heating block and heated to 30°C and let sit for one hour to reach temperature equilibration, then degassed by flushing with dry helium for 5 to 7 minutes. A small syringe was loaded with the bicarbonate sample, and depending on bicarbonate concentration, 100 to 600 µl of water sample was injected into the acid-charged exetainer®, taking care that none of the bicarbonate solution stuck to the underside or the topside of the septa. The samples were then allowed to react overnight before extraction and analysis. All samples were analyzed against a laboratory working standard calibrated against NBS-19 (‰ Vienna Peedee Belemnite (V-PDB)). ^{13}C analyses were typically better than ± 0.07 ‰.

Sediment Analyses

Sediment characteristics

A small representative subsample was taken from each sample bag for one core from Beldanga, one core from Hariharpara, and one core from Nabagram and let air dry on paper plates in the lab. After drying, similar observations of general physical characteristics of sediment samples (e.g. sediment color (dry) and grain size(s) [for creation of a litholog with sediment colors and grain size(s)], visible plant/organic matter, mineral content, etc.) made in the field were done in the lab.

Thin Section Petrography of sediments

For six sediment samples from June 2009 (BM-44 [~13 m], BM-64 [~20 m], BM-99 [~30 m], BM-115 [~35 m], NB-58 [~18 m], NB-79 [~24 m]), the same subsamples mentioned above (in

"Sediment Characteristics" section) were placed in separate small 20 ml HDPE scintillation vials (Wheaton; Cat. No. 0334172) and shipped to Spectrum Petrographics (http://www.petrography.com/) in Vancouver, Washington, to have thin sections (9.14 cm x 5.33 cm) made from the loose sediments. Epoxy was injected into the loose sediments, and once solidified, the hardened mass was glued to the glass thin section. The mass was then cut relatively thin and ground to a thickness of 30 μm and polished. Thin sections from January 2010 (BM-4 [~1 m], BM-6 [~2 m], BM-90 [~27 m], BM-100 [~30 m], BM-130 [~40 m], HK-20 [~6 m], HK-60 [~18 m], HK-130 [~40 m], KHN-50 [~15 m], KHN-100 [~30 m]) were also made in the same manner by the same company at a later date.

Once samples were returned from Spectrum Petrographics, each thin section was carefully analyzed with a polarizing light petrographic microscope (Leica DM EP Microscope) with objectives of 4x, 10x, and 40x (all 3 Leica Hi Plan), and oculars with 10x magnification (Model No. 13581008). During analysis of each slide, apparent textures/color variations were noted, major minerals and accessory minerals and their relative abundance within the sample were identified, along with any other noticeable/unique features, especially the textures. Mineralogy was determined by both plane-polarized light and cross-polarized light. Some key features used to identify minerals were relief, color, pleochroism, interference colors, birefringence, extinction angles, presence/absence of cleavage, and mineral shape/habit. Photomicrographs were taken with a camera (SPOT Insight QE, Model # 4.2) attached to Nikon Eclipse E-600 POL polarizing light microscope. SPOT Advanced Software was used for digital photo capture.

Scanning Electron Microscopy with Energy Dispersive X-Rays of sediments

Sediment samples from Beldanga (BM-44 [~13 m], BM-64 [~20 m], BM-90 [~27 m], BM-99 [~30 m], BM-115 [~35 m], BM-130 [~40 m]), Hariharpara (HK-50 [~15 m]), and Nabagram (NB-70 [~21 m]) were analyzed by scanning electron microscopy (SEM) with energy dispersive spectrum (EDS) (Hitachi S-3500N). Each sample was mounted on a separate aluminum SEM stub with a carbon coating. The sample was then coated with a conductive material (0.1% Au-Pd) to prevent accumulation of surface charging, which can occur when electron beams from the SEM are bombarding the sample and are not allowed to escape from the surface via a conductive path. If there is no such path, the image formed by the SEM will be very poor. Each sample was carefully scanned, aiming to delineate specific 'conspicuous' grains (any grain with an appearance different than the majority of surrounding grains) for analysis. When a grain of interest was observed, x-ray microanalysis (EDS) was done at several points on the grain. This technique generated a spectrum in

which the peaks corresponded to specific x-ray lines and the elements could be identified. The peaks were obtained as a result of the three basic components of the EDS at work. An x-ray detector detects and converts x-rays into electronic signals. Then a pulse processor measures the electronic signals to determine the energy of each x-ray detected. Finally, an analyzer interprets and displays the x-ray data. Several main elements of interest were As, Ca, P, Mg, K, Fe, Mn, Cr, Cu, and S. X-ray spectra were used as a 1st-order interpretation of the mineral being analyzed.

Hand-held X-Ray Fluorescence (initial screening) for total elemental compositions of sediments

Three total sediment cores (Beldanga core #2, Hariharpara core #2, Nabagram core #2) were analyzed by a hand-held x-ray fluorescence (XRF) analyzer (Thermo Scientific® Niton® Analyzer XL3t). Each sample was air-dried overnight at room temperature. After drying, all large, organic debris and non-representative material (twigs, roots, rock, etc.) were removed. Samples were homogenized, and then a representative portion was ground with a mortar and pestle. Additionally, two standard reference materials (SRM) (NIST Montana II Soil 2711a; USGS SDO-1 [Kane et al., 1990; Kuznetsova et al., 1999; Lozano and Bernal, 2005; Andrade et al., 2009]) were measured for quality assurance. Calibration was done before sample analysis began, after every 20 samples were analyzed, and at the end of sampling. This verification was performed by analyzing the Montana II Soil 2711a. A percent difference (%D) was calculated for each target analyte to ensure a %D of ± 20% of the certified value for each analyte. If %D fell outside of this acceptance range, the calibration curve was adjusted by varying the slope of the line and/or the y-intercept value for the analyte. The SRM was re-analyzed until the %D fell within ± 20%.

The sample analysis was initiated by exposing the sample to primary radiation from the source. Flourescent and backscattered x-rays from the sample entered through the detector window and were converted into electric pulses in the detector. Within the detector, energies of the characteristic x-rays were converted into a train of electric pulses, the amplitudes of which were linearly proportional to the energy of the x-rays. An electronic multi-channel analyzer measured the pulse amplitudes, which was the basis of qualitative x-ray analysis. The number of counts at a given energy per unit of time was representative of the element concentration in a sample and was the basis for quantitative analysis.

Analysis of Phosphate, Fe and Fe(II) of sediment core

Phosphate, Fe(II), Fe(III) and total Fe were measured at Queens College, Jamaica, New York, for 22 sediment samples from Beldanga core #1. Approximately a 0.5 g aliquot of wet sediment was leached in 10 ml of 1.2 M HCl diluted with N_2-purged water at 80°C in a water bath for 1 hour, after which the concentrations of Fe(II) and Fe(III) in the leachate were measured with ferrozine (Viollier et al., 2000; Horneman et al., 2004). The concentration of total Fe in the acidified supernatant was analyzed by HR-ICP-MS (Cheng et al., 2004).

Concentration of leachable arsenic and phosphate was measured by slightly modified molybdenum blue method (Dhar et al., 2004), but due to high interference caused by high levels of leachable phosphate in the leachate, arsenic could not be reliably quantified. However, phosphate concentrations were reliably measured in diluted leachate (1:10) by using HACH® DR 5000 UV-Vis Spectrophotometer (Dhar et al., 2004).

Total Digestion of sediments

Total digestion of 10 sediment samples (Beldanga: BM-20 [~6 m], BM-80 [~24 m], BM-90 [~27 m], BM-100 [~30 m], BM-130 [~40 m]; Nabagram: NB-10 [~3 m], NB-30 [~9 m], NB-60 [~18 m], NB-90 [~27 m], NB-110 [~34 m]) was done using a method modified from Zarcinas et al. (1996). Approximately 0.5 g of < 2 mm sediment from aquifer sediment cores was weighed out into restricted neck digest tubes, along with three separate duplicates of three of the same subsamples (Beldanga: BM-90 [~27 m], BM-130 [~40 m]; Nabagram: NB-60 [~18 m]) and placed in a digestion block. 5 ml of aqua regia (HNO_3:HCl 1:3) (1.25 ml of HNO_3 and then 3.75 ml of HCl) were added to each sample. The digestion block was left at room temperature overnight under the fume hood (KSU-Agronomy).

The next morning, each tube was swirled vigorously to make sure no soil was stuck on the bottom of the tubes. Small glass funnels were placed in each tube for refluxing. The digestion block was heated to 140°C for 2 hours (Hamon et al., 2004; Zarcinas et al., 2004). Samples were monitored every 10-15 minutes to make sure that the sediments had not bubbled up the tubes. After the 2 hours reflux period, tubes were removed from the block to let cool. De-ionized water was then added to bring total solution volume to 50 ml mark, mixing each sample well. Samples were then covered with clear plastic wrap and placed in a cold room (walk-in refrigerator) overnight.

The next day the solution of each sample was filtered through Whatman No. 42 filter paper into 15 ml plastic vials. Samples were then taken to the Inductively Coupled Plasma Mass

Spectrometer (ICP-MS) lab in the Department of Diagnostic Medicine/Pathobiology in the College of Veterinary Medicine at Kansas State University.

In the ICP-MS lab, prepared samples were analyzed by ICP-MS (Agilent ICP-MS 7500cx, Agilent Technologies, Wilmington, DE) for a panel of elements including magnesium (Mg), aluminum (Al), vanadium (V), chromium (Cr), manganese (Mn), iron (Fe), cobalt (Co), nickel (Ni), copper (Cu), zinc (Zn), arsenic (As), selenium (Se), molybdenum (Mo), silver (Ag), cadmium (Cd), barium (Ba), thallium (Tl), and lead (Pb). Hydrogen reaction and helium collision were used for interference removal, and argon dilution was used to extend the range of acceptable total dissolved solids concentrations up to 1%. Standards for elemental analyses by ICP-MS were obtained from Environmental Express (Mt. Pleasant, SC). High molecular weight elements, including Ag, Cd, Ba, Tl, and Pb were analyzed without the use of reaction cell interference removal. Selenium was analyzed in the hydrogen reaction mode, while the rest of the elements were analyzed in the helium collision mode. To account for sample matrix effects, scandium (Sc), rhodium (Rh), indium (In), lutetium (Lu) and bismuth (Bi) were used as fixed concentration internal standards in all samples and calibration standards.

Quantification was achieved by measurements of the count rate ratios between internal standards and the elements of interest, and based on linear regression models derived from a series of six standards with the following concentrations for each element: 0, 0.1, 1, 10, 100, 1000 µg/l. Element concentrations in blanks were used to correct sample-measured concentrations for background contaminants associated with analytical reagents and processes. System stability was verified by analysis of 10 µg/l and 100 µg/l standards at the end of each batch of samples. Acceptable stability was defined as < 20% variation between initial and end samples. Limits of detection were defined as three times the background standard deviation of a 10 µg/l standard, derived from seven independent analyses.

Sequential Extractions of sediments

Several sequential extraction methods were carefully evaluated and compared during this study (Tessier et al., 1979; Keon et al., 2001; Alam et al., 2001; Loeppert et al., 2003; He et al., 2010). Sequential extractions can be relatively simple methods to assess trace element pools of differential relative lability in soils and sediments, using reagents of increasing dissolution strength, where ideally, each reagent targets a specific solid phase associated with the trace element of interest (Wenzel et al., 2001), in this case arsenic. One potential limitation for using this method may be the

re-adsorption of As on remaining mineral phases during extraction (Wenzel et al., 2001 and references therein). After identifying the major minerals and accessory minerals present in the sediments for this study, the 5-step method of He et al. (2010) was most relevant and therefore was chosen for this study. This method targets first the more labile phases (physi-sorbed and chemi-sorbed) in which As can be easily mobilized in the types of environments found in the study area. Secondly, this method also aims at attacking amorphous and poorly crystalline hydrous oxides of Fe separately from the well-crystallized hydrous oxides of Fe, with which As is known to be associated in these types of sediments. The last step uses the EPA 3050B method to target residual phases.

Sequential extractions were done on all depths of a total sediment core (Beldanga core #2, 13 total samples) using methods described in He et al. (2010). Initially, the procedure was performed on three samples (BM-20 [~6 m], BM-90 [~27 m], BM-130 [~40 m]) and a NIST standard reference material (Montana II Soil 2711a) as a trial run to work out any intricacies or problems that possibly have arisen during the procedure. Later, sequential extractions were done on the remaining ten samples from Beldanga core #2. Concentrations of As, Mn, and Fe in the extractants of each sample from each step were measured by ICP-OES (KSU-Agronomy).

To begin the process, small (~1 g) subsamples of the wet samples were placed in previously weighed (to 0.001 g precision) plastic 50 ml centrifuge tubes in a N_2 glove box for a few days to dry. During drying of the samples, the extractant for the first step, 0.05 M $(NH_4)_2SO_4$, was made by adding 1.983 g of $(NH_4)_2SO_4$ powder to 300 ml of de-ionized water. Once samples were dry, or nearly so, they were removed from the N_2 atmosphere and weighed to nearest 0.001 g. Then 25 ml of the 0.05 M $(NH_4)_2SO_4$ were added to the samples via pipette. Samples were placed on a shaker for 4 hours to react with the ammonium sulfate. During the 4 hours, 7 multi-element standards (As, Mn, Fe) were prepared in the 0.05 M $(NH_4)_2SO_4$ matrix near expected concentrations. After 4 hours of shaking, samples were removed and centrifuged at ~2100 rpm for 10 minutes. The solution was decanted into a disposable syringe and passed through a 0.45 μm filter into a 13 mm x 90 mm plastic vial for analysis by ICP-OES. The remaining solution was filtered into small Evergreen vials for future analysis (by GFAAS). One wash step with 15 ml of de-ionized water was done at ~2100 rpm for 10-15 minutes. The remaining solution was decanted and discarded. Centrifuge tubes (with sample) were weighed to account for contribution from this step onto the following step.

The second step of the extraction process was the extraction of the specifically sorbed ions using 0.05 M $NH_4H_2PO_4$. $NH_4H_2PO_4$ was used because As and P have similar electron configurations and form triprotic acids with similar dissociation constants (Wenzel, et al., 2001), and at equal

concentrations phosphate outcompetes arsenate for adsorption sites in soils (Swartz et al., 2004) because of smaller size and higher charge density of phosphates (Manning et al., 1996). The 0.05 M strength was prepared by adding 1.15 g of $NH_4H_2PO_4$ granules to 300 ml of de-ionized water. Then 25 ml of 0.05 M $NH_4H_2PO_4$ solution was added via pipette to each 50 ml centrifuge tube and placed on the shaker overnight for 16 hours. Standards and samples from Step 1 were run (during shaking for the second step) on ICP-OES using wavelengths of 193.76, 257.61, 259.94 nm for As, Mn and Fe, respectively. Then 7 multi-element standards were prepared for As, Mn, and Fe using the 0.05 M $NH_4H_2PO_4$ as the matrix for the same concentrations of those made for the first step (As and Mn: 1, 1.5, 2, 2.5, 3, 4, 5 mg/l; Fe: 100, 125, 150, 175, 200, 225, 250 mg/l). After 16 hours of shaking, samples were centrifuged at ~2100 rpm for 10 minutes. The solution was decanted and filtered into ICP vials and Evergreen vials as mentioned above for the previous step. A wash step with 15 ml of de-ionized water was done at ~2100 rpm for 10-15 minutes. The remaining solution was decanted and discarded. Centrifuge tubes (with sample) were weighed to account for contribution from this step onto the following step.

The third step used a 0.2 M NH_4^+-oxalate buffer at pH 3.25 in the dark to attack the amorphous and poorly crystalline hydrous oxides of Fe (e.g. ferrihydrite) and Al. The 0.2 M NH_4^+-oxalate buffer strength was achieved by adding 8.526 g of NH_4^+-oxalate buffer granules to ~250 ml of de-ionized water, adjusting pH to 3.25 by adding ~4 ml of concentrated HCl (trace metal grade). De-ionized water was added to bring the final volume of solution up to 300 ml to make the 0.2 M NH_4^+-oxalate buffer. Next, 25 ml of 0.2 M NH_4^+-oxalate buffer at pH 3.25 was added to each centrifuge tube with a pipette and placed in a rack in a cardboard box and covered with aluminum foil (for darkness) then placed on a shaker for 4 hours. Standards and samples from Step 2 were run on ICP-OES. Then 7 multi-element standards were prepared for As, Mn, and Fe using the 0.2 M NH_4^+-oxalate buffer at pH 3.25 as the matrix for the same concentrations of those made for the first two steps. After 4 hours of shaking, samples were centrifuged at ~2100 rpm for 10 minutes. The solution was decanted and filtered into ICP vials and Evergreen vials as mentioned above for the previous steps. A wash step with 15 ml of de-ionized water was done at ~2100 rpm for 10-15 minutes. The remaining solution was decanted and discarded. Centrifuge tubes (with sample) were weighed to account for contribution from this step onto the following step.

The fourth step of the extraction process used 0.2 M NH_4^+-oxalate buffer + 0.1 M ascorbic acid at pH 3.25 to attack the crystalline hydrous oxides of Fe (e.g. goethite, hematite) and Al. The extractant was prepared by adding 8.526 g of 0.2 M NH_4^+-oxalate granules and 5.283 g of ascorbic

acid to ~250 ml of de-ionized water. Solution pH was adjusted to 3.25 by adding ~3.8 ml of HCl (trace metal grade) and bringing the volume up to 300 ml with de-ionized water to achieve proper strength. Then 25 ml of the extractant solution was carefully added via pipette to each centrifuge tube with sample. Centrifuge tubes were placed in a rack in a water bath and heated at 90°C ± 5°C for 30 minutes. During water bath, standards and samples from Step 3 were run on ICP-OES. Standards were made using respective extractant solution as the matrix for values of As, Mn, and Fe used in previous steps. Samples were centrifuged two times at ~2100 rpm (10 minutes first time and 15 minutes second time). As done in previous steps, samples were filtered into vials for analysis. Centrifuge tubes were weighed to account for contribution from earlier step onto the following step.

The final step of the procedure used EPA 3050B Method for extraction of metals in the residual phases. First, 10 ml of 1:1 HNO_3 (5 ml HNO_3:5 ml de-ionized water) were added to each centrifuge tube. Each centrifuge tube was then covered with a watch glass and placed in a water bath at ~90°C for 15 minutes. Samples were removed and let cool after the 15 minutes. Then 5 ml of concentrated HNO_3 were added to each sample, watch glasses were replaced, and samples were returned to water batch to reflux for 30 minutes. No brown fumes were observed, so samples were left in water bath at 90°C ± 6°C for ~2 hours to evaporate. Standards and samples from Step 4 were run on ICP-OES under same conditions as earlier steps. After 2 hours, samples were removed from water bath and let cool. Then 2 ml of de-ionized water was added to samples, followed by 3 ml of 30% H_2O_2 to facilitate effervescence. Samples were returned to water bath and heated at 90°C ± 5°C for two hours. During the first hour, a total of 10 ml of H_2O_2 was added in 1 ml aliquots to each sample due to continued effervescence of the samples. After two hours, samples were removed from water bath and centrifuged, decanted and filtered as done in the previous steps. Final weights of samples were recorded, and samples were stored in refrigerator. Standards were made using same concentrations as other steps in a 10:13:7 HNO_3:H_2O_2:de-ionized water matrix and run along with samples in the ICP-OES.

After achieving desirable results from this preliminary run, the remaining ten samples from Beldanga core #2 were subjected to the same procedure. Larger volumes of extractant were prepared for each step to accommodate the increased number of samples. New standards were prepared to better fit expected values (based on results from 'trial run') for each element. Leachates were analyzed via ICP-OES both immediately following each step and the next day using the same standards.

Chapter 5 - Results

Sediment Characterization

Two distinct sediment types were observed in this study. Sediments west of river Bhagirathi were orange-brown in color and primarily fine- to medium-grain sand with the upper few meters capped by a silty-clay layer on both sites (Nabagram and Kandi). The silty-clay layer in Kandi was thicker than the upper silty-clay layer in Nabagram. The color of these Pleistocene-age sediments results from oxidation of their Fe-rich minerals (Fig. 9). East of river Bhagirathi, Holocene sediments were mostly light to dark grey in color, owing to the highly reducing environment in the subsurface (Fig. 10). The stratigraphy was comprised of alternating silty-clay and fine- to medium-grain sand, capped with ~3 m of clay and another ~8 m of silty clay just below the clay. In one of the study areas (Beldanga), a thin layer of light-brown colored sediment was observed ~30 m below ground level (Fig. 11). The grey sediments east of the river were all part of the present-day floodplains of Bhagirathi.

Presentation of all results throughout this section is described in terms of three operationally-defined depths within the sediment cores: shallow - < 15 m; intermediate - 15 to 25 m; deep - > 25 m.

Mineralogy and Chemistry of Sediment Cores

Petrographic analysis

Petrography of thin sections made from disintegrated sediments revealed several distinctions between high and low As sediments, as well as changes in texture and mineralogy with depth. Mineralogy of sediments in all areas was predominantly quartz (45-60%) and feldspar (18-25%), followed by micas (biotite and muscovite, 10-20%). Modes were obtained via visual estimations of thin sections and then averaged for all samples. Textures and the presence and proportions of micas, amphiboles, carbonates, oxides, and other accessory minerals were the major differences among the sediments.

Beldanga (high-As area): The textures of sediments varied with depth, while relative proportions of angular to sub-angular quartz (50-60%) and feldspars (18-25%) remained fairly constant throughout the entire core. Abundance of mostly lath-shaped and highly weathered biotite

and muscovite was more prominent in the shallower depths (15%), decreased slightly in intermediate depths (10%), and then increased in the deeper sediments (~15%).

At shallow depths, sediments were predominantly comprised of fine-grained materials with clay agglomerates containing angular grains of quartz (~55%) and feldspar (~20%), which had a sieve-like texture. Some grains had Fe-oxide coatings (Fig. 12A). Fe-mottling was present among some of the Fe-rich clay agglomerates. Within the matrix of these agglomerates, biotite (~6-8%) and muscovite (~12-14%) were observed, with carbonates > amphiboles > apatite > zircon > chlorite.

Sediments from intermediate depths were very fine-grained and had an abundance of fragmented quartz and feldspar grains, with a fairly significant amount of fine-grained, weathered micas. Fe-oxides constituted ~6-8% of identifiable grains, along with a few apatite and zircon grains randomly scattered throughout the fine-grained, Fe-rich clayey matrix (Fig. 12B).

Figure 10: Orange-brown sandy Pleistocene sediments from west of river Bhagirathi – Nabagram (low-As area).

Figure 9: Grey sandy, micaceous Holocene sediments from east of river Bhagirathi – Beldanga (high-As area).

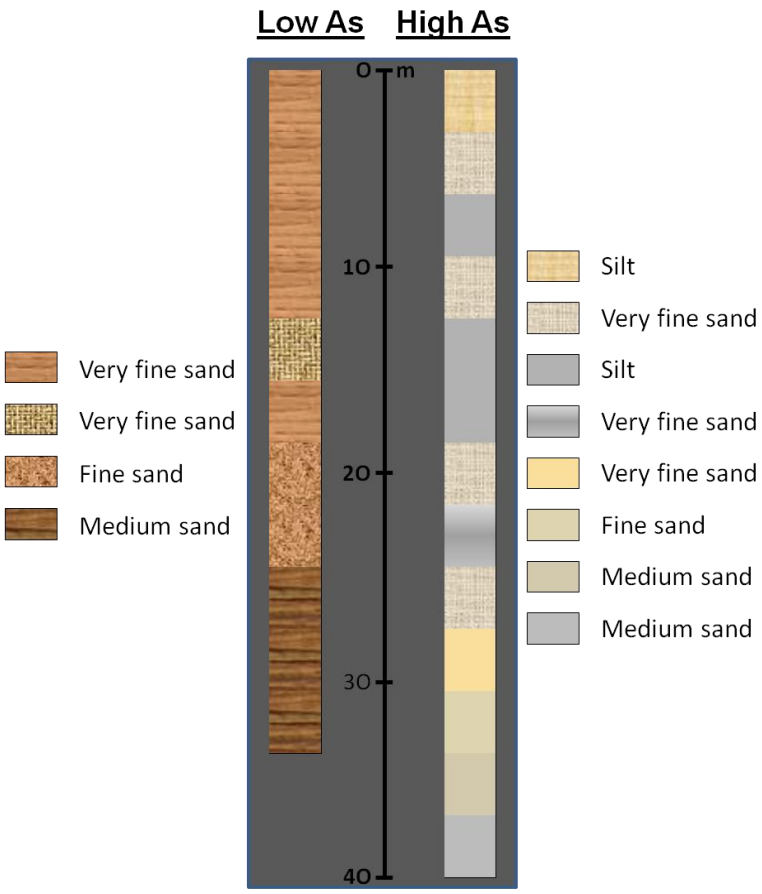

Figure 11: Wet sediment colors and textures of sediment cores from a low-As area (Nabagram) and a high-As area (Beldanga).

The texture of deeper sediments was generally coarse-grained, but also comprised of intermittent fine-grained material. More lath-shaped biotites and muscovites were included within the matrix of clay masses, where some clay agglomerates had outer rims of probable carbonate and/or iron-carbonate, and others had carbonate veins intersecting them (Fig. 12C). Fe-rich clays/coatings were observed on round, probable carbonate grains, along with flow-like structures encircling some of the other non-carbonaceous grains (Fig. 12D). Opaque minerals, presumed to be Fe-oxide or Fe-(oxy)hydroxides, constituted ~5 to 10% of the total mineral assemblage. Fine-grained, light-brown sandy sediments, constituted by a fair amount of Fe-oxide coated grains, with a significant amount of tiny, lath-shaped biotites and muscovites, were observed in one section. Several opaque Fe-rich grains were present as well, along with amphibole > chlorite > carbonates > apatite > zircon and rutile (Fig. 12E-H). *All photomicrographs are noted with PPL (plane-polarized light) or XPL (cross-polarized light).*

Hariharpara (high-As area): Petrographic analysis of another high-As area revealed similarities to those mentioned above in Beldanga sediments, and a few differences. Major similarities between the two cores were the relative proportions of quartz and feldspar, whose abundance varied slightly with depth throughout the whole core. Generally, mica contents (biotite, muscovite) were higher in Hariharpara than in Beldanga and remained relatively constant (~15%) throughout the entire core.

Sediments in the shallow depths were chiefly fine-grained. Numerous Fe-rich grains and micas were found in a gradation of colors from light yellowish-brown to dark brown to nearly black. A fine-grained matrix surrounded small, fragmented quartz and feldspar grains and small, weathered semi- lath-shaped micas (Fig. 13A). A significant amount of small apatite grains, with amphiboles, zircon, and a few carbonate concretions were randomly distributed within the sample.

In intermediate depth sediments where dissolved As concentrations were elevated, quartz and highly weathered feldspars constituted ~50% of the total mineral assemblage, and apart from that, weathered micas (~25%) and carbonates (~12%) dominated the mineralogy (Fig. 13B), with Fe-oxides ≈ amphiboles > apatite ≈ chlorite, and minor amounts of epidote, zircon and sphene.

Deeper sediments were medium to coarse sand. Mineralogy was comprised of ~65% quartz and feldspar, with ~15% micas (fairly large biotites and lath-shaped muscovites) and 15% carbonates (calcite, cements, grain coatings). Some Fe-oxides had a slight mottled appearance and in total constituted ~3-5% of all grains. Only a few amphiboles, apatite, chlorite, and epidote grains were identified in the deeper sediments.

Nabagram (low-As area): Core sediments were comprised of mostly Fe-stained/coated quartz and weathered feldspar (80%) with some micas (~12%) and Fe-oxides, and only a few accessory minerals were observed. No significant variation in texture/mineralogy with depth was observed in this core. Fe-oxide blobs were fairly abundant, occurring in various colors from light brown to black, which gave the sediments their overall brownish-orange color. Only a few individual grains of apatite, rutile and zircon were identified. No amphibole or chlorite was detected.

Kandi (low-As area): Sediments were dark brown in color with many variable-size clay agglomerates situated within a finer-grained matrix, which also encircled a few larger grains of quartz, feldspars, and Fe-oxides (Fig 14A). These dark brown Fe-rich clay agglomerates contained small quartz and feldspar fragments, but most grains were too fine to be identified. No depth-dependent variation was observed in this core except for iron leaching/mottling in the deeper sediments (Fig. 14B).

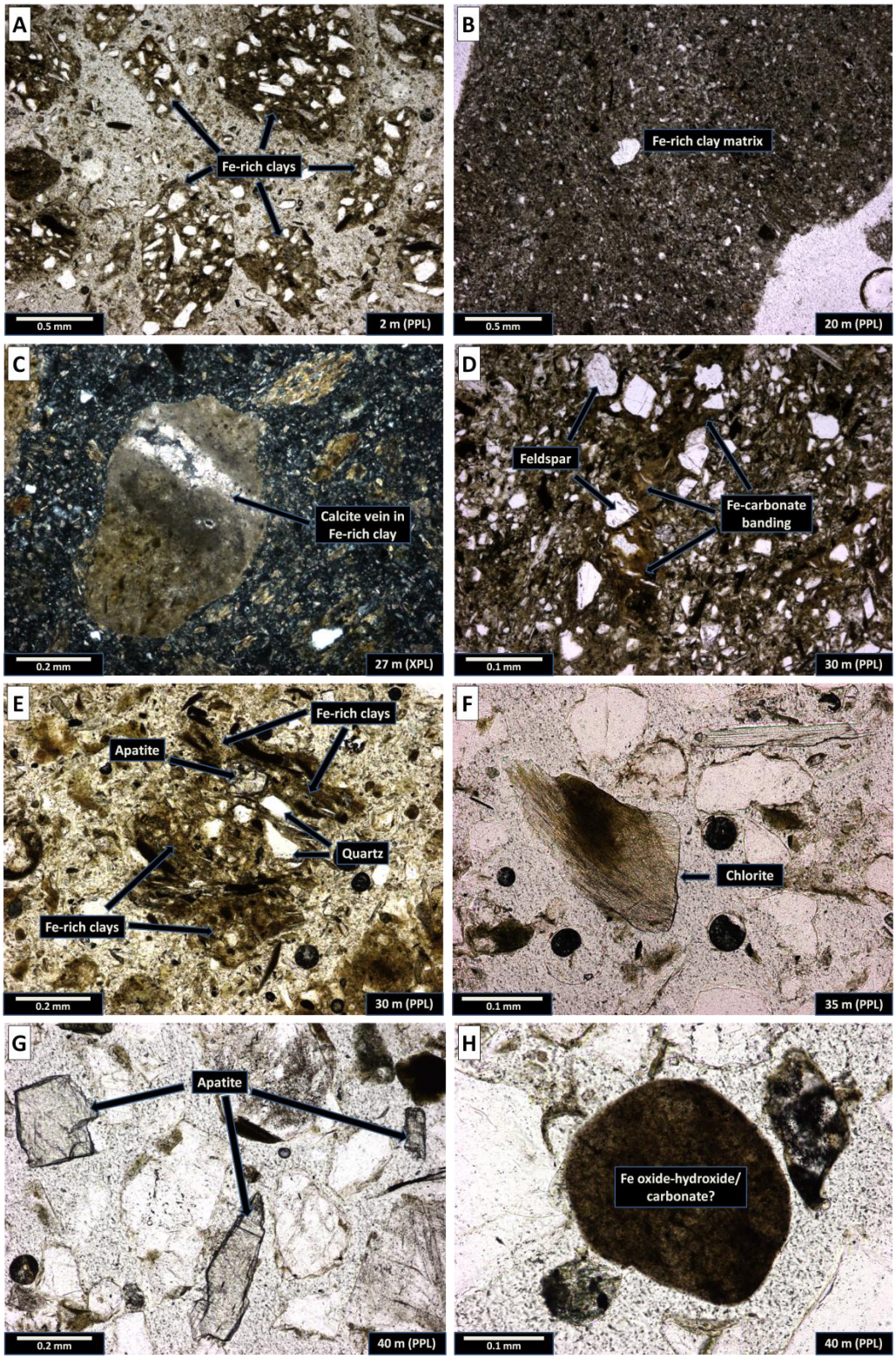

Figure 12: Photomicrographs showing dominant textures and mineralogy of sediment core from Beldanga (high-As area). Depth in lower right corner.

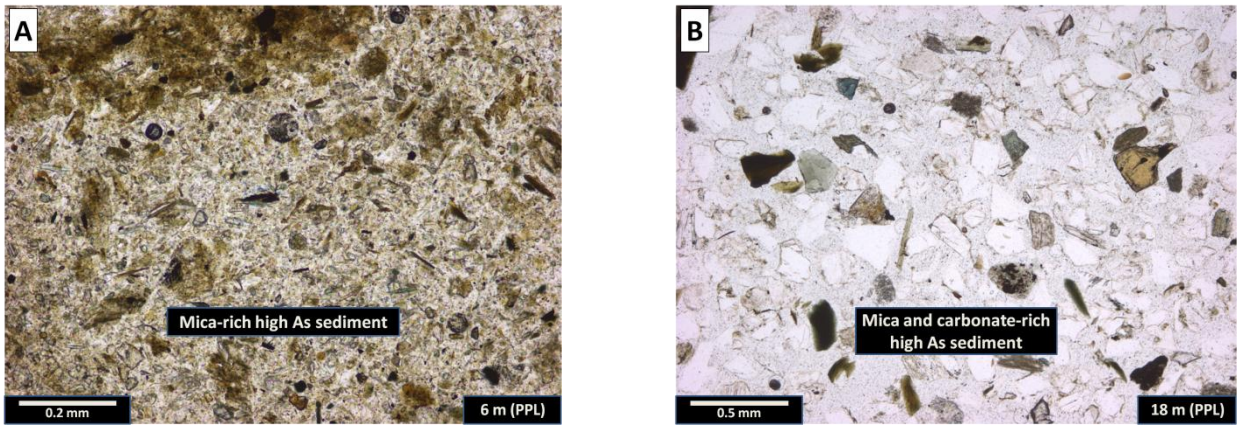

Figure 13: Photomicrographs of sediments from Hariharpara (high-As area). (A) High-As sediments rich in micas. (B) Carbonate- and mica-rich high-As sediments. Depth is in lower right corner.

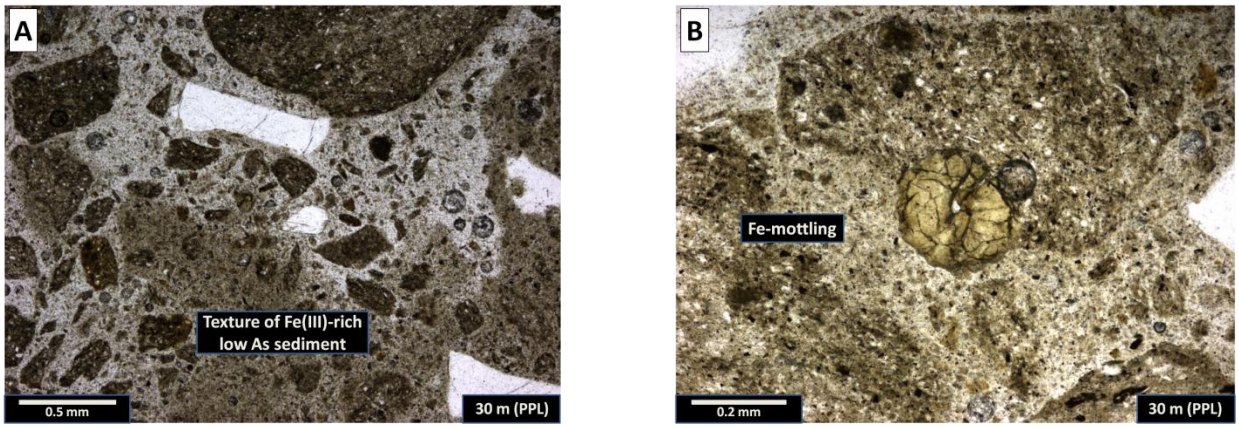

Figure 14: Photomicrographs of sediments from Kandi (low-As area). A. Iron mottling in low-As sediments. B. Fine-grained Fe(III)-rich low-As sediments. Depth is in lower right corner.

Scanning Electron Microscope Study with Energy Dispersive X-ray Spectra

Solid phase whole sediment analysis from shallow to deep aquifer sediments by scanning electron microscopy (SEM) revealed several key features of sediments from an area with high arsenic. A majority of the clay minerals detected were kaolinite. In Beldanga, the total Mg content in clays increased with depth from shallow to deep within the core (Fig. 15). Clays or fine-grained micas rich in Fe, K, and Mg, were observed in the deeper aquifer sediments. Also, copper was detected in the deepest part of the core, along with Fe, C, and silica.

Most grains from Hariharpara that were analyzed for elemental composition were alumino-silicates with minor amounts of Fe and K.

Nabagram sediments were predominantly angular quartz and feldspars.

No As was detected in any of the grains analyzed by SEM.

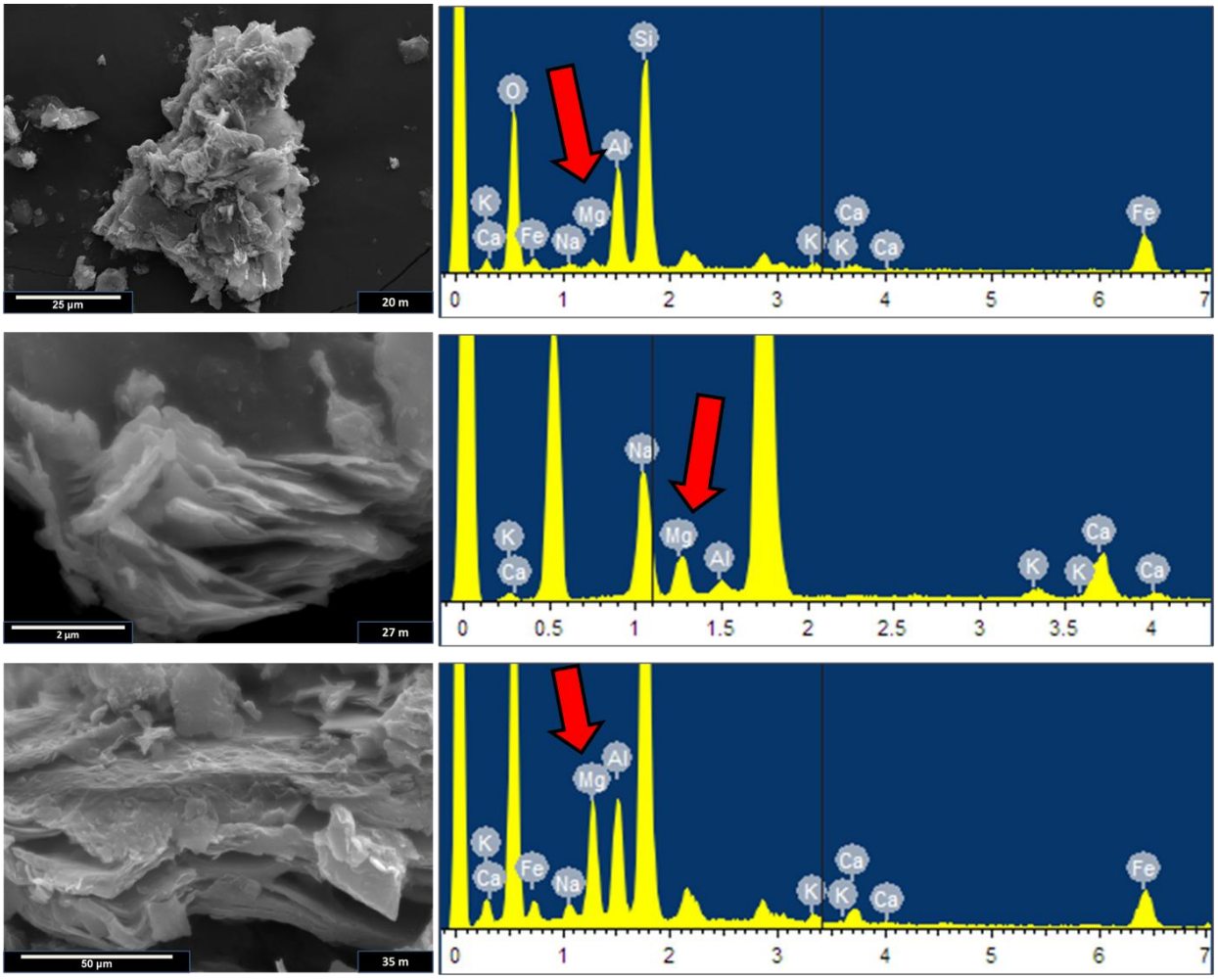

Figure 15: SEM photomicrographs of Beldanga (high-As area) clays; spectra showing elemental proportions on right.

X-Ray Fluorescence

Hand-held X-ray fluorescence (XRF) analysis of sediment cores from Beldanga, Hariharpara, and Nabagram revealed several relationships. The XRF detection limit for As was 11 ppm.

Beldanga: In core #2, As concentrations ranged from 2 to 18 ppm, with major peaks in concentration in shallow (6 m), and deep (27 and 40 m) sediments. Fe (7168 to 43,683 mg/kg) followed a similar pattern in changes with depth as As, from shallow to intermediate depths. K (8565 to 20,067 mg/kg) had a similar pattern with depth as As throughout the entire core (shallow to deep). No relationship was observed between As and Mn (146 to 678 mg/kg). Ca concentrations (3038 to 25,283 mg/kg) varied inversely with As throughout the majority of the core. Cr concentrations in the sediments varied from 0 to 95 mg/kg; Uranium concentrations ranged from 0 to 20 mg/kg; and Cu and Zn concentrations ranged from 0 to 52 mg/kg and 20 to 89 mg/kg, respectively. Depth patterns for Cr, U, Cu, Zn and As were very similar throughout the entire core (Fig. 16).

Hariharpara: Arsenic concentrations in the sediment ranged from 0 to 13 ppm throughout the entire core. In shallow sediments, As concentration averaged ~10 ppm, then decreased to < 2 ppm in the intermediate depth and deeper sediments. Fe and Mn ranged from 5954 to 38,733 mg/kg and 97 to 559 mg/kg, respectively, and followed the same pattern of variations in concentration with depth as arsenic. K (6979 to 17,567 mg/kg) and generally Ca (4636 to 30,150 mg/kg) concentrations followed a depth trend similar to arsenic. Cr concentrations in these sediments were high (16 to 77 mg/kg). U concentrations ranged from 3 to 22 mg/kg and showed no real relationship with arsenic. Similar to Beldanga, Cr, Cu (1 to 39 mg/kg), and Zn (11 to 64 mg/kg) displayed nearly identical patterns with depth, and were comparable to the As depth trend in these sediments (Fig. 17).

Nabagram: Elemental concentrations in these low-As sediments were significantly different than the high-As sediments. No As was detected via XRF in the orange-brown sediments. Overall, values for Fe (8330 to 24497 mg/kg), Mn (141 to 306 mg/kg), K (7637 to 12525 mg/kg), and Cu (0 to 32 mg/kg) were much lower in these low-As sediments compared to high-As sediments in Beldanga and Hariharpara. Cr and U had relatively the same range of values as in Hariharpara sediments. Zinc was slightly higher (18 to 58 mg/kg) than in Hariharpara, but similar to Beldanga sediments. Copper was detected at only two depths in the shallow sediments (Fig. 18).

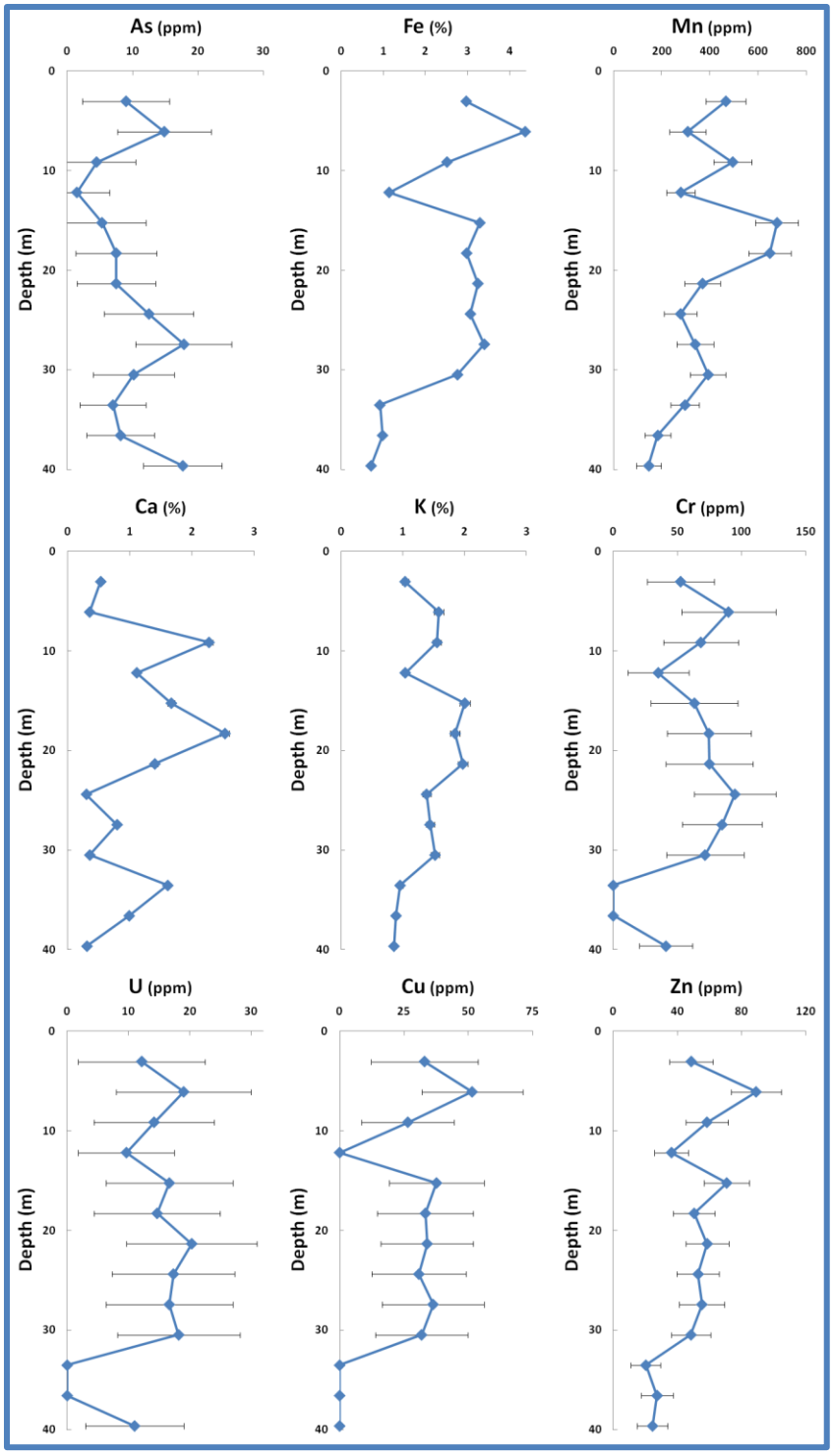

Figure 16: Major and trace element concentrations, in mg/kg or wt%, with depth in a sediment core from Beldanga (high-As area) measured by XRF. Horizontal lines represent ±2σ standard deviation from XRF analysis.

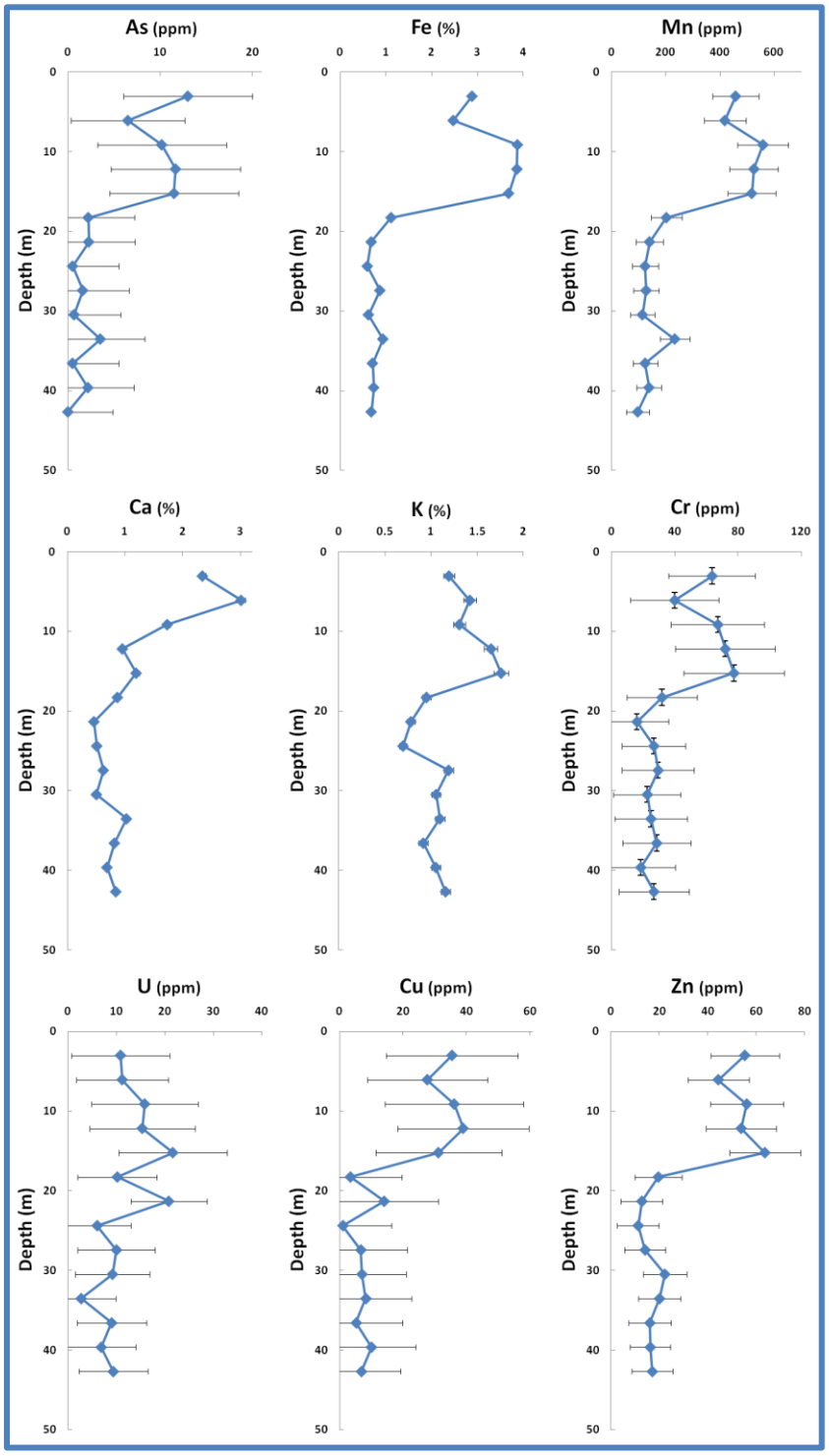

Figure 17: Major and trace element concentrations, in mg/kg or wt%, with depth in a sediment core from Hariharpara (high-As area) measured by XRF. Horizontal lines represent ±2σ standard deviation from XRF analysis.

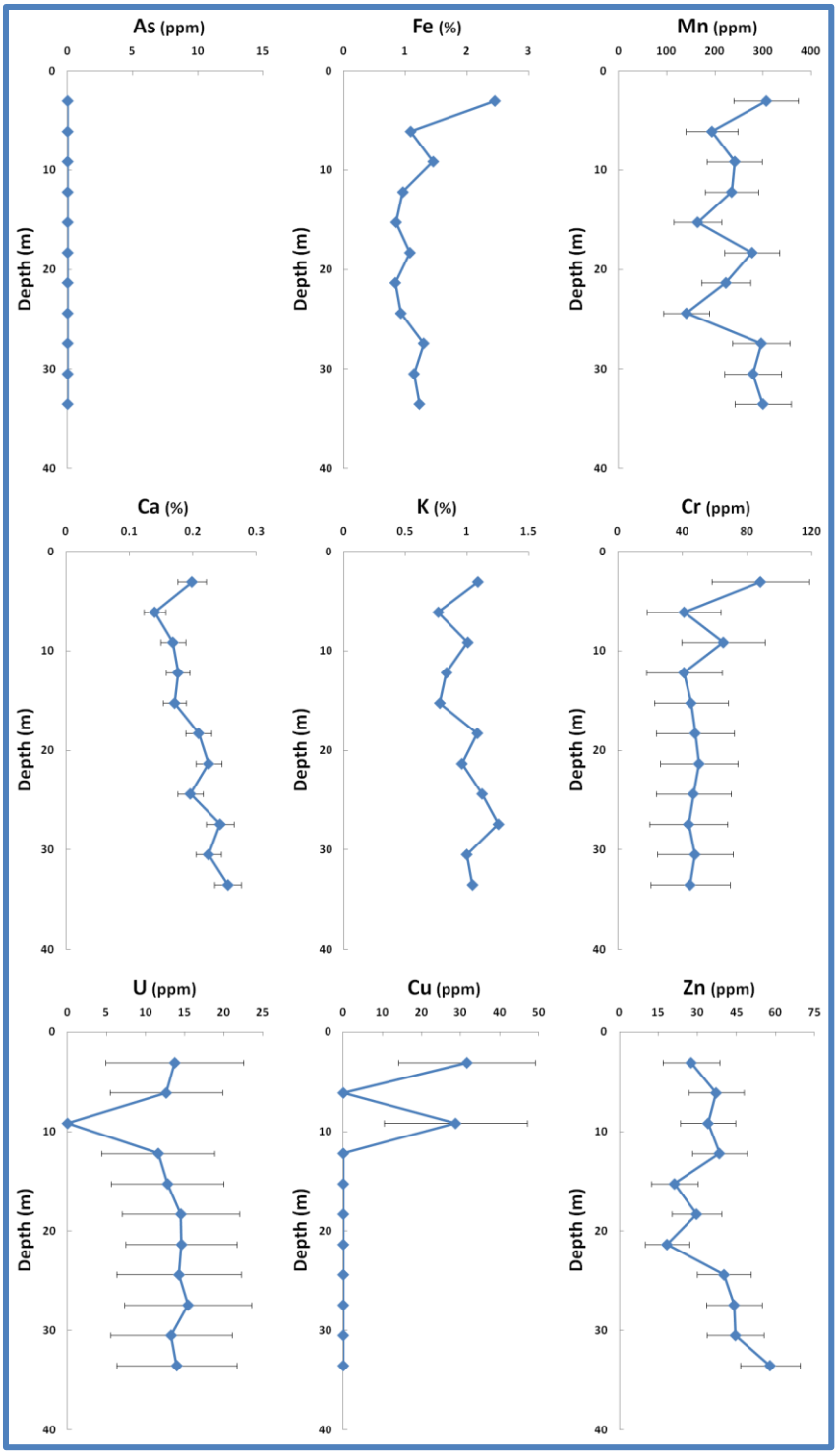

Figure 18: Major and trace element concentrations, in mg/kg or wt%, with depth in a sediment core from Nabagram (low-As area) measured by XRF. Horizontal lines represent ±2σ standard deviation from XRF analysis.

Iron Speciation and Phosphate in 'High-As' Sediments

Results for ferrous iron, total iron, and HCl-leachable phosphate values in sediments from Beldanga core #1 are presented here. Ferrous iron to total iron ratios for Beldanga core #1 generally ranged from 0.7 to 1 throughout the entire core, with one exception at 33 m, which had a ratio of 0.4 (Fig. 19). No consistent increase or decrease in Fe(II):Fe_T with depth was observed in this core.

In shallow sediments, phosphate concentrations increased with increasing Fe(II):Fe_T, then varied inversely with Fe(II):Fe_T throughout the intermediate depth and deeper sediments. Fe(II) concentrations generally decreased through the intermediate and deeper sediments, with the exception of one sharp increase in the deep sediments at 27 m (Fig. 20).

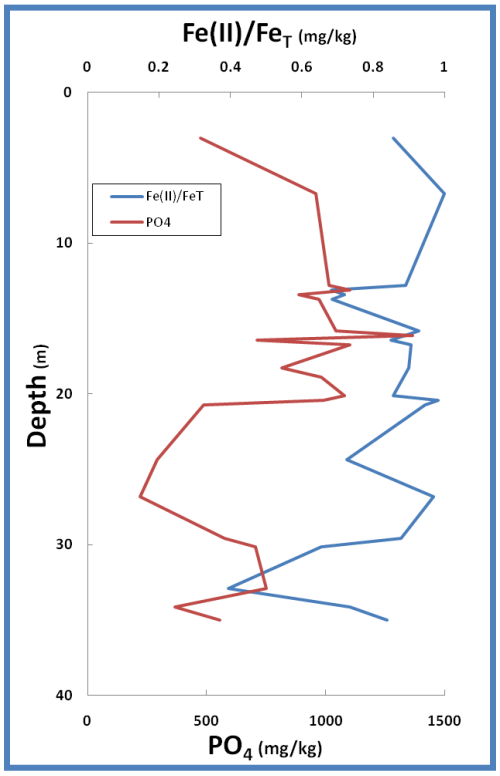

Figure 19: Fe(II):Fe_T ratio and phosphate concentrations with depth in sediment core from Beldanga (high-As area).

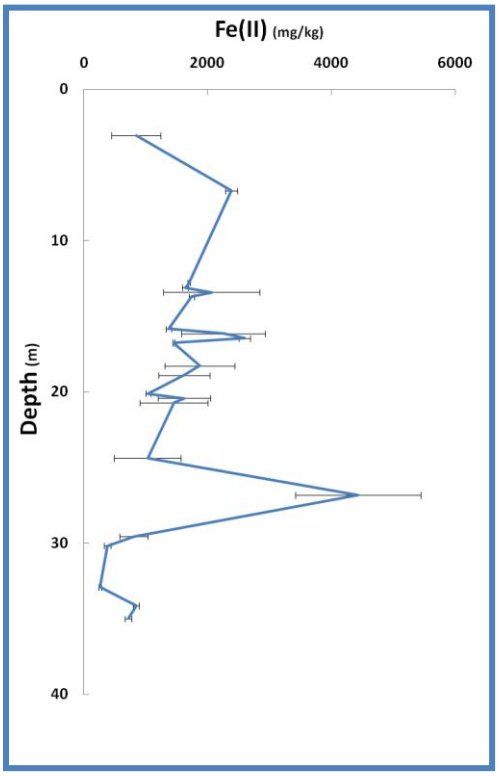

Figure 20: Fe(II) concentrations with depth in sediment core from Beldanga (high-As area). Horizontal lines represent standard deviation of two analyses by HR-ICP-MS.

Aqua Regia Digestion

Total digestion of sediments by aqua regia (Zarcinas et al. 1996) from Beldanga core #2 (Fig. 21) and Nabagram core #2 (Fig. 22) exhibited several correlations between As concentrations and concentrations of other elements. Correlations presented here all have confidence intervals > 95%.

Arsenic in Beldanga sediments showed some variations with depth. Arsenic concentrations of shallow and intermediate depth sediments were ~10 mg/kg, but increased to 18 mg/kg in the deeper sediments. Zn and Ca had the strongest positive correlations to As with $r^2 = 0.64$ and 0.59, respectively. Mn and Pb had weaker positive correlations to As with $r^2 = 0.31$ and 0.23, respectively. K and Mg had respective $r^2 < 0.16$ and 0.10. Al, Fe and Cu showed no real correlation with arsenic.

Shallow sediments (3 and 9 m) in Nabagram were found to have ~4 mg/kg As, while intermediate (18 m) depth and deeper (27 and 33 m) sediments all had As in the ~1 mg/kg range. Mn, Ca, Mg, and Zn all had negative correlations with As in the orange-brown sediments. Cu, Al, Pb, and Fe all had strongly to fairly significant r^2 values (0.91, 0.90, 0.71, 0.47, respectively), with 95% confidence interval. K showed no real correlation with As in these sediments.

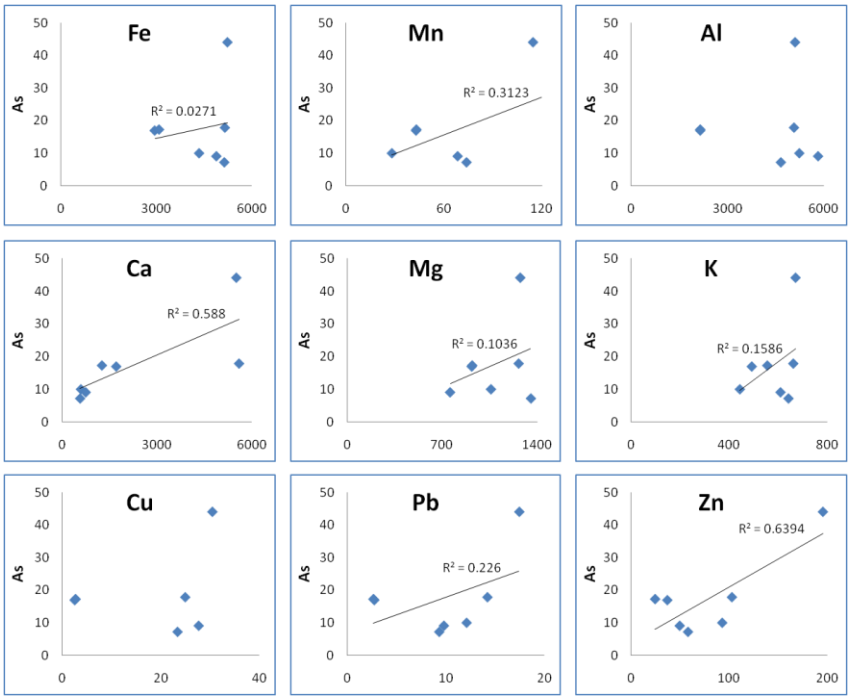

Figure 21: Specific element correlations with As in Beldanga core sediments (high-As) after aqua regia digestion and measurement by ICP-MS. All values reported in mg/kg.

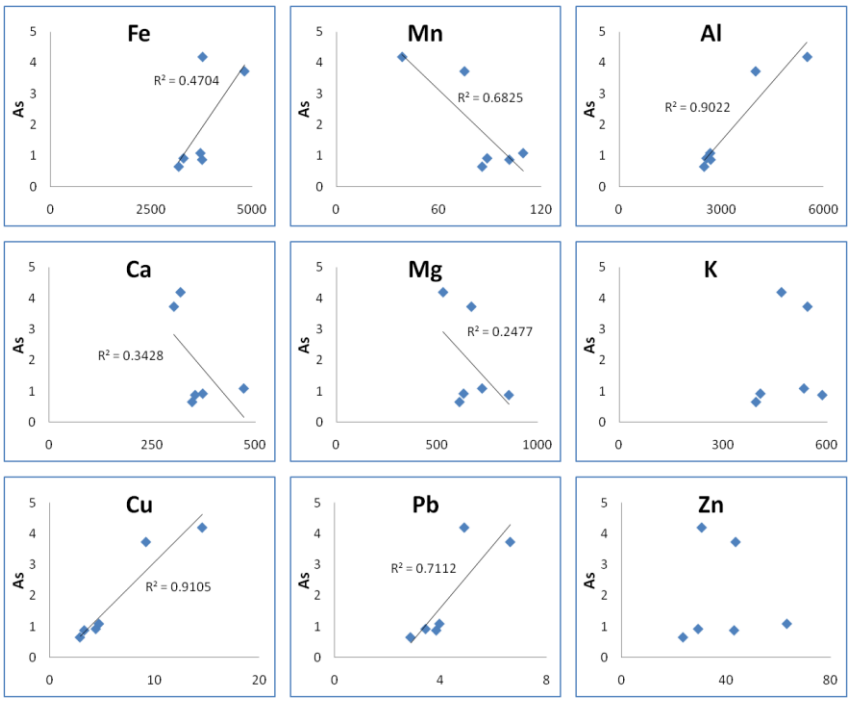

Figure 22: Specific element correlation with As in Nabagram core sediments (low-As) after aqua regia digestion and measurement by ICP-MS. All values reported in mg/kg.

Sequential Extraction Analysis

Sequential extractions were performed only on a high-As sediment core (Beldanga core #2). Results from sequential extractions of this core showed relative proportions in which As, Mn, and Fe are partitioned in various fractions in the sediments (Fig. 23, 24): non-specifically sorbed, specifically sorbed, amorphous and poorly crystalline hydrous oxides of Fe and Al, well crystallized hydrous oxides of Fe and Al, and residual minerals (e.g. quartz and feldspar). Comparison of leachates analyzed both immediately following each step and the next day using the same standards revealed nearly identical results for Mn and Fe, while there were a few variations with As values, especially for phases using $NH_4H_2PO_4$ and NH_4^+-oxalate buffer. It was concluded that for low concentration elements like As, specific sequential extraction steps should be dealt with using extra precaution and validation. For interpretation purposes, only the values measured immediately following completion of each step are reported here.

In the shallow sediments, a negligible amount (< 1%) of easily-exchangeable As was detected, while 26% of total As was P-extractable. A significant portion of As was associated with Fe hydroxides: ~23% for amorphous and poorly crystalline phases and ~20% for well-crystallized phases, while nearly 30% was in the residual phase. Approximately 6% of total Mn was found in the easily-exchangeable phase, and 9% of total Mn was in the P-extractable phase. In the amorphous and poorly-crystalline Fe hydroxide phase was 26% of the Mn, and only 17% Mn was locked in the well-crystallized phases of the hydroxides. No Fe was detected in either of the sorbed phases, while 19% and 29% of the total Fe were in the amorphous/poorly-crystalline phase and the well-crystallized phase, respectively. The remaining 52% of Fe was in the residual phase.

Sediments at intermediate depth had no easily exchangeable As, but 17% of total As was P-extractable. 26% and 13% of total As were associated with the amorphous/poorly-crystalline Fe hydroxide and well-crystallized phases, respectively, with 43% in the residual phase. Sorbed Mn accounted for ~8% of total Mn, while a major portion (30%) was associated with amorphous/poorly-crystalline Fe hydroxides, and only 5% with well-crystallized Fe hydroxides. No sorbed Fe was detected, so 29% was in amorphous/poorly-crystalline Fe hydroxides and 12% in well-crystallized Fe hydroxide phases.

Deep sediments showed the majority of the total As was in the P-extractable (~29%) and amorphous/poorly-crystalline Fe hydroxides (33%), while 16% was in the well-crystallized Fe hydroxides. The majority of Mn was in the residual phase (62%), ~10% was P-extractable, and the Fe hydroxide phases combined for 21% of total Mn. Fe was not detected in the sorbed phases. The amorphous/poorly-crystalline Fe hydroxide phase accounted for 14% total Fe, and the well-crystalline phase housed 17% of the total Fe concentration.

The total As concentrations for the sum of As concentrations from each of the five sequential extraction steps were all in good agreement with total As concentrations measured by ICP-MS from digestion by aqua regia and As concentrations measured by hand-held XRF (Fig. 25).

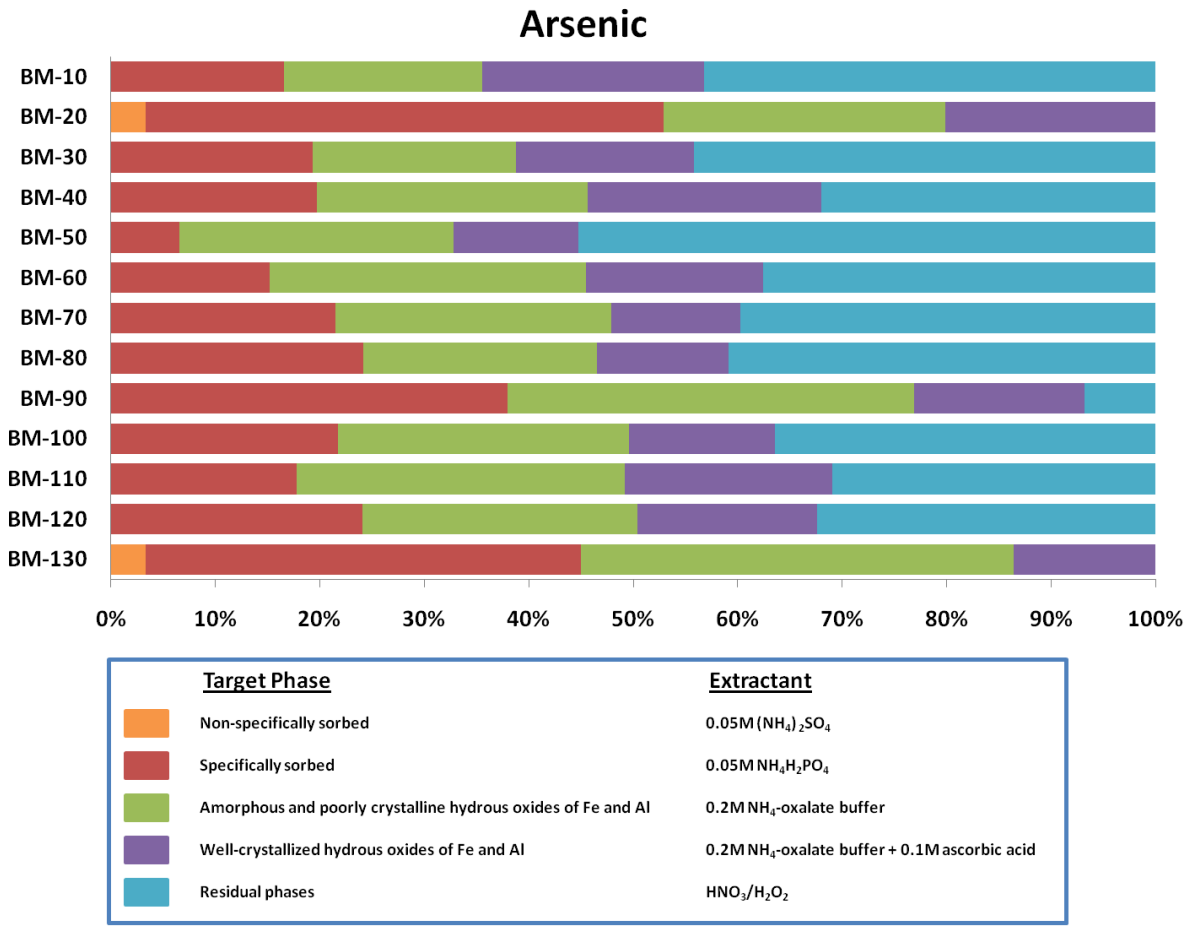

Figure 23: Partitioning of As among different fractions of sediments from an entire sediment core in Beldanga. Sediment depths ranged from ~3 m (10 ft) to ~40 m (130 ft) (e.g BM-10 = 10 ft (~3 m) depth; BM-130 = 130 ft (~40 m) depth).

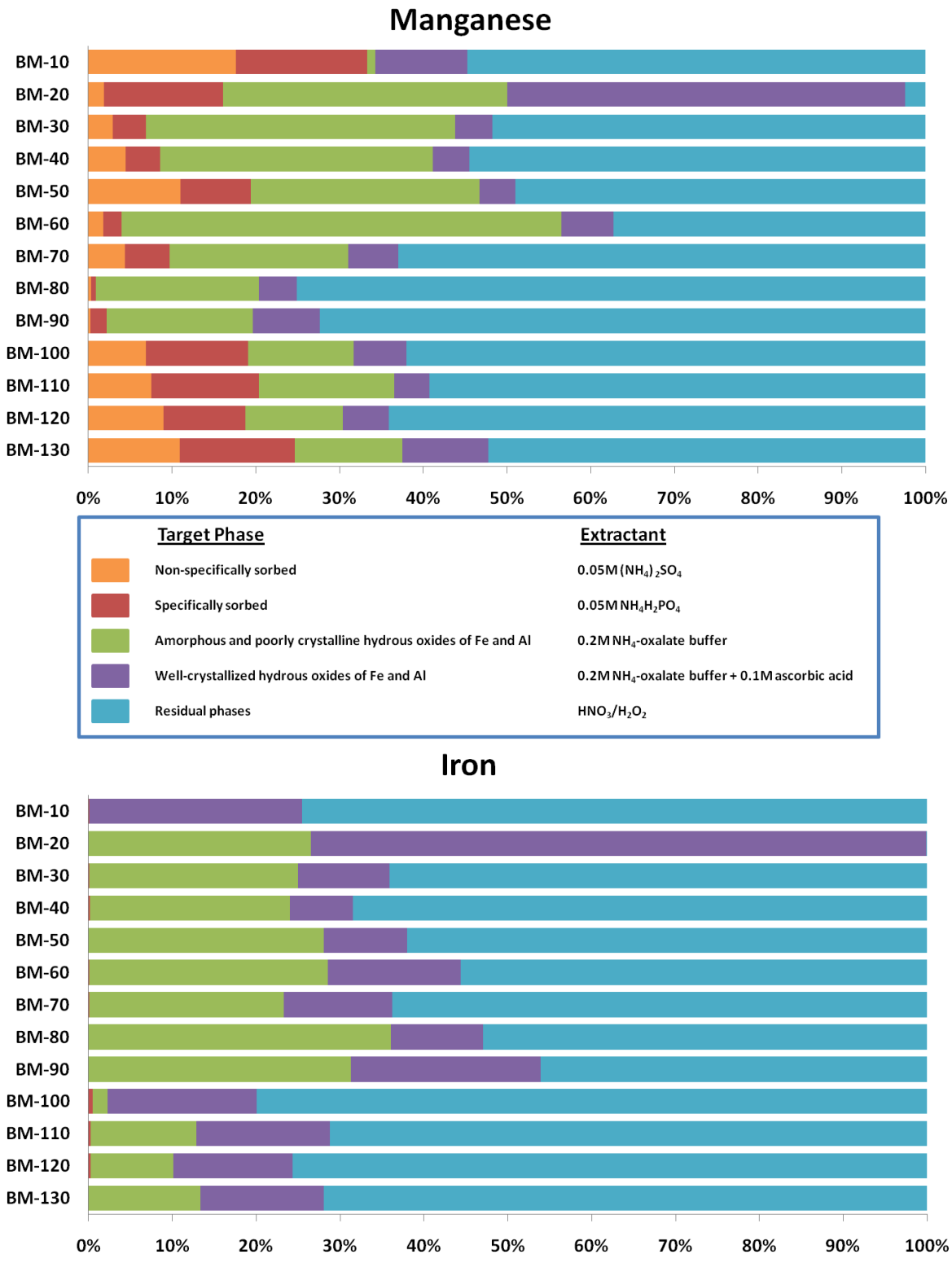

Figure 24: Partitioning of Mn (top) and Fe (bottom) among different fractions of sediments from an entire sediment core in Beldanga. Depths ranged from ~3 m (10 ft) to ~40 m (130 ft).

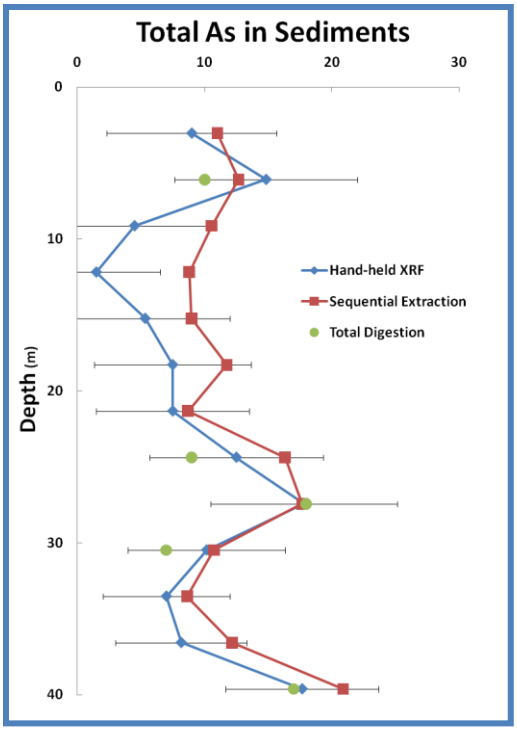

Figure 25: Comparison of total As concentrations measured by hand-held XRF, total digestion, and sequential extractions on sediment cores.

Water Chemistry

Field Analyses

HACH® Hydrolab® Results

Water samples collected in areas with high dissolved As concentrations (Beldanga, Hariharpara) in January 2010 had pH values at or near neutral range (Beldanga: [6.97 to 7.10]; Hariharpara: [6.87 to 7.04]). In areas with low dissolved As, pH values were distinctly above (Kandi: [7.3 to 7.7] and below (Nabagram: [6.4 to 7]) pH values for Beldanga and Hariharpara.

Conductivity of high-As waters in Beldanga ranged from 724 to 810 μS/cm and in Hariharpara ranged from 765 to 868 μS/cm. Low-As waters in Kandi had conductivity much higher (1358 to 1442 μS/cm) than Beldanga and Hariharpara, while Nabagram, another low-As area, had the lowest values (447 to 760 (μS/cm). Total Dissolved Solids (TDS) values for Beldanga and Hariharpara (463 to 518 mg/l and 489 to 555 mg/l, respectively) were higher than TDS values for Nabagram (286 to 486 mg/l), but much lower than TDS values for Kandi (869 to 923 mg/l).

Dissolved oxygen (DO) for high-As waters in Beldanga ranged from 2.3 to 4.0 mg/l, and from 3.2 to 4.7 mg/l in Hariharpara. DO values for low-As waters in Nabagram were in the range of 2.4 to 4.1 mg/l, and for low-As waters in Kandi, DO values were 2.6 to 4.9 mg/l.

Redox potential varied widely in Beldanga (67 to 388 mV) and somewhat less in Hariharpara (57 to 83 mV). Values for Nabagram were relatively higher (166 to 407 mV) and fairly low (32 to 310 mV) for Kandi (Fig. 26).

Field Test Kit Results

Waters with high cocnetrations of dissolved As were relatively high in HCO_3^- (Beldanga: [290 to 405 mg/l]; Hariharpara: [350 to 450 mg/l]). Less HCO_3^- (110 to 275 mg/l) was observed in low to no As waters in Nabagram. Kandi waters had low As concentrations and relatively high HCO_3^- values (400 to 500 mg/l).

Ammonium (NH_4^+) values for groundwaters were higher in areas with high As than in areas with low or no As. Beldanga waters had NH_4^+ concentrations of 0.2 to > 2 mg/l (with exception of one well in which no NH_4^+ was detected), and waters in Hariharpara ranged from 0.65 to 1.5 mg/l of NH_4^+. No NH_4^+ was detected in any of the wells sampled in Nabagram and Kandi.

In Beldanga groundwaters, HACH® Arsenic Field Test Kit showed two wells with high dissolved As (~50 µg/l, ~70 µg/l) and 2 wells with very high dissolved As (> 500 µg/l), and one well with low As (0 µg/l). Hariharpara had three wells with As concentrations greater than the maximum contaminant level of 50 µg/l (~70 µg/l, 70 to 300 µg/l, > 500 µg/l). In Nabagram, no As was detected by the field test kits. Kandi had four wells with dissolved As concentrations ~10 µg/l, one < 10 µg/l, and two with 0 µg/l.

Phosphate values for high-As waters were greater than phosphate values for low As waters. Hariharpara showed the highest phosphate of all the sites (2.4 to 4.1 mg/l), while Beldanga had a wider range (0.2 to 3 mg/l) of phosphate values. Both Nabagram and Kandi had much lower values of phosphate (0.2 to 1.1 mg/l and 0.5 to 1.2 mg/l, respectively) than the high-As waters of Beldanga and Hariharpara (Fig. 27).

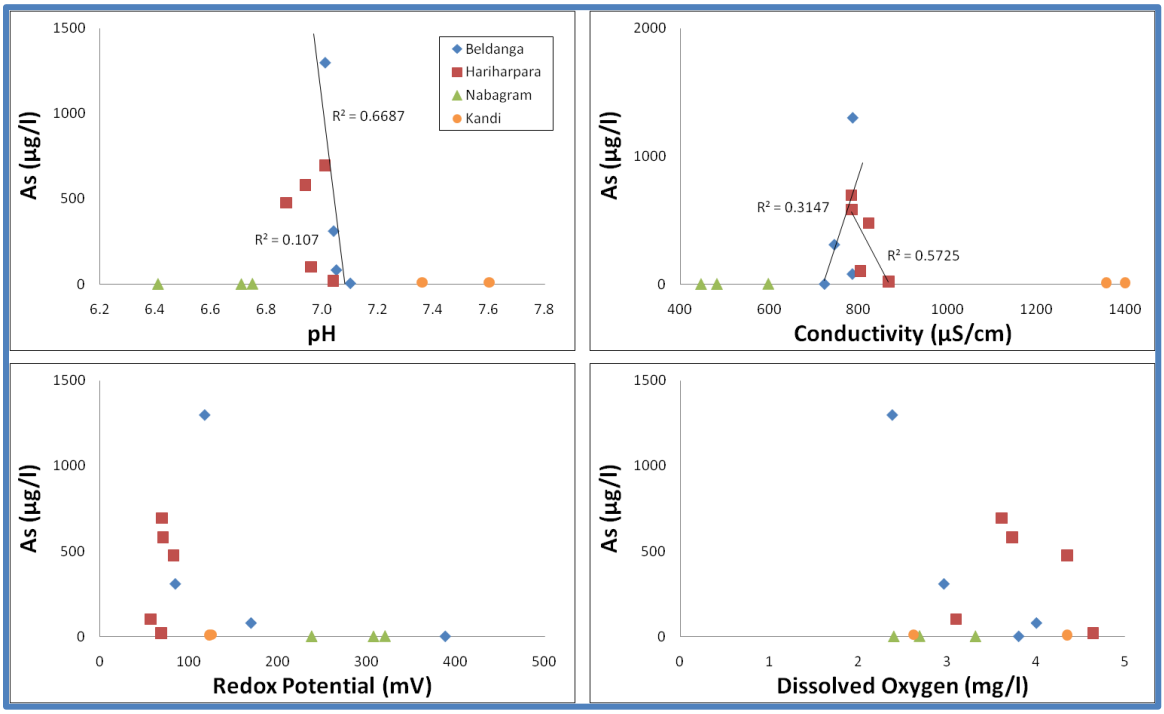

Figure 26: Water quality parameters plotted versus total dissolved As concentrations.

Figure 27: Values for alkalinity (top), ammonium (middle), and phosphate (bottom) concentrations of water samples plotted by tubewell number-location. All tubewells labelled with 'BM' and 'HK' are from the high-As areas, and tubewells labelled with 'NB' and 'KHN' are from low-As areas.

Laboratory Analyses

Total Arsenic and As(III) Analysis

Dissolved arsenic concentrations ranged from 0 to 3 μg/l and 0 to 11 μg/l in areas sampled west of river Bhagirathi (Nabagram and Kandi, respectively). East of Bhagirathi, As levels spanned a much wider range: 0 to 4622 μg/l in Beldanga, 19 to 695 μg/l in Hariharpara, 6 to 649 μg/l in Jalangi, and 3 to 641 μg/l in Naoda.

Shallow (< 60 m) groundwaters contained a wide range of dissolved As concentrations, which was highly spatially variable. In Beldanga, groundwater As levels from different wells screened at the same depth in the aquifer varied from 0 to > 4000 μg/l within a lateral distance of ~50 m (Fig. 28). Dissolved As concentrations in Hariharpara (and Jalangi and Naoda) varied laterally from < 50 μg/l to > 600 μg/l over a vertical distance of ~25 m (Fig. 29).

In Nabagram, dissolved As concentrations in groundwaters were 3 μg/l or less at similar depths (Fig. 30). Groundwaters from Kandi had low dissolved As concentrations in groundwaters. The maximum As concentration was 11 μg/l.

Deep (> 60 m) groundwaters were collected from four different wells (64 m (n=2) (Jalangi), 91 and 137 m (Naoda)), and their total dissolved As concentrations were 6, 37, 24, and 52 μg/l, respectively. The majority of the occurrence of elevated dissolved As concentrations in groundwater in this study was found in wells screened in the upper 50 m of the aquifer (Fig. 31). This is a typical bell-shaped curve of dissolved As concentrations at shallow depths that is a very common and consistent observation throughout the Bengal Basin.

Speciation of As done for 15 samples in the field (measured in the lab) revealed the dominant species to be As(III). As(III):As_T ranged from 0.55 to 0.98 for wells east of Bhagirathi, with an average ratio of 0.74 (Fig. 32). West of Bhagirathi, one well on which As speciation was done contained only 36% As(III). Overall, total dissolved As (and As(III)) concentrations increased from west to east.

Figure 28: Map of Beldanga (high-As area) showing the heterogeneity of lateral distribution of dissolved arsenic concentrations in groundwater. Arsenic concentrations (µg/l) are in red; tubewell depths (m) are in black in parentheses. Yellow circles indicate sampled tubewells where As concentrations were measured. Small green circles indicate sampled wells whose As concentrations have not yet been measured. Large red circles represent locations where subsurface sediment cores were collected.

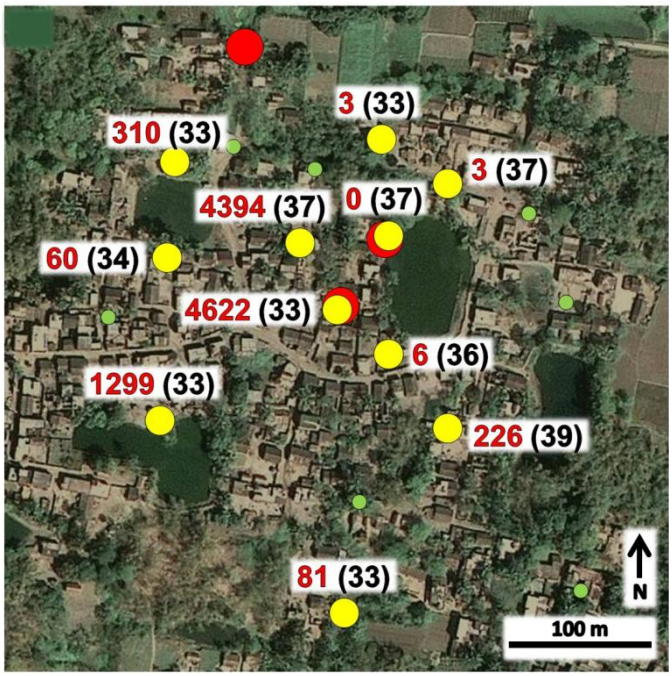

Figure 29: Map of Hariharpara (high-As area) showing heterogeneity of lateral and vertical distribution of dissolved arsenic concentrations in groundwater. Arsenic concentrations (µg/l) are in red; tubewell depths (m) are in black in parentheses. Yellow circles indicate sampled tubewells where arsenic concentrations were measured. Small green circles indicate sampled wells whose As concentrations have not yet been measured. Large red circles represent locations where subsurface sediment cores were collected.

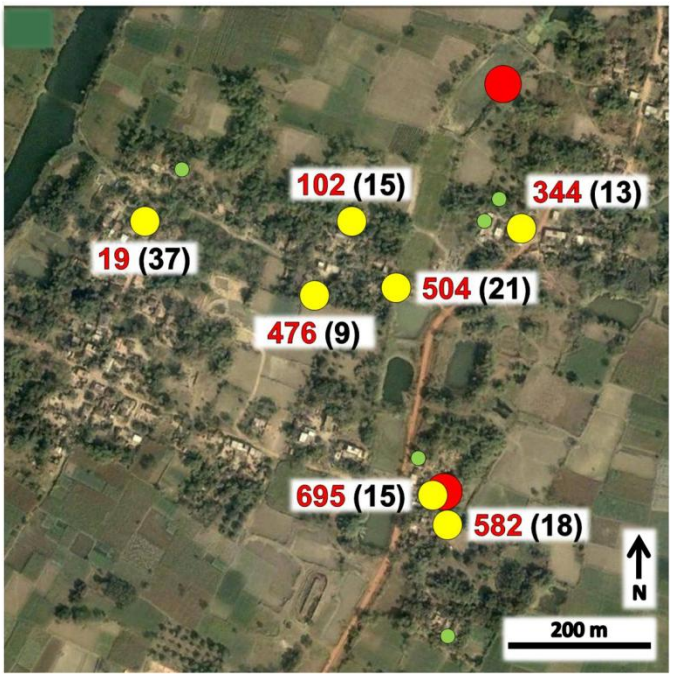

Figure 30: Map of Nabagram (low-As area) showing heterogeneity of lateral and vertical distribution of dissolved arsenic concentrations in groundwater. Arsenic concentrations (µg/l) are in red; tubewell depths (m) are in black in parentheses. Yellow circles indicate sampled tubewells where arsenic concentrations were measured. Small green circles indicate sampled wells whose As concentrations have not yet been measured. Large red circles represent locations where subsurface sediment cores were collected.

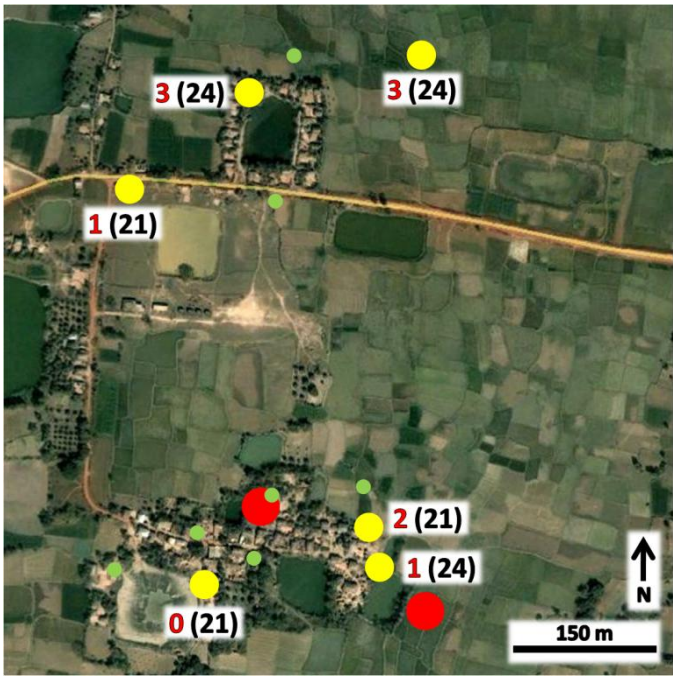

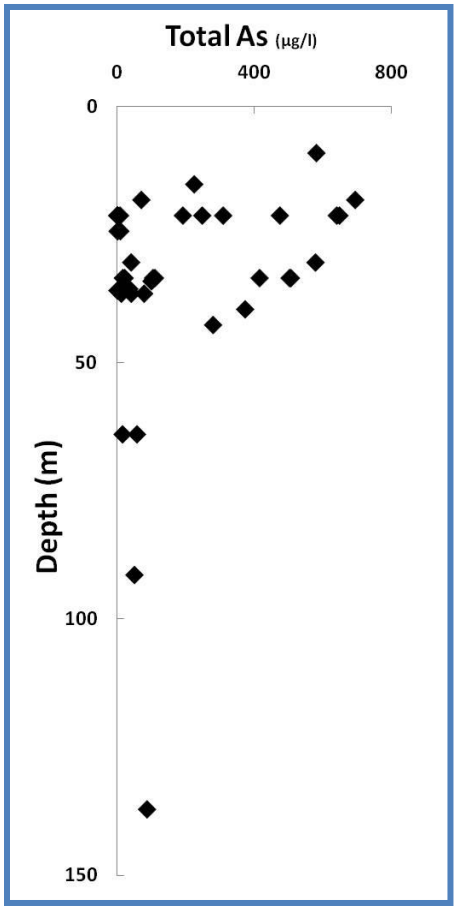

Figure 31: Concentrations of total dissolved As (µg/l) in groundwater plotted against depth (m). Major occurrence of dissolved As in groundwater is at depths < 50 m, which is a common phenomenon throughout the Bengal Basin.

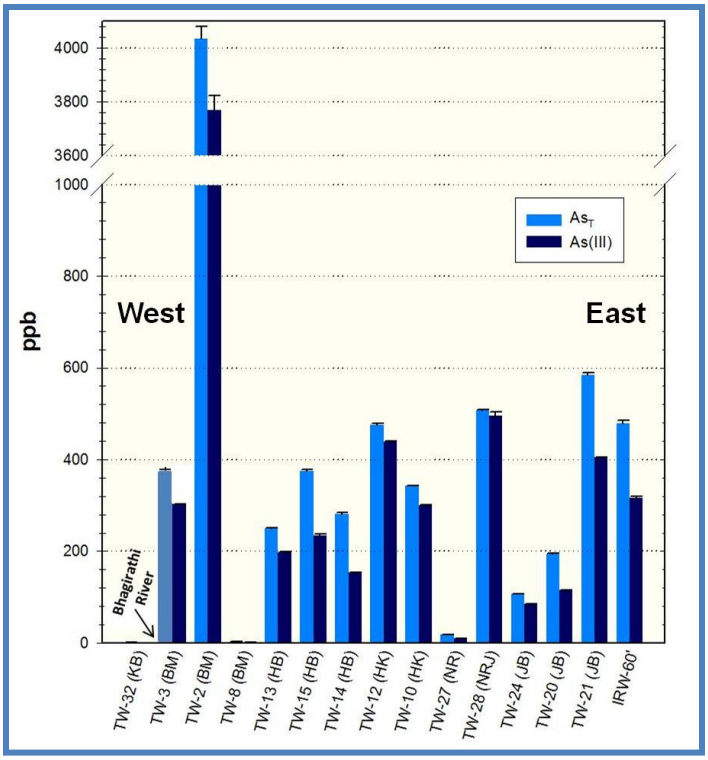

Figure 32: Total dissolved As (As_T) and As(III) concentrations (ppb (µg/l)) in groundwaters from 14 tubewells and one shallow irrigation well from Murshidabad. As_T in groundwater collected west of river Bhagirathi was < 1 µg/l (36% As(III)).

General Groundwater Parameters – Conductivity, TDS, DO, Alkalinity, Phosphate

Conductivity varied widely among the villages and within the villages. In Beldanga, conductivity fell within a fairly narrow range of values (755 to 833 μS/cm), as opposed the other villages which showed different values, like Hariharpara (608 to 1108 μS/cm), Jalangi (785 to 1066 μS/cm), and Naoda (717 to 1457 μS/cm). Conductivity in Nabagram waters varied from 454 to 1153 μS/cm. Conductivity of the pondwater in Hariharpara had a much lower value (198 μS/cm) than the pond water in Jalangi (909 and 709 μS/cm). Four of the five river waters ranged from 211 to 235 μS/cm in conductivity, while one river water sample measured 831 μS/cm.

TDS for high-As waters in Beldanga ranged from 339 to 385 mg/l, Hariharpara ranged from 283 to 515 mg/l, Jalangi ranged from 388 to 494 mg/l, and Naoda ranged from 357 to 710 mg/l. TDS in low-As waters of Nabagram ranged from 218 to 561 mg/l. Pond water from Hariharpara had a low TDS value of 97 mg/l, while the two pond waters in Jalangi had much higher TDS values (345 and 443 mg/l). TDS of river waters ranged from 103 to 114 mg/l.

DO was fairly high for high-As waters in Beldanga, Hariharpara, Jalangi, and Naoda (7.09 to 8.85 mg/l; 7.59 to 8.68 mg/l; 4.64 to 8.69 mg/l; 8.40 to 8.74 mg/l, respectively), DO values for Nabagram ranged from 6.28 to 8.83 mg/l. The Hariharpara pond had higher DO at 7.73 mg/l, while the two Jalangi pond waters had 3.21 and 2.27 mg/l. River waters had DO from 8.75 to 9.35 mg/l.

Alkalinity (as bicarbonate) in the four high-As areas ranged from 290 to 440 mg/l in Beldanga, 225 to 510 mg/l in Hariharpara, 325 to 525 mg/l in Jalangi, and 325 to 455 mg/l in Naoda. Bicarbonate values were much lower in Nabagram, ranging from 110 to 140 mg/l. The pond in Hariharpara had 60 mg/l of bicarbonate, and the two ponds in Jalangi had 210 and 170 mg/l bicarbonate. Bicarbonate of river waters ranged from 50 to 120 mg/l.

In Beldanga, phosphate values range from 0 to 4.6 mg/l. Waters with lower phosphate values had lower As values, and waters with higher concentrations of phosphate had higher concentrations of As. Phosphate ranged from 0.6 to 4.6 mg/l in Hariharpara, 0.1 to 4.5 mg/l in Jalangi, and only one sample from Naoda was measured for phosphate and had 4.6 mg/l phosphate. Phosphate was not measured in waters from Nabagram (see Appendix A).

Cations

Dissolved Fe was relatively low (1.2 to 2.6 mg/l) in Beldanga, but much higher in Hariharpara (4.0 to 9.3 mg/l), Jalangi (8.7 to 22.3 mg/l, with one irrigation well water having only 0.5 mg/l), and Naoda (3.1 mg/l). Low-As water in Nabagram had 4.1 mg/l Fe.

Magnesium in high-As waters ranged from 24 to 29 mg/l in Beldanga, 22 to 39 mg/l in Hariharpara, 26 to 35 mg/l in Jalangi, and 29 mg/l in Naoda. For low-As Nabagram water, Mg was 24 mg/l.

Calcium was lowest in high-As waters of Beldanga (91 to 110 mg/l). Hariharpara had Ca values from 100 to 140 mg/l, Jalangi from 118 to 160 mg/l, and Naoda (110 mg/l). Nabagram had 159 mg/l Ca in its low-As waters.

Potassium concentrations in high-As waters in Beldanga were in the range of 0.5 to 2.1 mg/l, Hariharpara was 1.8 to 3.7 mg/l, Jalangi was 2.0 to 3.2 mg/l, and Naoda was 2.3 mg/l. No K was detected in Nabagram (0 mg/l) (see Appendix A).

Anions

Concentrations of Cl^- for high-As areas ranged from 6 to 67 mg/l in Beldanga, < 1 to 70 mg/l in Hariharpara, 2 to 49 mg/l in Jalangi, and 2 to 84 mg/l in Naoda, while waters with low As concentrations in Nabagram had higher Cl^- concentrations (41 to 200 mg/l).

Dissolved SO_4^{2-} was not detected in Beldanga, and only in three of ten wells in Hariharpara (5 to 10 mg/l), five of eight wells in Jalangi (1 to 48 mg/l), and five of six in Naoda (4 to 48 mg/l). All wells sampled in Nabagram had dissolved SO_4^{2-} whose concentrations ranged from 10 to 48 mg/l.

Nitrate values were lower in high-As waters. Nitrate was detected in only one well (1.8 mg/l) in Beldanga, only one well (1.4 mg/l) in Hariharpara, two wells (1.4 and 5.8 mg/l) in Jalangi, and one well in Naoda had 51 mg/l of nitrate. Two wells with low-As waters in Nabagram had nitrate values of 3.7 and 31 mg/l.

Nitrite was detected in high-As waters in only one well in Beldanga (1.4 μg/l), none in Hariharpara or Jalangi, and in three wells in Naoda (5.2, 6.1, and 10.6 μg/l). No nitrite was detected in low-As waters of Nabagram (Fig. 33) (see Appendix A).

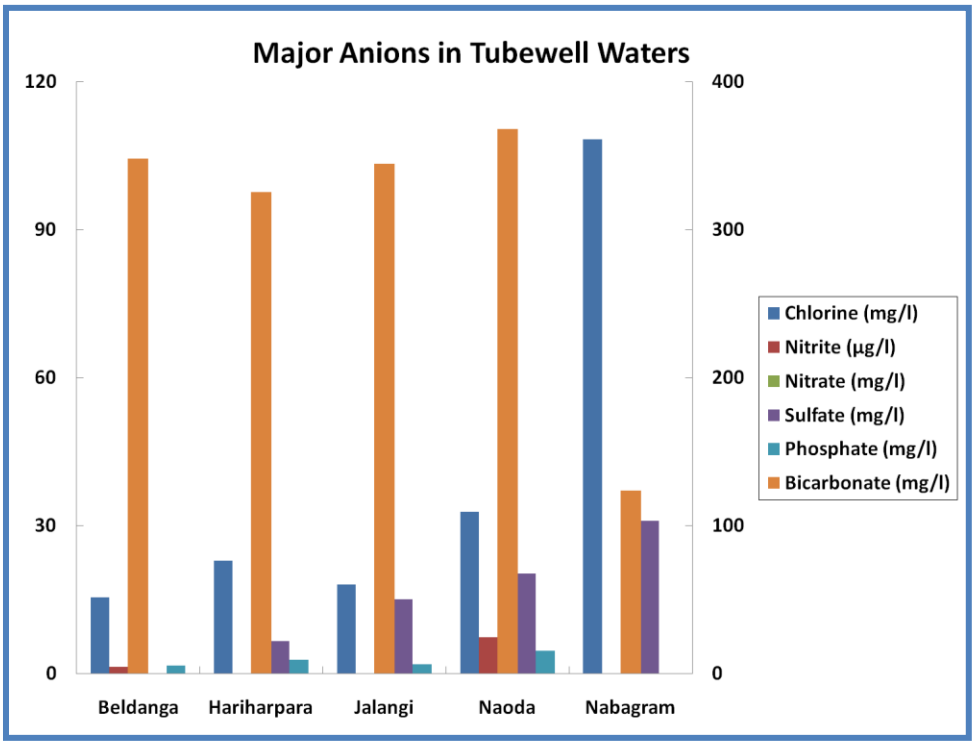

Figure 31: Major anions of tubewell waters are displayed here for each respective area (high-As: Beldanga, Hariharpara, Jalangi, Naoda; low-As: Nabagram). Y-axis is concentration in mg/l, except for nitrite (µg/l). Bicarbonate values are plotted on the right y-axis.

δ^2H & $\delta^{18}O$

Stable isotope values of δ^2H and $\delta^{18}O$ of tubewell, irrigation, pond and river waters showed several relationships (Fig. 34).

Precipitation: Wet season precipitation fell on and slightly below the global meteoric water line (GMWL) ($\delta^2H=8*\delta^{18}O+10$; Craig, 1961) and the local meteoric water line (LMWL) ($\delta^2H=7.2*\delta^{18}O+7.7$; Mukherjee et al., 2007b), while dry season precipitation fell further below the GMWL and LMWL (Fig. 22).Values for δ^2H and $\delta^{18}O$ for local wet season precipitation were -49‰, -64‰, and -46‰ for δ^2H and -7.3‰, -9.3‰, and -6.7‰ for $\delta^{18}O$ (Mukherjee et al., 2007b). Local dry season precipitation values for δ^2H and $\delta^{18}O$ were -32‰, -31‰, -36‰ and -31‰ for δ^2H and -5.1‰, -5.1‰, -4.7‰, and -4.7‰ for $\delta^{18}O$ (Mukherjee et al., 2007b).

Rivers: Major rivers of the region (Bhagirathi, Ganges) plotted above the GMWL. River waters ranged from -53.3‰ to -51.8‰ for δ^2H and from -8.2‰ to -7.9‰ for $\delta^{18}O$, while a smaller river (Muyarakshi) in Kandi had values of -13.87‰ and -1.89‰ for δ^2H and $\delta^{18}O$, respectively.

Ponds: When δ^2H was plotted against $\delta^{18}O$, the majority of the pond waters fell below the GMWL and the LMWL. δ^2H values for pond waters ranged from -55.5‰ to 3.7‰, and $\delta^{18}O$ values ranged from -8.4‰ to 2.2‰.

Tubewells: Regionally, most tubewell waters plotted on or near the GMWL and the LMWL. Values for all tubewell waters ranged from -42.1‰ to -9.3‰ for δ^2H and from -6.8‰ to -1.5‰ for $\delta^{18}O$. Deeper (> 60 m) tubewell waters had lighter $\delta^{18}O$ values (-34.3‰ and -42.1‰), while shallow (< 60 m) tubewell waters were more enriched and showed no clear relationship with depth (Fig. 35).

Irrigation wells: Irrigation wells had δ^2H values that ranged from -36‰ to -21.6‰ and $\delta^{18}O$ values ranged from -6.1‰ to -3.7‰. Deeper (91 and 137 m) irrigation wells had lighter $\delta^{18}O$ values than shallow (< 30 m) irrigation wells, which had heavier values for $\delta^{18}O$ at -5.9‰ and -6.1‰. δ^2H and $\delta^{18}O$ values of tubewell and irrigation waters showed generally showed no correlation with As concentrations (Fig. 36).

Separately, three different areas (Beldanga, Hariharpara and Nabagram) showed several relations. In Beldanga, 80% of tubewell waters plotted on or above the GMWL and LMWL (Fig. 37). In Hariharpara, ~90% of tubewell waters fell on or above the GMWL and LMWL (Fig. 38). In Nabagram, all tubewell and irrigation waters fell on or *below* the GMWL and LMWL (Fig. 39).

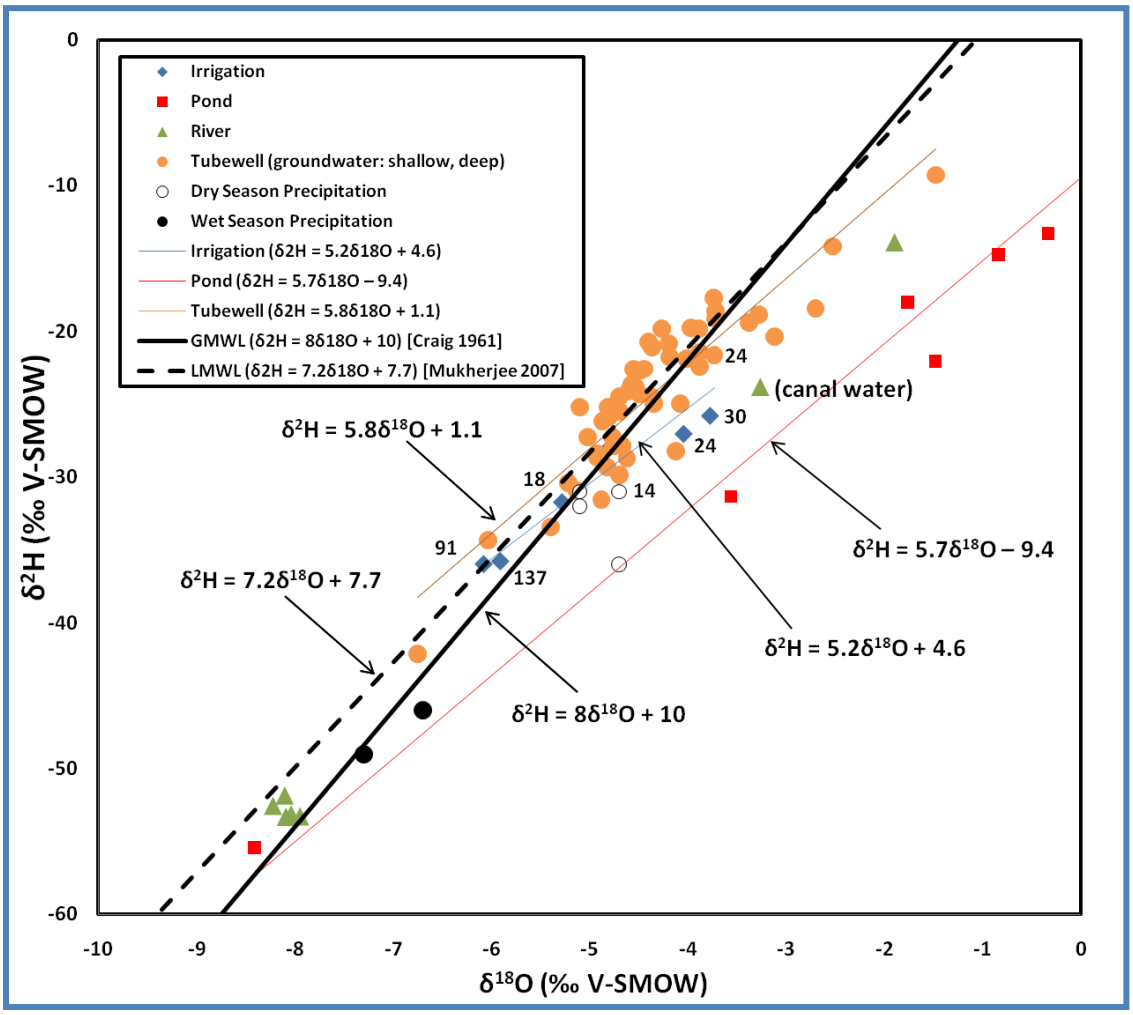

Figure 32: Stable isotope plots of δ^2H and $\delta^{18}O$ calibrated to (Vienna-Standard Mean Ocean Water (V-SMOW) for tubewell, irrigation, pond, river, and precipitation (dry and wet seasons) waters from Murshidabad district. Global meteoric water line (GMWL) and local meteoric water line (LMWL) are shown with their slope-intercept equations. Numbers near blue diamonds represent depth (m) of respective irrigation well waters.

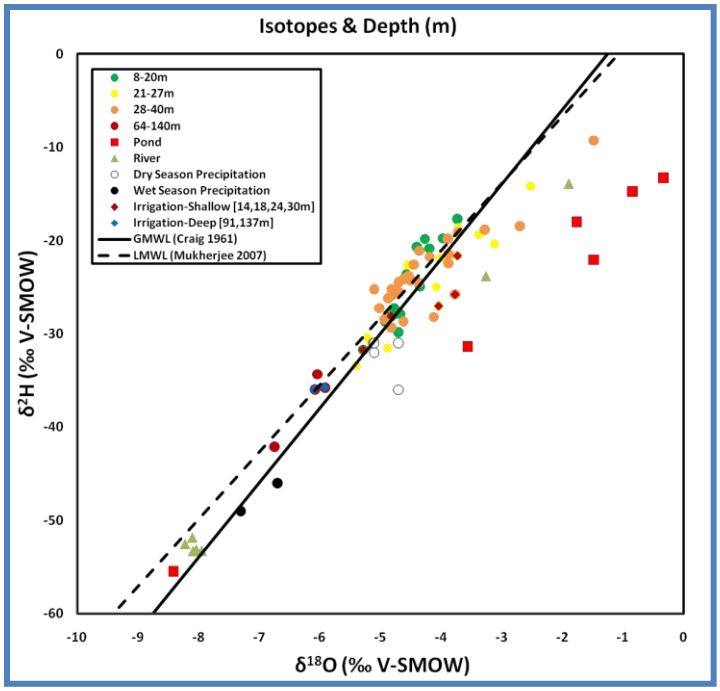

Figure 33: δ^2H and $\delta^{18}O$ plots similar to Figure 34, but here tubewell and irrigation wells are subdivided into different depth ranges noted by different colored circles and diamonds.

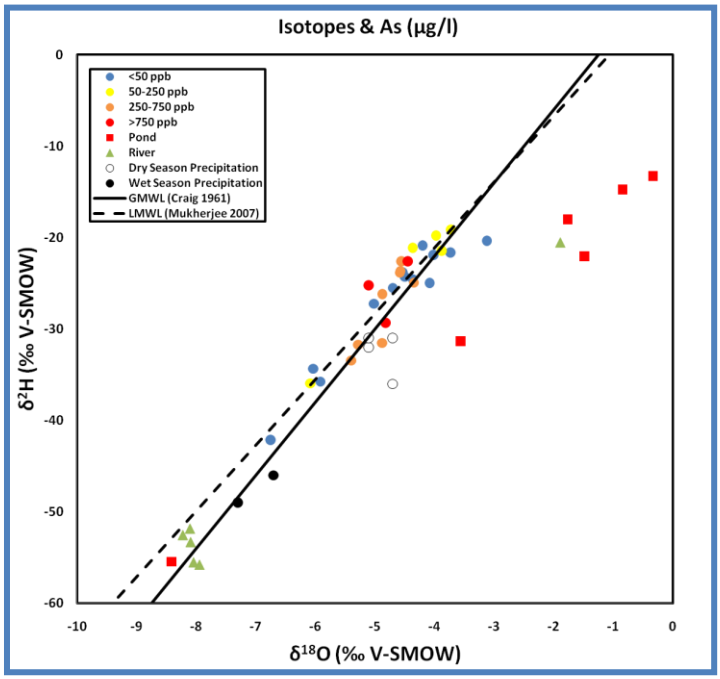

Figure 34: δ^2H and $\delta^{18}O$ plots where tubewell and irrigation wells are subdivided into different ranges of dissolved As concentrations (µg/l) noted by different colored circles.

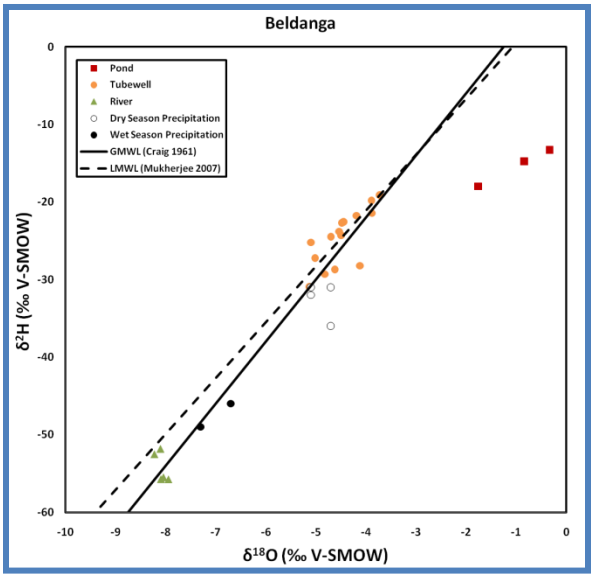

Figure 37: Beldanga (high-As area): δ^2H and $\delta^{18}O$ plots with river, pond, tubewell, and precipitation (dry and wet seasons) waters. Majority of tubewell waters plot above the GMWL and LMWL.

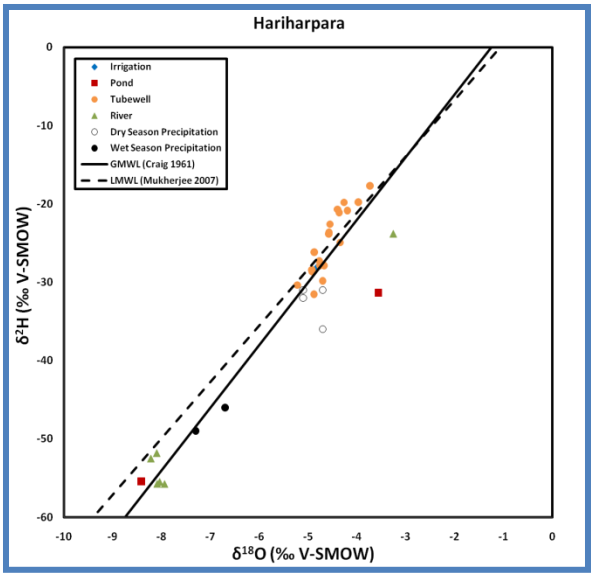

Figure 38: Hariharpara (high-As area): δ^2H and $\delta^{18}O$ plots with river, pond, tubewell, irrigation, and precipitation (dry and wet seasons) waters. Majority of tubewell waters plot above the GMWL and LMWL.

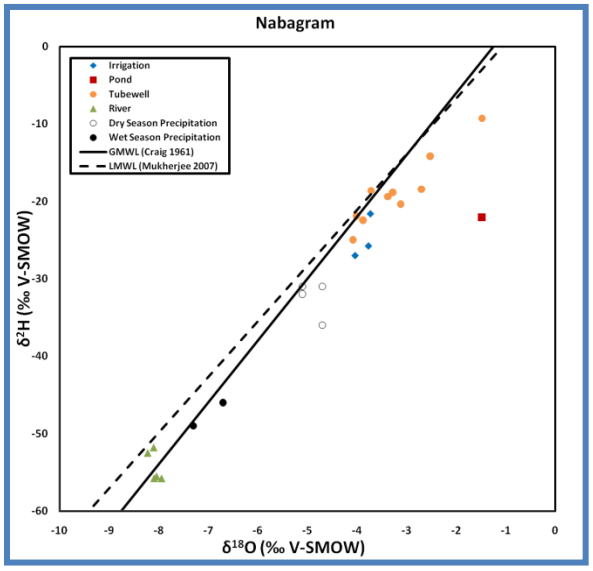

Figure 35: Nabagram (low-As area): δ^2H and $\delta^{18}O$ plots with river, pond, tubewell and precipitation (dry and wet seasons) waters. Majority of tubewell waters plot below the GMWL and LMWL.

δ^{13}C-DIC

Values for δ^{13}C of dissolved inorganic carbon (DIC) in tubewell and irrigation well waters revealed several conclusions (Fig. 40). δ^{13}C values of high-As waters (e.g. Beldanga) fell in the range of -7.45‰ to -10.57‰, except for TW-37(BM) which showed a δ^{13}C value of -9.70‰ and no dissolved As. In Hariharpara, the δ^{13}C value for TW-48(HK) screened at 9 m was -12.64‰. δ^{13}C values for wells screened at 15 m fell between -5.77‰ and 6.64‰, with the exception of TW-49(HK) whose δ^{13}C value was -14.33‰. All five tubewell waters had As concentrations > 100 µg/l. One tubewell (37 m) had δ^{13}C value of -7.58‰ and a dissolved As concentration of 19 µg/l.

Nabagram tubewell and irrigation well waters had lighter δ^{13}C values (-10.79‰ to -12.86‰) over a depth range of 21 to 30 m. Only one tubewell (TW-59(NB)) had a heavier (-8.76‰) value for δ^{13}C at 23 m depth. Four tubewell waters from Kandi at depths of 30 and 34 m had δ^{13}C values between -8.28‰ to -9.43‰, and all had dissolved As ≤ 11 µg/l.

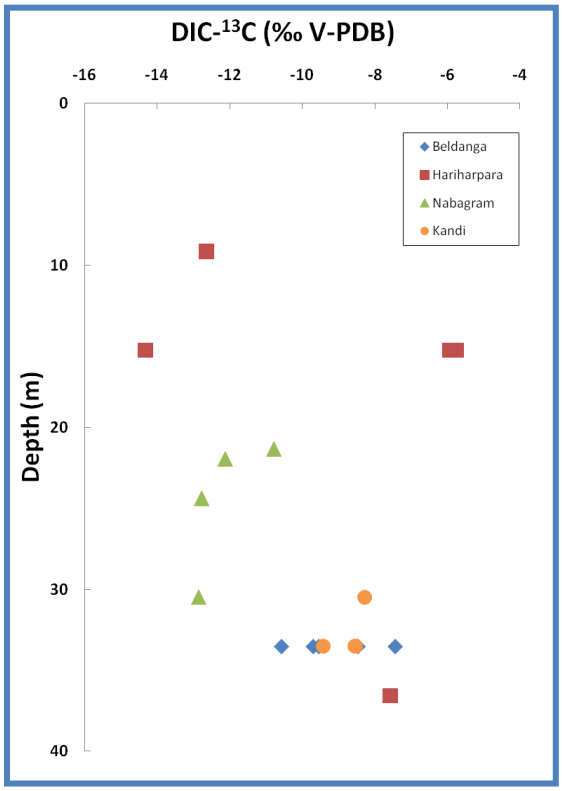

Figure 36: Stable isotope values of ^{13}C in dissolved inorganic carbon (DIC) in water samples - calibrated to ‰ Vienna-Peedee Belemnite (V-PDB) - plotted as a function of depth (m).

Chapter 6 - Discussion

Sediment Geochemistry

Physical Characterization

The first obvious difference between sediments in low-As areas versus sediments in high-As areas is color. West of the river Bhagirathi are the orange-brown to red-brown Pleistocene sediments identified as having low to no dissolved As in their groundwaters. Since Fe(II) minerals are usually black, the orange-brown color of the sediments is likely due to a higher proportion of Fe(III) minerals than Fe(II) or mixed Fe(II)/Fe(III) minerals (van Geen et al., 2003).

No As was detected in these sediments via XRF, and only in the shallow sediments (3 and 10 m) in Nabagram was As found greater than 1 mg/kg (~4 mg/kg) from total digestion of sediments by aqua regia. This may be a reflection of the grain sizes of the aquifer particles, generally fine to medium sand, in which As is less likely to associate except when it is present within an Fe-rich coating on the sand. These types of Pleistocene aquifers probably contain little to no dissolved As for several reasons. If As was previously present in these aquifers, it could have been flushed from the aquifer during the mid-late Pleistocene Glacial Maximum when hydraulic gradients were steeper than they are today. This may be a reasonable explanation if recent deposition west of Bhagirathi was relatively As-free. Another plausible scenario is As could be stored in the ubiquitous Fe-rich coatings (or Fe-rich phases) found on many aquifer particles (Imam et al., 1997) which have been shown to contain more than 2000 mg/kg As in some cases (Ravenscroft et al., 2005 and references therein). Arsenic could also be sequestered in the Fe(III) oxyhydroxides due to the oxidizing nature of the sandy aquifers. However, the presence of As in such coatings was not detected on any grains from the Pleistocene aquifers in this study.

Grey Holocene sediments of the present floodplains east of Bhagirathi contain on average relatively low amounts of As in the solid-phase when compared to global average values of As in unconsolidated sediments (typically 3 to 10 mg/kg; Smedley and Kinniburgh, 2002), but high and variable concentrations of As are observed in the groundwater (Charlet et al., 2007). Variations in As content with depth in both Beldanga and Hariharpara appear to be a function of grain size and/or mineralogy.

Petrography and Mineralogy of Sediment Cores

Mineralogy between high-As areas and low-As areas in this study shows significant differences. It is known that certain minerals can house a suite of trace elements, including arsenic. Minerals likely to be found in a highly weathered, fluvial environment, with which As can be associated are metal oxides (particularly Fe and Mn) (Ahmed et al., 2004), since they have high specific surface area and thus a high adsorption capacity (Zahid et al., 2009), sulfides (Polizzotto et al., 2006; Saunders et al., 2008 and references therein) and accessory minerals like apatite (Smedley et al., 2002; Mailloux et al., 2009; Neuman et al., 2010); or it can be absorbed on the surfaces of other minerals like carbonates (Smedley and Kinniburgh, 2002) and clays like illite (Lin and Puls, 2000, 2003; Pal et al., 2002), kaolinite (Raymahashay et al., 2003; Mukherjee et al., 2009b and references therein), and sometimes associated with chlorite (Pal et al., 2002). These types of minerals (with the exception of sulfides which are yet to be studied) were all found within the aquifer sediments in the study areas of Beldanga and Hariharpara, and could be potential sources and/or sinks for As, depending upon redox conditions of aquifer sediment-water interfaces, nature of organic matter, and sediment texture(s) (Tareq et al., 2003).

In Beldanga and Hariharpara, micas and clays rich in Fe, Mg (chlorite, which can contain up to 31 mg/kg As [Pal et al., 2002]), Mn, presumably Fe oxides, apatite (average 210 mg/kg As in Himalayan apatite [Mailloux et al., 2009]), and calcite (and possibly other carbonates) were found in relatively greater proportions within As-rich zones compared to As-poor zones. This is in agreement with a study by Charlet et al. (2007) in Chakdaha, another high-As area to the south of Murshidabad.

In shallow sediments in Beldanga, high concentrations of Fe, K, and Al were observed, along with prominent lath-shaped biotite grains. Biotite has been shown to sorb As on its surface (Seddique et al., 2008; Hasan et al., 2009; Nath et al., 2009). High amounts of As correlating with high Ca, Mg, Fe, K, and Al in the deeper sediments could also result from presence of biotite (Mg, Fe, K, and Al) and carbonates (Ca, Fe, Mg), which were both observed in significant amounts in thin sections.

In Hariharpara, the highest As found in the grey sediments was in the shallow sediments (< 15 m), which had sediment grain size in the range of clay to very fine sand, with majority being silt. The mineralogy of these sediments was analogous to those in Beldanga (which is expected in an alluvial-deltaic basin), although there was slightly higher (~5% more) mica content in the sediment cores in Hariharpara. In these shallow sediments (6 m), it is postulated that As may be associated with Fe (and Mn) oxyhydroxides, which were found within thin sections with a gradation of colors, owing to various amounts of Fe content. Amphiboles, apatite, and carbonate concretions are

associated with As, at least in the shallow and intermediate depths of the sediment cores. In the intermediate depths of the sediment core, weathering of biotites (Seddique et al., 2008; Hasan et al., 2009) and Fe-oxides (Swartz et al., 2004), and possibly carbonates (Smedley and Kinniburgh, 2002) may be responsible for releasing As into the groundwater. Light-brown, fine sand with some silt and clay that contained Fe-oxyhydroxides was observed in the deeper aquifer sediments. Also present were weathered feldspars with what appeared to be Fe-rich coatings, Fe-carbonates, Mg-rich clay (chlorite), other carbonates and apatite, all of which were observed in thin section. However, the majority of minerals found in Beldanga and Hariharpara were not observed in Nabagram or Kandi, most likely due to different sediment provenances (Acharyya and Shah, 2007; Mukherjee et al., 2009a).

In summary, the possible mineral phases that can host As in these sediments were Fe (and Mn) (oxy)(hydr)oxides, biotite, apatite, amphiboles, carbonates, and clays.

Major and Trace Element Geochemistry of Sediment Cores

The highest amounts of As were identified in the shallow and deeper sediments in Beldanga within the silt/very fine sand fractions. Other high concentrations of As in sediments were found in the deepest depths of the core in the grey, fine to medium size sand. The proportion of Fe(II):Fe_T in the shallow core sediments was ~0.85, indicating a strongly reducing environment. An even stronger reducing condition was found in one zone in deeper sediments in Beldanga where Fe(II) accounted for nearly 100% of total Fe. Sediment phosphate concentrations were higher when Fe(II):Fe_T ratios were lower, which could be explained by reductive dissolution of Fe-oxyhydroxides (McArthur et al., 2001). Studies have shown that reduction of Fe-oxyhydroxides and concomitant release and mobilization of phosphate into solution may result in competitive anion exchange with arsenate (or possibly arsenite) sorbed on other minerals, especially since the highest amounts of P-extractable As are found in sediments with high ratios of Fe(II):Fe_T (Zheng et al., 2005 and references therein). When phosphate (and sometimes carbonate) concentrations are high in sediments, this may limit the capacity of the sediments to sorb arsenic oxyanions (Harvey et al., 2002 and references therein).

Mg, Fe, Mn, K and Al were also found in higher concentrations with higher amounts of As in the deeper sediments, which may have an association with minerals like biotite and other Fe- and Mg-rich clays (e.g. chlorite) (Hasan et al., 2009). Arsenic sequestration into secondary mineral phases like siderite, rhodochrosite, or vivianite upon dissolution of Fe-oxyhydroxides is possible if

favorable conditions exist in a local environment (McArthur et al., 2001; Saunders et al., 2005; Datta et al., 2009), although these phases have not yet been identified in this study.

A strong correlation between As, Cu, and Zn, where respective patterns with depth were nearly identical in both Beldanga and Hariharpara, may indicate the presence of Cu and Zn sulfides, and hence it might be possible for As to exist in a sulfide phase.

Of the Beldanga sediments on which digestion by aqua regia was done, concentrations of As were consistent with As values obtained by XRF. One sample from 27 m was run in duplicate, and showed a significant difference between As concentrations (18 and 44 mg/kg), owing to the heterogeneity within these types of sediments.

A weak correlation of aqua regia-extractable Fe and As may be related to differences in mineralogy between the high and low As sediments, a major portion of Fe being retained in more refractory minerals (possibly accompanied by a significant redistribution of As to a mobilizable phase on the surface of aquifer particles (Horneman et al., 2004)), or it may just be due to heterogeneity of the sediments.

The fairly significant positive correlation observed between As and Zn in Beldanga may not be real due to the one high As value (44 mg/kg) accounting for the high r^2 value. If it is real, then Zn may be associated with As within sulfides or possibly clay minerals. Correlation between As and Ca does seem to be present, and may result from the presence of calcite, other carbonates, and/or amphiboles. The slight correlation of As with Mn relates that As might be associated with Mn-oxides or clay minerals. The association of Pb with As can result from carbonates, Fe-oxides, clays, and organic matter (Magrisso et al., 2009). Mg and K relations with As in these sediment may be in the form of biotite or other clay minerals, and possibly mafic minerals (for Mg) like amphiboles. No correlation of As exists with Al, at least determined by aqua regia digestion. This is likely due to an association of As with other non-Al-bearing minerals. The associations of As and other elements in Nabagram is not statistically significant mainly due to very few (and relatively low) values of As identified in these sediments, which may explain the basis of this relationship.

Sequential Extractions of Sediment Cores

Sequential extractions showed the compartmentalization of As within various fractions of sediments within the sediment core from Beldanga. These sequential extractions were not performed on sediments from Nabagram, simply because very little (< 4 mg/kg, and < 1 mg/kg in most cases) As was detected in bulk sediments. Sediments from Beldanga had a relatively greater amount of As,

thus giving reasonable As values using these extractions. Selective As extraction studies by Charlet et al. (2007) showed two major sinks for As: amorphous Fe(III) oxide (34% ± 8% of total extracted As) and acid volatile sulfides (AVS) and/or carbonates (19% ± 7% of total extracted As), both of which are reasonable fractions on which As can be adsorbed and co-precipitated.

HCO_3^- and PO_4^{3-} were the dominant ions in the aquifer which compete with As species for adsorption sites on mineral surfaces, thus releasing As into groundwater. The results presented in the current study are in partial agreement with Charlet et al. (2007). The main difference is that the present study did not target an AVS and/or carbonate phase, but rather a 'specifically-sorbed' phase, which could also account for some As adsorbed on carbonates.

In shallow sediments in Beldanga (high-As core), 0.4 mg/kg (~3% of total As) was in the easily-exchangeable phase, which indicates that it could be easily displaced from the sediment and mobilized into the groundwater. Silicates, sulfides, and organic matter are not affected in this phase, and Fe and Mn oxides should not be significantly solubilized (Tessier, et al., 1979). Also in the shallow sediments, 6.3 mg/kg (~50% of total As) was in the specifically-sorbed (to mineral surfaces (e.g. goethite (Keon et al., 2001)) phase. Arsenic in this phase can be desorbed through competitive ion exchange processes with the high amounts of phosphate observed (Acharyya et al., 1999). Approximately 3.4 mg/kg (~27% of total As) was associated with amorphous and poorly-crystalline hydrous Fe oxides, which are thermodynamically unstable under anoxic conditions (Tessier et al., 1979). Manganese concentrations in the Beldanga sediments were 14 and 33 mg/kg (14% and 32% of total Mn) was found in the same respective fractions. Sediment was grey in color at this depth, indicating enough reducing conditions that the Fe- (and Mn) oxyhydroxides could be dissolving over time, thus releasing structurally bound/co-precipitated arsenic.

The bulk of As in deeper sediments was found in the specifically-sorbed phase (6.7 mg/kg As; ~38% of total As) and in the amorphous and poorly-crystalline phase (6.9 mg/kg As; ~39% of total As). Approximately 17% of total Mn was associated with amorphous and poorly-crystalline hydrous Fe oxides, while most (~72%) of the Mn in the deeper aquifer sediments was in the residual phase.

In a zone within the deeper sediments, where chiefly light-brown fine sand (with some silt and clay) is found, ~80% of total Fe is Fe(II). Approximately 22% (2.3 mg/kg) of total As in this depth zone was found in the specifically-sorbed phase. A greater proportion of As was identified in association with amorphous/poorly-crystalline Fe-oxyhydroxides and well-crystallized Fe-oxyhydroxides (3.2 mg/kg and 2.1 mg/kg, respectively). In the deeper sediments, Mn was in the

easily exchangeable phase (~10%), specifically-sorbed (~13%), and amorphous Fe-oxyhydroxide phases (~14%).

At the deepest depth (40 m) in the sediment core, 0.7 mg/kg of As (~3%) was in the easily exchangeable phase and 8.7 mg/kg (~42%) in the specifically-sorbed phase. Arsenic was also correlated with Fe-oxyhydroxides (amorphous: 8.7 mg/kg; ~42%; crystalline: 2.9 mg/kg; ~14%), and with relatively low phosphates and higher proportions of Fe(II):Fe_T in the sediments. Hence, As may be easily mobilized into groundwater at this depth.

van Geen et al. (2008) noted that each mg/kg of P-extractable As in sediments is highly correlated to ~250 μg/l of dissolved As in pore waters. This scenario holds true in the deeper sediments in the sediment core from Beldanga. When values for P-extractable As in sediments from zone(s) where the highest dissolved As concentrations were found are added together, there should be ~4100 μg/l of dissolved As in the groundwater. Remarkably, the tubewell situated just beside the location from where the sediment core was collected had a dissolved As concentration of 4036 μg/l. Such an elevated concentration of dissolved As as in this case may result from competitive ion-exchange processes, coupled with reductive dissolution of As-bearing Fe-minerals.

Summary of Sediment Characterization

Several distinct differences were found among sediments from low-As areas (Nabagram and Kandi) and high-As areas (Beldanga and Hariharpara), and within the high-As sediment cores themselves. First and foremost, the color of sediments was orange-brown to reddish-brown in the low-As areas, which is indicative of high proportions of Fe(III) and mixed Fe(II)/Fe(III) phases (i.e. redox conditions). In high-As areas, sediment colors were chiefly light to dark grey (with a few light brown zones) in the high-As areas. A depositional environment rich in organic matter facilitates the complete reduction of FeOOH (McArthur et al., 2004). Dissolved As concentrations are high (> 50 μg/l) where there is complete reduction of FeOOH, so the FeOOH has released all its sorbed As into solution. At this point, the aquifer becomes grey in color as FeOOH disappears (McArthur et al., 2004). When sorbed As is released by Mn oxides, it does not remain in solution if FeOOH reduction is incomplete, rather the As sorbs to FeOOH, and the sediments tend to be brown in color.

Low-As areas consisted of predominantly quartz and feldspars, with minor amounts of micas and calcite, while high As areas had a varied mineral suite: consisting of quartz, feldspars, biotite, muscovite, amphiboles, calcite (and other carbonates), Fe-(oxy)(hydr)oxides, accessory minerals (apatite, zircon, sphene, epidote, etc.), and clays (chlorite, kaolinite, possibly illite). High Fe(II):Fe_T

values corresponded with (relatively) low phosphate concentrations in the sediments (and vice versa) in Beldanga, for which competitive ion-exchange (upon reductive dissolution of Fe-oxyhydroxides) seems to be a plausible explanation. Also, the biotite and apatite in high-As zones may be weathering to release As from the sediments, which is evidenced by sequential extraction results of As being predominantly present in the specifically-sorbed phase and associated with amorphous and poorly-crystalline hydrous oxides of Fe (and Al and Mn), as well as a significant amount of As in the residual phases in some instances.

Another point to be made here is that results from total digestions and sequential extractions and results from hand-held XRF are correlated. An advantage of using sequential extractions versus XRF is that particular mineral phases with which specific elements (e.g. As, Mn, Fe) are associated was easily and accurately identified. On the other hand, as an initial screening tool, hand-held XRF gave reasonable values and is therefore deemed reliable for this purpose.

Water Chemistry

General Water Attributes

Chemical signatures of waters with high dissolved As concentrations often showed distinct differences when compared with waters with little or no dissolved arsenic. High-As waters in Beldanga and Hariharpara had circumneutral pH values. Low-As waters in Nabagram and Kandi had pH values below and above circumneutral pH values, respectively. As-enriched waters in Beldanga and Harihapara had moderate 720-860 μS/cm conductivity values, while conductivity values of low-As waters (Nabagram and Kandi) were below and above the range of conductivity values for high-As waters. This may be explained by lower dissolved ion concentrations in Nabagram due to extensive flushing from the higher elevation Pleistocene aquifer**.**

Dissolved oxygen (DO) and oxidative redox potential (ORP) in high-As waters in Beldanga and Hariharpara were slightly higher than would be expected for high-As waters, but were still in the upper range of anoxic or sub-oxic condition for most samples. These higher values may have resulted from rapid partial oxidation during sampling, while DO and ORP for low-As waters were fitting for generally highly oxidized aquifers.

Speciation and Spatial Variability of Arsenic in Waters in Murshidabad

Areas west of Bhagirathi have waters with low concentrations of dissolved As most likely due to a combination of the following reasons: only minor amounts of arsenic (majority < 1 mg/kg) were detected in the solid phase; anoxic conditions are not prevalent (waters were high in SO_4^{2-}) in the Pleistocene aquifers in this study area that can facilitate reduction of Fe-oxyhydroxides; and presence of extremely low concentrations (or complete absence in some wells) of phosphate and low HCO_3^- concentrations (Nabagram) that, if present, possibly could compete with arsenate for adsorption sites on mineral surfaces.

Groundwater east of Bhagirathi contained elevated concentrations of dissolved As, at mg/l levels in some wells. A probable cause for significantly elevated levels of dissolved As in the groundwaters here is the reducing condition in the aquifers, which is enhanced when coupled with microbial oxidation of natural organic matter (BGS and DPHE, 2001; Harvey et al., 2005 and references therein). Two tubewells in Beldanga located < 50 m apart had what are believed to be the highest concentrations of As reported in West Bengal (previously 3.7 mg/l, Stüben et al., 2003) at 4.6 mg/l and 4.4 mg/l. Wells located ~50 m northeast and ~30 m southeast of the high-As wells contain 0 and 6 μg/l, respectively. Wells sampled ~100 m northeast of these "hotspots" contain only 3 μg/l of As, all of which have well screens at nearly the same depth. This could be due to local variations in groundwater flow paths caused by well pumping, or a redox front (Nickson et al., 1998; Nath et al., 2005). McArthur et al. (2008) attributed this type of spatial variation to microbial weathering of As-rich lenses associated with paleomeanders comprising pockets of As-bearing minerals on the flanks of a buried paleochannel or oxbow lake.

In Hariharpara, Jalangi, and Naoda, high groundwater As concentrations were vertically distributed over a range of 25 m that could result from As release in the shallow subsurface and later transport to depth in the highly permeable sandy aquifers, as also the case cited by Polizzotto et al., 2006. It can also be due to a wide zone of As bearing minerals undergoing reductive dissolution in these grey sediments, or possibly a combination of both scenarios.

In high-As areas like Beldanga, Hariharpara, and Jalangi, deeper groundwaters (> 60 m) are slightly contaminated (one well showed As at 52 μg/l), which may be explained by very low As concentrations in the sediments or possibly from As-bearing waters from above making their way along narrow flow paths into deeper parts of the aquifers. This means that even the deeper aquifers are at risk to As contamination and may not provide safe drinking water in the future (Mukherjee et al., 2010).

The majority of the total As being As(III) for all samples in which As speciation was done is a reflection of the redox conditions of the aquifers, whether it is widespread or localized only in some areas. These high As(III):As_T ratios may also be a function of the differences in distribution coefficient for As(III) and As(V) (Naidu et al., 2009). As(III) is more mobile in the subsurface (Polizzotto et al., 2006). In the presence of strongly reducing conditions in the subsurface, As(III) remains stable as As(V) is continuously reduced to As(III). Thus, accumulation of As(III) around certain well screens, coupled with possible microbial reduction of ferric iron and As(V), could be a plausible scenario to explain some of the highest As(III):As_T ratios.

Ionic Constituents in Waters from Murshidabad

Differences in chloride values may reflect age and residence times of groundwater in the Pleistocene and Holocene aquifers, as well as the number of times the aquifers have been flushed (Dhar et al., 2008).

High HCO_3^- concentrations may correlate with weathering of carbonates and degradation of organic matter under local reducing conditions coupled with Fe-(oxy)(hydr)oxide dissolution (Mukherjee-Goswami et al., 2008 and references therein). The presence of high ratios of Fe(II):Fe_T in Beldanga indicate reducing conditions that, upon dissolution of the Fe-bearing hydrous oxides, could release HCO_3^- into the groundwater, along with phosphate and arsenic. Dissolved phosphate and As concentrations both show positive correlation with HCO_3^- concentrations. Low concentrations of HCO_3^- and relatively high oxygen content in waters with low dissolved As may indicate unfavorable conditions for both carbonate dissolution or reduction and subsequent dissolution of Fe oxyhydroxides.

Nitrate and nitrite values were low simply due to the reducing condition of the aquifers in high-As areas.

A reason sulfate values are less in water with high As may be due to a negligible amount of sulfide minerals present in the sediment (although they were not really targeted in this study). It would be expected under these reducing conditions that S-bearing minerals would not undergo complete or possibly not even partial dissolution. The low amounts of sulfate detected may have been dissolved in the shallow subsurface where more oxidizing conditions existed and then transported to depth via groundwater flow (Polizzotto et al., 2006).

In well waters where cations were measured, dissolved Fe was generally lower in Beldanga than in other high-As areas (Hariharpara, Jalangi, Naoda). One well in Jalangi (TW-20(JB)) had

extremely high dissolved Fe (22.3 mg/l), with relatively high K (3.2 mg/l), Ca (136.6 mg/l) and Mg (31.8 mg/l), along with 190 μg/l of As, which may be a result of weathering of biotite and/or Fe- and Mg-rich clays. The deepest (137 m) well sampled (IRW-2(JB)) had only 0.5 mg/l dissolved Fe, the lowest of all sampled well waters.

Overall, concentrations of dissolved Mg and Ca were relatively similar, owing possibly to weathering of mafic and felsic minerals. Pond and river waters had much lower dissolved Mg and Ca concentrations than all the groundwaters (shallow and deep), resulting from the different recharge(s) for each type of aforementioned waters.

Values for K were somewhat higher in Hariharpara, Jalangi and Naoda than in Beldanga. No dissolved K was detected in Nabagram, which may be from lack of micas and clay minerals, or possibly from aquifer flushing.

Hydrogen and Oxygen Isotopes as Indicators of Groundwater Recharge

Overall, plots of δ^2H versus $\delta^{18}O$ for all water samples were consistent with results from previous work in West Bengal (Mukherjee et al., 2007b) and Bangladesh (Stute et al., 2007). Monsoonal precipitation values from Mukherjee et al., 2007b, plotted along the GMWL and showed a high degree of depletion (and a moderate evaporation effect), while some δ^2H and $\delta^{18}O$ values for dry season precipitation plotted below the GMWL and LMWL, and showed a much less degree of depletion than monsoonal precipitation for the local region.

River samples had lighter $\delta^{18}O$ values and slight evaporative enrichment from the LMWL since they were chiefly fed by highly depleted snowmelt from the Himalayas (Stüben et al., 2003), except for a small canal (SW-1(HK)) in Hariharpara and the river Muyarakshi in Kandi. These two exceptions showed a fair amount of evaporative enrichment which indicates more evaporation than groundwaters and slightly less than the pond waters. This may be due to their flow rates, which were very low, almost comparable to the stagnant ponds.

δ^2H and $\delta^{18}O$ values for the majority of groundwaters from tubewells fell along the GMWL and LMWL, mainly in the range of -5‰ and -3‰ and -17‰ and -32‰, respectively, which was in agreement with work done by Sikdar and Sahu (2009) in the same region. Shallow (8 to 20 m) groundwaters mostly plotted above the GMWL and LMWL, revealing that these waters were not affected by evaporation (Sikdar and Sahu, 2009). Intermediate depths (21 to 40 m) were mainly clustered along the GMWL and LMWL between -30‰ and -19‰ for δ^2H and from -5‰ and -4‰ for $\delta^{18}O$, mostly owing to non-evaporative waters. The two deepest (64 m) tubewells sampled were

more depleted than all the other tubewells, suggesting a 'paleo-recharge' during a different climatic period (Mukherjee et al., 2007b) and possibly a separation from the shallower aquifer from which most of the other well water samples were collected.

Shallow (14 to 30 m) irrigation wells ranged from -31.71‰ to -21.61‰ for δ^2H and -3.73‰ to -5.28‰ for $\delta^{18}O$ and all plotted below the LMWL, indicating slight evaporative enrichment. The two deep (91 and 137 m) irrigation wells were even more depleted than the shallow irrigation wells but plotted along the LMWL, above the GMWL, suggesting a recharge from long ago, possibly during a period of different climate. This is just a conjecture since $^3H/^3He$ dating was not done in this study.

All pond waters plotted significantly below the GMWL and LMWL [δ^2H: -22.06‰ to 3.69‰; $\delta^{18}O$: -3.56‰ to 2.19‰] (with the exception of PW-2(HK) from Hariharpara, which had values [δ^2H: -55.45‰; $\delta^{18}O$: -8.341‰] more depleted than river waters) and had a local evaporation line defined by $\delta^2H=5.7\delta^{18}O-9.4$ (similar to results from Sengupta et al., 2008). These values indicate a significant degree of evaporative enrichment due to the stagnant nature of the pond waters. Since pond waters showed a significant amount of evaporative enrichment, it is plausible to believe pond waters had a very minor contribution, if any, to recharge of groundwaters in this study. Additionally, there is little to no evidence from this study to relate dissolved As concentrations in groundwater to stable isotope signatures of δ^2H and $\delta^{18}O$.

When values for δ^2H and $\delta^{18}O$ are viewed on the local-scales, several more trends become apparent. In Beldanga, all tubewell water $\delta^{18}O$ values were between -5.10‰ and -3.72‰, as were the dry season precipitation $\delta^{18}O$ values, while the pond water $\delta^{18}O$ values were -1.76‰ and -0.33‰ and highly enriched in evaporation. This suggests that dry season precipitation, and not pond waters, may be a major source of recharge for the shallow aquifer, at least in the general vicinity of this particular village in Beldanga. Local winter (dry season) precipitation in this regions happens from localized moisture accumulation combined with intense evaporation of local surface water bodies such as ponds and canal waters.

In Hariharpara, 85% of the 20 tubewell waters plotted above the GMWL, and 75% plotted on or above the LMWL, all within the range of -5.22‰ to -3.73‰ for $\delta^{18}O$. The largest pond (sampled January 2010) in the village had a $\delta^{18}O$ value of -3.56‰, and showed a high evaporative enrichment. The same pond was sampled in June 2009, and had a $\delta^{18}O$ value of -8.41‰, which was even more depleted than the nearby major river Bhagirathi. Currently, there is no good explanation for this observation. Additionally, the small canal at the edge of the village plotted much below the GMWL

and LMWL, showing evaporative enrichment. This may result from influence by the pond water (or vice versa), or in conjunction with the pond water, which in turn influences the shallow groundwater beneath the village with some slight mixing. However, additional studies would be needed to prove (or disprove) this.

All tubewell and irrigation well waters in the low-As area of Nabagram plotted on or below the LMWL and the GMWL, which is significantly different from Beldanga and Hariharpara. Some of the tubewells were more enriched than others in Nabagram and also more so than those in Beldanga and Hariharpara, and the pond water was heavily enriched in evaporation. This may be due to some slight mixing between dry season precipitation and pond water, or it may also result from evaporation of precipitation water during infiltration.

Since $\delta^{2}H$ and $\delta^{18}O$ and values for precipitation (Mukherjee et al., 2007b), river waters, and groundwaters (both shallow and deep irrigation and tubewell waters) all plotted on or just below the GMWL and the LMWL, with most of the pond waters plotted significantly below this line, indicating a degree of evaporative enrichment, the major recharge mechanism for the aquifer in this study appeared to be dry season precipitation, rather than monsoonal precipitation or pond water. Had groundwaters plotted below the GMWL and LMWL, then there may had been evidence of some degree of mixing between pond water and precipitation and/or river water, but generally they did not, except slightly in the case of Nabagram. Lighter values for $\delta^{18}O$ in deeper wells may result from older water that was recharged from similar type precipitation farther north and has followed a longer flow path for a long period of time and may have been subjected to some evaporation. However, this is just speculation since groundwater dating was not done in this study.

δ^{13}C-Dissolved Inorganic Carbon of Waters in Murshidabad

Dissolved organic carbon (DOC) brought to depth by recent irrigation has been shown to facilitate reduction of Fe-oxyhydroxides in shallow aquifers, releasing As into groundwater (Harvey et al., 2002). DOC is mobilized from sediments into groundwater when it is oxidized to dissolved inorganic carbon (DIC) (Zheng et al., 2004) or when water containing younger DIC mixes with these DOC-containing sediments (Harvey et al., 2005 and references therein). DIC values (^{13}C) of waters can be explained by fractionation during carbonate reduction (Harvey et al., 2002), and can act as tracers to represent CO_2 outgassing from water, leaving the heavier ^{13}C-DIC behind in the water. Heavier values for ^{13}C-DIC indicate exchange with atmospheric CO_2, while lighter values of ^{13}C-DIC indicate carbonate and/or organic rich (e.g. bacteria) components in the matrices (Neumann et al.,

2010). Concentrations of NH_4^+ (and Ca^{2+}) follow the same depth trend as the As profile in the shallow aquifers, and DOC and DIC both increase with increasing As to the depth where As peaks (Harvey et al., 2002). DIC and other products of organic carbon oxidation (i.e. NH_4^+) are strongly correlated with dissolved As concentrations in this study. High dissolved HCO_3^- concentrations in waters with low dissolved oxygen, suggest that the source of DIC includes a component of respired CO_2 derived from organic matter oxidation either during infiltration through soil or along the flow path of water (Zheng et al., 2004), which is also supported from more negative δ^{13}C-DIC values (McArthur et al., 2001). When ^{13}C-DIC values are lighter (i.e. < -10‰), As concentrations are generally lower, as are pH and NH_4^+ (exemplified by values in waters from Nabagram). In this study, waters with ^{13}C-DIC values > -10‰ (less organic matter) are prone to have elevated As concentrations, higher pH and higher NH_4^+ values. The correlation between NH_4^+ and As may be explained by respiration of DOC producing ammonia and CO_2, the latter inducing calcite (or other carbonate) dissolution (Harvey et al., 2002), which were found in abundance in sediments from several arseniferous zones in this study area.

Summary of Water Chemistry

A probable cause for significantly elevated levels of dissolved As in the groundwaters in our field study area is the reducing condition in the aquifers, which is enhanced when coupled with microbial oxidation of natural organic matter (BGS and DPHE, 2001; Harvey et al., 2005 and references therein). Concentrations of dissolved constituents in water points to reducing conditions (high Fe, HCO_3^-, PO_4^{3-}, NH_4^+, and elevated As(III):As_T; with low NO_3^-, NO_2^-, Cl^- and SO_4^{2-}) (Tareq et al., 2003) in high-As areas. Stable isotope values for δ^2H and δ^{18}O indicate dry season precipitation as predominant source of recharge to the aquifers. The spatial variability of dissolved As concentrations is complex and may be the result of multiple factors including spatially and temporally variable flow paths induced by flooding conditions and well-pumping, buried As-rich lenses (e.g. peat layers), distribution of microbial communities, etc., of which many are outside the scope of this project. Deeper groundwaters though show very low dissolved As, but they can be sustainable as As-safe zones in the long run. Low-As areas consisted of low Fe, HCO_3^-, PO_4^{3-}, NH_4^+, and high Cl^- and SO_4^{2-}, where lighter δ^{13}C-DIC values mainly corresponded with lower pH, low NH_4^+, and low arsenic.

Chapter 7 - Conclusions

West of river Bhagirathi, low As concentrations are found in groundwaters (< 10 μg/l). This results from a lack of solid-phase As in the orange-brown Pleistocene sediments (generally < 1 mg/kg), as well as the oxidizing condition present within the aquifers, which prevents reductive dissolution of hydrous Fe-oxides and subsequent mobilization of As into the groundwater. These aquifers are likely to remain as As-safe zones, at least for the immediate future.

East of Bhagirathi, dissolved As concentrations are significantly elevated in the shallow aquifers (< 60 m), where stable isotope data shows dry season precipitation to be a probable main source of groundwater recharge. The presence of reducing conditions within the high-As aquifers is evident from high Fe(II):Fe_T in sediments and high As(III):As_T in the groundwaters. Also further corroborating the notion of reducing conditions here are elevated levels of dissolved Fe, HCO_3^-, PO_4^{3-}, NH_4^+, and low NO_3^-, NO_2^-, Cl^-, and SO_4^{2-}. These factors point to reductive dissolution of hydrous Fe-oxides, and weathering of As-bearing clays, biotite, and apatite. This study shows that reduction of Fe-oxyhydroxides and concomitant release and mobilization of phosphate into solution may result in competitive ion exchange with arsenate (or possibly arsenite) sorbed on other minerals, since highest amounts of P-extractable As are found in sediments with high ratios of Fe(II):Fe_T. For each mg/kg of P-extractable As in sediments in Beldanga, ~250 μg/l of dissolved As were found in pore waters. Hence this study promotes the fact that both reductive dissolution and competitive ion exchange are probable release mechanisms of geogenic arsenic from solid phases into groundwaters. Microbial oxidation of natural organic matter, as evidenced from δ^{13}C-DIC values, is likely a major contributor to reductive mineral weathering processes that play a role in As mobilization in these sediments. These factors and processes may be occurring individually or simultaneously in different parts of the aquifer, and thus a synergistic effect could be leading to these unprecedented levels (> 4 mg/l) of As in the groundwater. Variable flow paths caused by well-pumping and the heterogeneous nature of the paleo depositional environment are other major factors controlling the high spatial variability of As in these fluvial environments.

Though relatively low (< 52 μg/l) amounts of As were detected in the deeper (> 60 m) aquifers, great caution should be used when exploring new possibilities for alternative drinking water sources in this region. Also, since irrigation wells in the region are pumping excessive volumes of deeper groundwater, deeper aquifers should be used solely as a drinking water source and not be

exploited for irrigation because over-pumping could lead to drawdown and subsequent contamination of the deeper aquifer.

West Bengal, like Bangladesh and other neighboring regions characterized by deltaic systems, is facing a crisis of As-tainted drinking waters in its local to regional aquifers. Local populations have been suffering from this calamity for more than a decade. Any arsenic research goes beyond the science; the reality of advocating science lies where risk assessment, safe mitigation and alternative measures are implemented to alleviate sufferings of the people. It has been estimated that 200 million people worldwide are at risk from drinking water containing high concentrations of arsenic, a number which is expected to increase due to recent lowering of the recommended standard for arsenic concentrations in drinking waters to 10 μg/l. Some authorities are considering lowering this value even further. This current work tried to link the occurrence of geogenic arsenic in different environments and potential contamination of groundwaters and their probable effect on human society. Much more research is needed to understand the propogation of arsenic in the food chain, finding optimal mitigation measures, sustaining deep aquifers, and overall, providing arsenic safe drinking water and food to millions of people in this region.

References

Acharyya, S.K., Chakraborty, P., Lahiri, S., Raymahashay, B.C., Guha, S., Bhowmik, A. 1999. Arsenic poisoning in the Ganges delta. Nature. 401, 545.

Acharyya, S.K. and B.A. Shah. 2007. Groundwater arsenic contamination affecting different geologic domains in India – a review: influence of geologic setting, fluvial geomorphology and Quaternary stratigraphy. J. Env. Sci. Health. 42, 1795-1805.

Ahmed, K.M., Bhattacharya, P., Hasan, M.A., Akhter, S.H., Alam, S.M.M., Bhuyian, M.A.H., Imam, M.B., Khan, A.A., Sracek, O. 2004. Arsenic enrichment in groundwater of the alluvial aquifers in Bangladesh: an overview. App. Geochem. 19, 181-200.

Alam, M.G.M., Tokunaga, S., Maekawa, T. 2001. Extraction of arsenic in a synthetic arsenic-contaminated soil using phosphate. Chemosphere. 43, 1035-1041.

Andrade, S., Ulbrich, H.H., Janasi, V.A., Navarro, M.S. 2009. The determination of total hydrogen, carbon, nitrogen and sulfur in silicates, silicate rocks, soils and sediments. Geostandards and Geoanalytical Research. 33, 337-345.

Appelo, C.A.J. and D. Postma. 1996. Geochemistry, Groundwater and Pollution. Rotterdam: Balkema.

Armienta, M.A. and N. Segovia. Arsenic and fluoride in the groundwater of Mexico. Environ. Geochem. Health. 30, 345-353.

Baig, J.A., Kazi, T.G., Shah, A.Q., Kandhro, G.A., Afridi, H.I., Arain, M.B., Jamali, M.K., Jalbani, N. 2010. Speciation and evaluation of Arsenic in surface water and groundwater samples: A multivariate case study. Ecotoxic. And Environ. Safety. 73, 914-923.

BGS and DPHE (British Geological Survey and Department of Public Health and Engineering), 2001. Arsenic contamination of groundwater in Bangladesh. *In*: Kinniburgh, D.G., Smedley, P.L. (Eds.), British Geological Survey (Technical Report, WC/00/19. 4 Volumes) British Geological Survey, Keyworth.

Bostick, B.C. and S. Fendorf. 2003. Arsenite sorption on troilite (FeS) and pyrite (FeS_2). Geochem. Cosmochim. Acta. 67, 909-921.

Bundschuh, J., Farias, B., Martin, R., Storniolo, A., Bhattacharya, P., Cortes, J., Bonorino, G., Albouy, R. 2004. Groundwater arsenic in the Chaco-Pampean Plain, Argentina: Case study from Robles County, Santiago del Estero Province. App. Geochem. 19, 231-243.

Bundschuh, J., Perez-Cerrera, A., Litter, M.I. 2008. Distribucion del arsenico en las regones Iberica e Iberoamericana. Ed. Prog. Iberoamericano de Ciencia y Technol. para el Desarrollo, Buenos Aires, Argentina. Available at: http://www.cnea.gov/ar/xxi/ambiental/iberoarsen.

Bundschuh, J., Armineta, M.A., Birkle, P., Bhattacharya, P., Matschullat, J., Mukherjee, A.B. 2009. Natural Arsenic in Groundwater of Latin America. *In*: Bundschuh, J. and P. Bhattacharya (series eds): Arsenic in the environment, Volume 1. CRC Press/Balkema Publisher, Leiden, The Netherlands.

Burgess, W.G., Hoque, M.A., Michael, H.A., Voss, C.I., Breit, G.N., Ahmed, K.M. 2010. Vulnerability of deep groundwater in the Bengal Aquifer System to contamination by arsenic. Nat. Geosci. 3, 83-87.

Burnol, A. and L. Charlet. 2010. Fe(II)—Fe(III)-bearing phases as a mineralogical control on the heterogeneity of arsenic in Southeast Asian groundwater. Environ. Sci. Technol. 44, 7541-7547.

Charlet, L. and Polya D.A. 2006. Arsenic in shallow, reducing groundwaters in southern Asia: An environmental health disaster. Elements. 2, 91-96.

Charlet, L., Chakraborty, S., Appelo, C.A.J., Roman-Ross, G., Nath, B., Ansari, A.A., Lanson, M., Chatterjee, D., Mallik, S.B., 2007. Chemodynamics of an arsenic "hotspot" in a West Bengal aquifer: A field and reactive transport modeling study. App. Geochem. 22, 1273-1292.

Chapman Conference. 2009. AGU Chapman Conference on Arsenic in Groundwater of Southeast Asia. Siem Reap, Cambodia, 24-27 March. (http://www.agu.org/meetings/chapman/2009/acall/)

Chappelle, F.H. 2001. Ground-water microbiology and geochemistry, John Wiley & Sons Ltd, New York.

Chen, Y., Parvez, F., Gamble, M., Islam, T., Ahmed, A., Argos, M., Graziano, J.H., Ahsan, H. 2009. Arsenic exposure at low-to-moderate levels and skin lesions, arsenic metabolism, neurological functions, and biomarkers for respiratory and cardiovascular diseases: Review of recent findings from the Health Effects of Arsenic Longitudinal Study (HEALS) in Bangladesh. Toxicol. Appl. Pharmacol. 239, 184-192.

Cheng, Z., Zheng, Y., Mortlock, R., van Geen, A., 2004. Rapid multielement analysis of groundwater by high-resolution inductively coupled plasma mass spectrometry. Anal. and Bioanal. Chem. 379, 513-518.

Clauer, N., and Chaudhuri, S. 1995. Clays in Crustal Environments (Isotope dating and Tracing). Springer, 359 p.

Coplen, T.B. 1994. Reporting of stable hydrogen, carbon, and oxygen isotope abundances. Pure & Appl. Chem. 66, 273-276.

Craig, H., 1961. Isotopic Variations in Meteoric Waters. Science. 133, 1702-1703.

Cullen, W.R. and K.J. Reimer. 1989. Arsenic speciation in the environment. Chemical Reviews. 89, 713-764.

Das, D., Basu, G., Chowdhury, T.R., Chakraborty, D. 1995. Bore-hole soil-sediment analysis of some As affected areas. *In*: Proc. Int. Conf. on Arsenic in groundwater: cause, effect and remedy.

Datta, S., Mailloux, B., Jung, H.B., Hoque, M.A., Stute, M., Ahmed, K.M., Zheng, Y., 2009. Redox trapping of arsenic during groundwater discharge in sediments from the Meghna riverbank in Bangladesh. Proc. Natl. Acad. Sci. 106, 16930-16935.

Datta,S., Neal, A., Johannesson, K., Haug, J., Sarkar, D., Sur,P., Purkait, B. 2010a. Geochemical and mineralogical contrasts between low and very high arsenic affected areas in Murshidabad district, West Bengal, India. Arsenic in Geosphere and Human Diseases. Eds. Jean, J.S., Bundschuh, J., Bhattacharya, p. 110-111.

Datta, S., Johannesson, K., Neal, A., Haug, J., Socki, R., Ocheltree, T. 2010b. Stable isotopic evaluation of arsenic hotspots and low As areas in Murshidabad, West Bengal, India. GSA Abstracts with Programs, Vol. 42, No. 5, p. 551. Abstract # 181534. National meeting, Denver, CO.

Dhar, R.K., Biswas, B.K., Samanta, G., Mandal, B.K., Chakraborti, D., Roy, S., Jafar, A., Islam, A., Ara, G., Kabir, S., Khan, A.W., Ahmed, S.A., Hadi, S.A., 1997. Groundwater arsenic calamity in Bangladesh. Current Science. 73, 48-59.

Dhar, R. K., Y. Zheng, P. Rubenstone, van Geen, A. 2004. A rapid colorimetric method for measuring arsenic concentration in groundwater. Analytica Chimica Acta. 526, 203-209.

Dhar, R.K., Zheng, Y., Stute, M., van Geen, A., Cheng, Z., Shanewaz, M., Shamsudduha, M., Hoque, M.A., Rahman, M.W., Ahmed, K.M., 2008. Temporal variability of groundwater chemistry in shallow and deep aquifers of Araihazar, Bangladesh. J. Cont. Hydrol. 99, 97-111.

Dowling, C.B., Poreda, R.J., Basu, A.R., Peters, S.L. 2002. Geochemical study of arsenic release mechanisms in the Bengal Basin groundwater. Water Resour. Res. 38, 1173.

Dzombak D.A. and F.M.M. Morel. 1990. Surface Complexation Modeling- Hydrous Ferric Oxide. John Wiley, New York.

Ficklin, W.H. 1983. Separation of As(III) and As(V) in ground waters by ion-exchange. Talanta. 30, 371-373.

Fendorf, S., Michael, H.A., van Geen, A. 2010. Spatial and temporal variations of groundwater arsenic in South and Southeast Asia. Science. 328, 1123-1127.

Garai, R., Chakraborty, A.K., Dey, S.B., Saha, K.C. 1984. Chronic arsenic poisoning from tube-well water. J. Indian Med. Assoc. 82, 34-35.

Garcia, M.E. and J. Bundschuh. 2006. Control mechanisms of seasonal variation of dissolved arsenic and heavy metal concentrations in surface waters of Lake Poopo basin, Bolivia. GSA Annual Meeting, Philadelphia, 22-25 Oct, 2006. 38(7):320.

Garzanti, E., Ando, S., France-Lanord, C., Vezzoli, G., Censi, P., Galy, V., Najman, Y. 2010. Mineralogical and chemical variability of fluvial sediments 1. Bedload sand (Ganga-Brahmaputra, Bangladesh). Earth Plan. Sci. Letters. 299, 368-381.

Ghosh, A.K., Sarkar, D., Bhattacharyya, P., Maurya, U.K., Nayak, D.C. 2006. Mineralogical study of some arsenic contaminated soils of West Bengal, India. Geoderma. 136, 300-309.

Goodbred, S.L., Kuehl, S.A., Steckler, M.S., Sarker, M.H. 2003. Controls on facies distribution and stratigraphic preservation in the Ganges-Brahmaputra delta sequence. Sed. Geol. 155, 301-316.

Guha Mazumder, D.N., Haque, R., Ghosh, N., Binay, K.D., Santra, A., Chakraborty, D., Smith, A.H. 1998. Arsenic levels in drinking water and the prevalence of skin lesions in West Bengal, India. Int. J. Epidemiol. 21, 871-877.

Hamon, R.E., McLaughlin, M.J., Gilkes, R.J., Rate, A.W., Zarcinas, B., Robertson, A., Cozens, G., Radford, N., Bettenay, L. 2004. Geochemical indices allow estimation of heavy metal background concentrations in soils. Global Biogeochemical Cycles. 18, GB1014.

Haque, S.E., Johannesson, K.H. 2006. Arsenic concentrations and speciation along a groundwater flow path: The Carrizo Sand aquifer, Texas, USA. Chem. Geol. 228, 57-71.

Haque, S., Junfeng, J., Johannesson, K.H. 2008. Evaluation mobilization and transport of arsenic in sediments and groundwaters of Aquia aquifer, Maryland, USA. J. Cont. Hydrol. 99, 68-84.

Harvey, C.F., Swartz, C.H., Badruzzaman, A.B.M., Keon-Blute, N., Yu, W., Ali, M.A., Jay, J., Beckie, R., Niedan, V., Brabander, D., Oates, P.M., Ashfaque, K.N., Islam, S., Hemond, H.F., Ahmed, M.F., 2002. Arsenic mobility and groundwater extraction in Bangladesh. Science. 298, 1602-1606.

Harvey, C.F., Swartz, C.H., Badruzzaman, A.B.M., Keon-Blute, N., Yu, W., Ali, M.A., Jay, J., Beckie, R., Niedan, V., Brabander, D., Oates, P.M., Ashfaque, K.N., Islam, S., Hemond, H.F., Ahmed, M.F., 2005. Groundwater arsenic contamination on the Ganges Delta: biogeochemistry,

hydrology, human perturbations, and human suffering on a large scale. C.R. Geoscience. 337, 285-296.

Harvey, C.F., Ashfaque, K.N., Yu, W., Badruzzaman, A.B.M., Ali, M.A., Oates, P.M., Michael, H.A., Neumann, R.B., Beckie, R., Islam, S., Ahmed, M.F. 2006. Groundwater dynamics and arsenic contamination in Bangladesh. Chem. Geol. 228, 112-136.

Hasan, M.A., von Brömssen, M., Bhattacharya, P., Ahmed, K.M., Siker, A.M., Jacks, G., Sracek, O., 2009. Geochemistry and mineralogy of shallow alluvial aquifers in Daudkandi upazila in the Meghna flood plain, Bangladesh. Environ. Geol. 57, 499-511.

He, Y.T., Fitzmaurice, A.G., Bilgin, A., Choi, S., O'Day, P., Horst, J., Harrington, J., Reisinger, H.J., Burris, D.R., Hering, J.G. 2010. Geochemical processes controlling arsenic mobility in groundwater: A case study of arsenic mobilization and natural attenuation. App. Geochem. 25, 69-80.

Hopenhayn, C. 2006. Arsenic in drinking water: impact on human health. Elements. 2, 103-107.

Hopenhayn-Rich, C., Biggs, M.L., Fuchs, A., Bergoglio, R., Tello, E.E., Nicolli, H., Smith, A.H. 1996. Bladder-cancer mortality associated with arsenic in drinking water in Argentina. Epidemiol. 7, 117-124.

Hoque, M.A., Khan, A.A., Shamsudduha, M., Hossain, M.S., Islam, T., Chowdhury, S.H. 2009. Near surface lithology and spatial variation of arsenic in the shallow groundwater: southeastern Bangladesh. Environ. Geol. 56, 1687-1695.

Horneman, A., van Geen, A., Kent, D., Mathe, P. E., Zheng, Y., Dhar, R. K., O'Connell, S., Hoque, M.A., Aziz, Z., Shamsudduha, M., Seddique, A., Ahmed, K. M. 2004. Decoupling of arsenic and iron release to Bangladesh groundwater under reducing conditions. Part I: Evidence from sediment profiles. Geochim. Cosmochim. Acta. *68*, 3459-3473.

Imam, B., Alam, M., Akhter, S.H., Choudhury, S.Q., Hasan, M.A., Ahmed, K.M. 1997. Sedimentological and mineralogical studies on arsenic contaminated aquifers in Bangladesh. Department of Geology, Dhaka University, for Bangladesh Water Development Board.

Itai, T., Takahashi, Y., Seddique, A.A., Maruoka, T., Mitamura, M. 2010. Variations in the redox state of As and Fe measured by X-ray absorption spectroscopy in aquifers of Bangladesh and their effect on As adsorption. App. Geochem. 25, 34-47.

Jakariya, M., Vahter, M., Rahman, M., Wahed, M.A., Hore, S.K., Bhattacharya, P., Jacks, G., Persson, L.A. 2007. Screening of arsenic in tubewell water with field test kits: evaluation of the method from public health perspective. Sci. Total Environ. 379, 167-175.

Jung, H.B., Zheng, Y. 2006. Enhanced recovery of arsenite sorbed onto synthetic oxides by L-ascorbic acid addition to phosphate solution: calibrating a sequential leaching method for the speciation analysis of arsenic in natural samples. Water Res. 40, 2168-2180.

Kane, J.S., Arbogast, B.F., Leventhal, J.S. 1990. Characterization of Devonian Ohio Shale SDO-1 as a USGS geochemical reference sample. Geostandards Newsletter. 14, 169-196.

Keon, N.E., Swartz, C., Brabander, D.J., Harvey, C., Hemond, H.F. 2001. Validation of an arsenic sequential extraction method for evaluation mobility in sediments. Env. Sci. Technol. 35, 2778-2784.

Kocar, B.D., Herbel, M.J., Tufano, K.J., Fendorf, S. 2006. Contrasting effects of dissimilatory iron(III) and arsenic(V) reduction on arsenic retention and transport. Environ. Sci. Technol. 40, 6715-6721.

Kuznetsova, A.I., Rusakova, Y.A., Zarubina, O.V. 1999. Quality tests for determination of trace elements in mineral samples. J. Anal. Chem. 54, 898-902.

Langmuir, D. 1997. Aqueous environmental geochemistry. Upper Saddle River, New Jersey, Prentice Hall, 600 p.

Lawson, M., Ballentine, C.J., Polya, D.A., Boyce, A.J., Mondal, D., Chatterjee, D., Majumder, S., Biswas, A. 2008. The geochemical and isotopic composition of ground waters in West Bengal: tracing ground-surface water interaction and its role in arsenic release. Mineralogical Magazine. 72, 441-444.

Lin, Z. and Puls, R.W. 2000. Adsorption, desorption and oxidation of arsenic affected by clay minerals and aging process. Environ. Geol. 39, 753-759.

Lin, N.F., Tang, J., Bian, J.M. 2002. Characteristics of environmental geochemistry in the arseniasis area of the Inner Mongolia of China. Environ. Geochem. Health. 24, 249-259.

Lin, Z. and Puls, R.W. 2003. Potential indicators for the assessment of arsenic natural attenuation in the subsurface. Adv. Environ. Res. 7, 825-834.

Loeppert, R.H., Jain, A., Abd El-Haleem, M.A., Biswas, B.K. 2003. Quantity and speciation of arsenic in soils by chemical extraction. *In*: Biogeochemistry of environmentally important trace elements. 42-56.

Lozano, R. and J.P. Bernal. 2005. Characterization of a new set of eight geochemical reference materials for XRF major and trace element analysis. Revista Mexicana de Ciencias Geologicas. 22, 329-344.

Luo, Z.D., Zhang, Y.M., Ma, L. 1997. Chronic arsenicism and cancer in inner Mongolia – consequences of well-water arsenic level greater than 50 mg/L. *In*: Arsenic Exposure and Health Effects (eds C.O. Abernathy, R.L. Calderon and W.R. Chappell), Chapman and Hall, London.

Magrisso, S., Belkin, S., Erel, Y. 2009. Lead bioavailability in soil and soil components. Water Air and Soil Pollution. 202, 315-323.

Mailloux, B.J., Alexandrova, E., Keimowitz, A.R., Wovkulich, K., Freyer, G.A., Herron, M., Stolz, J.F., Kenna, T.C., Pichler, T., Polizzotto, M.L., Dong, H., Bishop, M., Knappett, P.S.K., 2009. Microbial mineral weathering for nutrient acquisition releases arsenic. App. Env. Microbiol. 75, 2558-2565.

Manning, B.A, and Goldberg, S. 1996. Modeling competitive adsorption of arsenate with phosphate and molybdate on oxide minerals. Soil Sci. Soc. Am. J. 60, 121-131.

Mason, B. and L.G. Berry. 1978. Elements of Mineralogy. New York. Freeman.

McArthur, J.M., Ravenscroft, P., Safiulla, S., Thirlwall, M.F., 2001. Arsenic in groundwater: Testing pollution mechanisms for sedimentary aquifers in Bangladesh. Water Resour. Res. 37, 109-117.

McArthur, J.M., Banerjee, D.M., Hudson-Edwards, K.A., Mishra, R., Purohit, R., Ravenscroft, P., Cronin, A., Howarth, R.J., Chatterjee, A., Talukder, T., Lowry, D., Houghton, S., Chadha, D.K., 2004. Natural organic matter in sedimentary basins and its relation to arsenic in anoxic ground water: the example of West Bengal and its worldwide implications. App. Geochem, 19, 1255-1293.

McArthur, J.M., Ravenscroft, P., Banerjee, D.M., Milsom, J., Hudson-Edwards, K.A., Sengupta, S., Bristow, C., Sarkar, A., Tonkin, S., Purohit, R., 2008. How paleosols influence groundwater flow and arsenic pollution: A model from the Bengal Basin and its worldwide implication. Water Resour. Res. 44, W11411.

McArthur, J.M., Banerjee, D.M., Sengupta, S., Ravenscroft, P., Klump, S., Sarkar, A., Disch, B., Kipfer, R. 2010. Migraton of As, and $^{3}He/^{3}H$ ages, in groundwater from West Bengal: Implications for monitoring. Water Res. 44, 4171-4185.

Meng, X.G., Bang, S., Korfiatis, G.P. 2000. Effects of silicate, sulfate, and carbonate on arsenic removal by ferric chloride. Water Res. 34, 1255-1261.

Michael, H.A. and C. Voss. 2009. Controls on groundwater flow in the Bengal Basin of India and Bangladesh: regional modeling analysis. Hydrogeol. J. 17, 1561-1577.

Morgan, J.P. and W.G. McIntire. 1959. Quaternary geology of Bengal Basin, East Pakistan, and India. GSA Bulletin. 70, 319-342.

Mukherjee, A., Fryar, A.E., Howell, P.D. 2007a. Regional hydrostratigraphy and groundwater flow modeling in the arsenic-affected areas of the western Bengal basin, West Bengal, India. Hydrogeol. J. 15, 1397-1418.

Mukherjee, A., Fryar, A.E., Rowe, H. D., 2007b. Regional scale stable isotopic signatures of recharge and deep groundwater in the arsenic affected areas of West Bengal, India. 334, 151-161.

Mukherjee, A., von Brömssen, M., Scanlon, B., Bhattacharya, P., Fryar, A.E., Hasan, M.A., Ahmed, K.M., Chatterjee, D., Jacks, G., Sracek, O., 2008. Hydrogeochemical comparison and effects of overlapping redox zones on groundwater arsenic near the Western (Bhagirathi sub-basin, India) and Eastern (Meghna sub-basin, Bangladesh) margins of the Bengal Basin. J. Cont. Hydrol. 99, 31-48.

Mukherjee, A., Fryar, A.E., Thomas, W.A., 2009a. Geologic, geomorphic and hydrologic framework and evolution of the Bengal basin, India and Bangladesh. J. Asian Earth. Sci. 34, 227-244.

Mukherjee, A., Fryar, A.E., O'Shea, B.M. 2009b. Major occurrences of elevated arsenic in groundwater and other natural waters. *In*: Arsenic: environmental chemistry, health threats and waste treatment. John Wiley & Sons Ltd, New York.

Mukherjee, A., Fryar, A.E., Bhattacharya, P. 2010. Regional to local-scale extent and controls on existence of deeper groundwater arsenic in western parts of Bengal Basin. GSA Program with Abstracts. 42, 550.

Mukherjee-Goswami, A., Nath, B., Jana, J., Sahu, S.J., Sarkar, M.J., Jacks, G., Bhattacharya, P., Mukherjee, A., Polya, D.A., Jean, J., Chatterjee, D., 2008. Hydrogeochemical behavior of arsenic-enriched groundwater in the deltaic environment: Comparison between two study sites in West Bengal, India. J. Cont. Hydro. 99, 22-30.

Naidu, R., Smith, E., Owens, G., Bhattacharya, P., Nadebaum, P. 2006. Managing arsenic in the environment from soil to human health. Australia: CSIRO Publishing, 656 p.

Naidu, R., Smith, E., Huq, S.M.I, Owens, G., 2009. Sorption and bioavailability of arsenic in selected Bangladesh soils. Environ. Geochem. Health. 31, 61-68.

Nath, B., Berner, Z., Basu Mallik, S., Chatterjee, D., Charlet, L., Stuben, D., 2005. Characterization of aquifers conducting groundwaters with low and high arsenic concentrations: a comparative case study from West Bengal, India. Mineral Magazine. 69, 841-853.

Nath, B., Sahu, S.J., Jana, J., Mukherjee-Goswami, A.; Roy, S., Sarkar, M.J., Chatterjee, D. 2008. Hydrochemistry of arsenic-enriched aquifer from rural West Bengal, India: A study of the arsenic exposure and mitigation option. Water Air Soil Pollut. 190, 95-113.

Nath, B., Chakraborty, S., Burnol, A., Stuben, D., Chatterjee, D., Charlet, L. 2009. Mobility of arsenic in the sub-surface environment: An integrated hydrogeochemical study and sorption model of the sandy aquifer materials. J. Hydrol. 364, 236-248.

Neal, A., Datta, S., Haug, J., Johannesson, K., Purkait, B., Sarkar, D., Sur, P. 2009. Geochemistry of arsenic hotspots in Murshidabad and surrounding areas in West Bengal, India. GSA Abstracts with Programs, Vol. 41, No. 7, p. 463. Abstract # 163397. National meeting, Portland, OR.

Neal, A., Haug, J., Socki, R., Ocheltree, T., Petroske, E., Johannesson, K., Dhar, R., Datta, S. 2010a. Understanding heterogeneity in sediment geochemistry in contrasting groundwater arsenic bearing environments in Murshidabad, West Bengal, India. GSA Abstracts with Programs, Vol. 42, No. 5, p. 551. Abstract # 182258. National meeting, Denver, CO.

Neal, A., Haug, J., Johannesson, K., Purkait, B., Datta, S. 2010b. Comparative geochemical analysis of arsenic hotspots and low-As areas in Murshidabad, West Bengal, India. Goldschmidt Conference. International meeting, Knoxville, TN.

Neal, A., Datta, S., Johannesson, K., Haug, J., Purkait, B. Geochemistry of arsenic hotspots and surrounding areas in Murshidabad, West Bengal, India. 2010c. GSA Abstracts with Programs, Vol. 42, No. 2, p. 95. Abstract # 170471. NC/SC regional meeting, Branson, MO.

Neumann, R.B., Ashfaque, K.N., Badruzzaman, A.B.M., Ali, M.A., Shoemaker, J.K., Harvey, C.F., 2010. Anthropogenic influences on groundwater arsenic concentrations in Bangladesh. Nat. Geosci. 3, 46-52.

Nicolli, H.B., Suriano, J.M., Peal, M.A.G., Ferpozzi, L.H., Baleani, O.A. 1989. Groundwater contamination with arsenic and other trace-elements in an area of the Pampa, province of Cordoba, Argentina. Environ. Geol. Water Sci. 14, 3-16.

Nickson, R., McArthur, J.M., Burgess, W.G., Ahmed, K.M., Ravenscroft, P. Rahman, M., 1998. Arsenic poisoning in Bangladesh groundwater. Nature. 395, 338.

Nickson, R., McArthur, J.M., Ravenscroft, P., Burgess, W.G., Ahmed, K.M. 2000. Mechanism of arsenic release to groundwater, Bangladesh and West Bengal. App. Geochem. 15, 403-413.

Nordstrom, D.K. 2000. An overview of arsenic mass poisoning in Bangladesh and West Bengal India. *In*: Young, C. (Ed.), Minor Elements 2000. Processing and Environmental Aspects of As, Sb, Se, Te, and Bi. Society for Mining, Metallurgy and Exploration, p. 21-30.

Nordstrom, D.K. 2002. Public health – worldwide concerns of arsenic in groundwater. Science. 296, 2143-2145.

O'Shea, B.M. 2006. Delineating the source, geochemical sinks and aqueous mobilization processes of naturally occurring arsenic in a coastal sandy aquifer, Stuarts Point, New South Wales, Australia. Ph.D. thesis. University of New South Wales, Sydney.

Pal, T., Mukherjee, P.K., Sengupta, S., Bhattacharya, A.K., Shome, S. 2002. Arsenic pollution in groundwater of West Bengal, India – An insight into the problem by subsurface sediment analysis. Gondwana Res. 5, 501-512.

Parvez, F., Chen, Y., Brandt-Rauf, P.W., Slavkovich, V., Islam, T., Ahmed, A., Argos, M., Hassan, R., Yunus, M., Haque, S.E., Balac, O., Graziano, J.H., Ahsan, H. 2010. A prospective study of respiratory symptoms associated with chronic arsenic exposure in Bangladesh: findings from the Health Effects of Arsenic Longitudinal Study (HEALS). Thorax. 65, 528-533.

PHED (Public Health Engineering Department). 1991. Arsenic pollution in groundwater in West Bengal. Report of arsenic investigation project to the National Drinking Water Mission, Delhi, India.

Plant, J.A., Kinniburgh, D.G., Smedley, P.L., Fordyce, F.M., Klinck, B.A. 2003. Arsenic and Selenium. British Geological Survey, Keyworth, Nottingham, UK. 50 p.

Polizzotto, M.L., Harvey, C.F., Sutton, S.R., Fendorf, S., 2005. Processes conducive to the release and transport of arsenic into aquifers of Bangladesh. Proc. Natl. Acad. Sci. 102, 18819-18823.

Polizzotto, M.L., Harvey, C.F., Li, G., Badruzzman, B., Ali, A., Newville, M., Sutton, S., Fendorf, S., 2006. Solid-phases and desorption processes of arsenic within Bangladesh sediments. Chem. Geology. 228, 97-111.

Polizzotto, M.L., Kocar, B.D., Benner, S.G., Sampson, M., Fendorf, S. 2008. Near-surface wetland sediments as a source of arsenic release to ground water in Asia. Nature. 454, 505-U5.

Radloff, K.A., Cheng, Z.Q., Rahman, M.W., Ahmed, K.M., Mailloux, B.J., Juhl, A.R., Schlosser, P., van Geen, A. 2007. Mobilization of arsenic during one-year incubations of grey aquifer sands from Araihazar, Bangladesh. Environ. Sci. Technol. 41, 3639-3645.

Rahman, M.M., Naidu, R., Bhattacharya, P. 2009. Arsenic contamination in groundwater in the Southeast Asia region. Environ. Geochem. Health. 31, 9-21.

Ravenscroft, P. 2003. Overview of the hydrogeology of Bangladesh. *In*: Rahman, A.A., Ravenscroft, P. (eds.) Groundwater resources development in Bangladesh. The University Press, Dhaka 43-86.

Ravenscroft, P., Burgess, W.G., Ahmed, K.M., Burren, M., Perrin, J., 2005. Arsenic in groundwater of the Bengal Basin, Bangladesh: Distribution, field relations, and hydrogeological setting. Hydrogeo. J. 13, 727-751.

Raymahashay, B.C., Khare, A.S. 2003. The arsenic cycle in Late Quaternary fluvial sediments: mineralogical considerations. Current Science. 84, 1102-1104.

Reza, A.H.M.S., Jean, J-S., Yang, H-J., Lee, M-K., Woodall, B., Liu, C-C., Lee, J-F., Luo, S-D. 2010. Occurrence of arsenic in core sediments and groundwater in the Chapai-Nawabganj District, northwestern Bangladesh. Water Res. 44, 2010-2037.

Saha, A.K. and C. Chakrabarti. 1995. Geological and geochemical background of the As bearing groundwater occurrences of West Bengal. *In*: Proc. Int. Conf. on Arsenic in groundwater: cause, effect and remedy.

Sankararamakrishnan, K., Chauhan, D., Nickson, R.T., Tripathi, R.M., Iyengar, L. 2008. Evaluation of two commercial field test kits used for screening of groundwater for As in northern India. Sci. Total Environ. 401, 162-167.

Saunders, J.A., Mohammad, S., Korte, N.E., Lee, M.K., Fayek, M., Castle, D., Barnet., M.O. 2005. Groundwater geochemistry, microbiology, and mineralogy in two arsenic-bearing Holocene alluvial aquifers from the United States. Advances in arsenic research - integration of experimental and observational: studies and implications for mitigation. ACS Symposium Series. 915, 191-205.

Saunders, J.A., Lee, M.K., Shamsudduha, M., Dhakal, P., Uddin, A., Chowdhury, M.T., Ahmed, K.M. 2008. Geochemistry and mineralogy of arsenic in (natural) anaerobic groundwaters. App. Geochem. 23, 3205-3214.

Seddique, A.A., Masuda, H., Mitamura, M., Shinoda, K., Yamanaka, T., Itai, T., Maruoka, T., Uesugi, K., Ahmed, K.M., Biswas, D.K. 2008. Arsenic release from biotite into a Holocene aquifer in Bangladesh. App. Geochem. 23, 2236-2248.

Sengupta, S., McArthur, J.M., Sarkar, A., Leng, M.J., Ravenscroft, P., Howarth, R.J., Banerjee, D.M. 2008. Do ponds cause arsenic-pollution of groundwater in the Bengal Basin? An answer from West Bengal. Environ. Sci Technol. 42, 5156-5164.

Sikdar, P.K. and P. Sahu. 2009. Understanding wetland sub-surface hydrology using geologic and isotopic signatures. Hydrol. Earth Syst. Sci. 13, 1313-1323.

Sinha, R., Kettanah, Y., Gibling, M.R., Tandon, S.K., Jain, M., Bhattacharjee, P.S., Dasgupta, A.S., Ghazanfari, P. 2009. Craton-derived alluvium as a major sediment source in the Himalayan Foreland Basin of India. GSA Bulletin. 121, 1596-1610.

Smedley, P.L. and D.G. Kinniburgh, 2002. A review of the source, behavior, and distribution of arsenic in natural waters. App. Geochem. 17, 517-568.

Smedley, P.L., Nicolli, H.B., Macdonald, D.M.J., Barros, A.J., Tullio, J.O. 2002. Hydrogeochemistry of arsenic and other inorganic constituents in groundwaters from La Pampa, Argentina. App. Geochem. 17, 259-284.

Smedley, P.L., Kinniburgh, D.G., Macdonald, D.M.J., Nicolli, H.B., Barros, A.J., Tullio, J.O., Pearce, J.M., Alonso, M.S. 2005. Arsenic associations in sediments from the loess aquifer of La Pampa, Argentina. App. Geochem. 20, 989-1016.

Smith, A.H., Lingas, E.O., Rahman, M. 2000. Contamination of drinking-water by arsenic in Bangladesh: a public health emergency. Bulletin of the World Health Organziation. 78, 1093-1103.

Smith, A.H., Steinmaus, C.M. 2009. Health effects of arsenic and chromium in drinking water: recent human findings. Annual Review of Public Health. 30, 107-122.

Stüben, D., Berner, Z., Chandrasekharam, D., Karmakar, J., 2003. Arsenic enrichment in groundwater of West Bengal, India: geochemical evidence for mobilization of As under reducing conditions. App. Geochem. 18, 1417-1434.

Stute, M., Zheng, Y., Schlosser, P., Horneman, A., Dhar, R.K., Datta, S., Hoque, M.A., Seddique, A.A., Shamsudduha, M., Ahmed, K.M., van Geen, A., 2007. Hydrological control of As concentrations in Bangladesh groundwater. Water Resour. Res. 43, W09417.

Subramanian, V. 1996. The sediment load of India – an update. Erosion and Sediment Yield: Global and Regional Perspectives (Proceedings of the Exeter Symposium). IAHS Publ. 236.

Sur, P. 2006. Mineralogical and geochemical investigations of sediments and waters from river Ganges with special application to arsenic contamination of groundwaters in the aquifers of Murshidabad district, West Bengal. M.Sc. Thesis.

Swartz, C.H., Keon-Blute, N., Badruzzaman, B., Ali, A., Brabander, D., Jay, J., Bensancon, J., Islam, S., Hemond, H.F., Harvey, C.F. 2004. Mobility of arsenic in a Bangladesh aquifer: inferences from geochemical profiles, leaching data, and mineralogical characterization. Geochim. Cosmochim. Acta. 68, 4539-4557.

Tareq, S.M., Safiullah, S., Anawar, H.M., Rahman, M.M., Ishizuka, T. 2003. Arsenic pollution in groundwater: a self-organizing complex geochemical process in the deltaic sedimentary environment, Bangladesh. Sci. Total Environ. 313, 213-226.

Tessier, A., Campbell, P.G.C., Bisson, M. 1979. Sequential extraction procedure for the speciation of particulate trace metals. Anal. Chem. 51, no. 7.

van Geen, A., Zheng, Y., Versteeg, R., Stute, M., Horneman, A., Dhar, R., Steckler, M., Gelman, A., Small, C., Ahsan, H., Graziano, J.H., Hussain, I., Ahmed, K.M., 2003. Spatial variability of arsenic in 6000 tube wells in a 25 km^2 area of Bangladesh. Water Resour. Res. 39, 1140.

van Geen, A., Protus, T., Cheng, Z., Horneman, A. 2004. Testing groundwater for arsenic in Bangladesh before installing a well. Environ. Sci. Technol. 38, 6783-6789.

van Geen, A., Cheng, Z., Seddique, A.A., Hoque, M.A., Gelman, A., Graziano, J.H., Ahsan, H., Parvez, F., Ahmed, K.M. 2005a. Reliability of a commercial kit to test groundwater for arsenic in Bangladesh. Environ. Sci. Technol. 39, 299-303.

van Geen, A., Cheng, Z., Seddique, A.A., Hoque, M.A., Gelman, A., Graziano, J.H., Ahsan, H., Parvez, F., Ahmed, K.M. 2005b. Response to comment on "Reliability of a commercial kit to test groundwater for arsenic in Bangladesh". Environ. Sci. Technol. 39, 5503-5504.

van Geen, A., Zheng, Y., Cheng, Z., Aziz, Z., Hornmean, A., Dhar, R.K., Mailloux, B., Stute, M., Weinman, B., Goodbred, S., Seddique, A.A., Hoque, M.A., Ahmed, K.M. 2006. A transect of groundwater and sediment properties in Araihazar, Bangladesh: Further evidence of decoupling between As and Fe mobilization. Chem. Geol. 228, 85-96.

van Geen, A., Zheng, Y., Goodbred, S., Horneman, A., Aziz, Z., Cheng, Z., Stute, M., Mailloux, B., Weinman, B., Hoque, M.A., Seddique, M.A., Hossain, M.S., Chowdhury, S.H., Ahmed, K.M. 2008a. Flushing history as a hydrogeological control on the regional distribution of arsenic in shallow groundwater of the Bengal Basin. Environ. Sci. Technol. 42, 2283-2288.

van Geen, A., Radloff, K., Aziz, Z., Cheng, Z., Huq, M.R., Ahmed, K.M., Weinman, B., Goodbred, S., Jung, H.B., Zheng, Y., Charlet, L., Metral, J., Chakraborty, S., Gajurel, A.P., Upreti, B.N. 2008b. Comparison of arsenic concentrations in simultaneously-collected groundwater and aquifer particles from Bangladesh, India, Vietnam, and Nepal. App. Geochem. 23, 3244-3251.

van Geen, A. 2008c. Environmental science – Arsenic meets dense populations. Nat. Geosci. 1, 494-496.

Viollier, E., Inglett, P.W., Hunter, K., Roychoudhury, A.N., Cappellan, P. 2000. The ferrozine method revisited: Fe(II)/Fe(III) determination in natural waters. App. Geochem. 15, 785-790.

von Brömssen, M., Larsson, S.H., Bhattacharya, P., Hasan, M.Z., Ahmed, K.M., Jakariya, M., Sikder, M.A., Sracek, O., Biven, A., Dousova, B., Patriarca, C., Thunvik, R., Jacks, G. 2008. J. Cont. Hydro. 99, 137-149.

Wasserman, G.A., Liu, X.H., Parvez, F., Ahsan, H., Factor-Litvak, P., van Geen, A., Slavkovich, V., Lolacono, N.J., Cheng, Z.Q., Hussain, L., Momotaj, H., Graziano, J.H. 2004. Water arsenic

exposure and children's intellectual function in Araihazar, Bangladesh. Environ. Health Perspect. 112, 1329-1333.

Weinman, B., Goodbred, S.L., Zheng, Y., Aziz, Z., Steckler, M., van Geen, A., Singhvi, A.K., Nagar, Y.C. 2008. Contributions of floodplain stratigraphy and evolution to the spatial patterns of groundwater arsenic in Araihazar, Bangladesh. GSA Bulletin. 120, 1567-1580.

Welch, A.H., Lico, M.S., Hughes, J.L. 1988. Arsenic in ground water of the western United States. Ground Water. 26, 333-347.

Wenzel, W.W., Kirchbaumer, N., Prohaska, T., Stingeder, G., Lombi, E., Adriano, D.C. 2001. Arsenic fractionation in soils using improved sequential extraction procedure. Anal. Chem. Acta. 436, 309-323.

Wilkie, J.A and J.G. Hering 1998. Rapid oxidation of geothermal As(III) in streamwaters of the eastern Sierra Nevada. Environ. Sci. Technol. 32, 657-662.

Yu, W.H., Harvey, C.M., Harvey, C.F. 2003. Arsenic in groundwater in Bangladesh: A geostatistical and epidemiological frame work for evaluating health effects and potential remedies. Water. Resour. Res. 39, 1146.

Zahid, A., Hassan, M.Q., Breit, G.N., Balke, K.D., Flegr, M. 2009. Accumulation of iron and arsenic in the Chandina alluvium of the lower delta plain, Southeastern Bangladesh. Env. Geochem. Health. 31, 69-84.

Zarcinas, B.A., McLaughlin, M.J., Smart, M.K. 1996. The effect of acid digestion technique on the performance of nebulization systems used in inductively coupled plasma spectrometry. Commun. Soil Sci. Plant Anal. 27, 1331-1354.

Zarcinas, B.A., Pongsakul, P., McLaughlin, M.J., Cozens, C.G. 2004. Heavy metals in soils and crops in southeast Asia. 2. Thailand. Environ. Geochem. Health. 26, 359-371.

Zheng, Y., Stute, M., van Geen, A., Gavrieli, I., Dhar, R., Simpson, H.J., Schlosser, P., Ahmed, K.M., 2004. Redox control of arsenic mobilization in Bangladesh groundwater. App. Geochem. 19, 201-214.

Zheng, Y., van Geen, A., Stute, M., Dhar, R., Mo, Z., Cheng, Z., Horneman, A., Gavriell, I., Simpson, H.J., Versteg, R., Steckler, M., Grazioli-Venier, A., Goodbred, S., Shahnewaz, M., Shamsudduha, M., Hoque, M.A., Ahmed, K.M. 2005. Geochemical and hydrogeological contrasts between shallow and deeper aquifers in two villages of Araihazar, Bangladesh: Implications for deeper aquifers as drinking water sources. Geochim. Cosmochim. Acta. 69, 5203-5218.

Appendix A - Water Analyses

This section contains general data for water samples and results from laboratory analyses.

Water Chemistry Data

General data for water samples collected during June 2009 (continued on next page).

Sample ID	Latitude (N)	Longitude (E)	Well Depth (m)	Conductivity (µS/cm)	TDS (mg/l)	Dissolved Oxygen (mg/l)	HCO_3^- (mg/l)	As_T (µg/l)	As(III) (µg/l)	PO_4^{3-} (mg/l)
TW-1 (BM)	23°56.371	88°16.167	36.6	753	339	7.84	440			3.6
TW-2 (BM)	23°56.359	88°16.174	33.5	829	372	7.92	385	4035	3750	4.3
TW-2a (BM)	23°56.359	88°16.174	33.5	825	373	8.2	335			
TW-3 (BM)	23°56.396	88°16.130	33.5	819	363	7.64	334	310	375	1
TW-4 (BM)	23°56.372	88°16.131	34.1	772	352	7.09	290			
TW-5 (BM)	23°56.331	88°16.131	33.5	817	375	7.96	330			1
TW-6 (BM)	23°56.351	88°16.187	35.7	833	385	8.83	360			0.1
TW-7 (BM)	23°56.327	88°16.210	39.6	798	370	8.85	310			
TW-8 (BM)	23°56.399	88°16.187	36.0	762	352	8.52	335	3	2	0
TW-9 (BM)	23°56.353	88°15.994	33.5	796	371	8.63	360			
TW-10 (HK)	24°03.692	88°21.588	0.0	863	404	8.17	360	340	300	3.2
TW-11 (HK)	24°03.671	88°21.509	21.3	685	323	8.28	250			4.2
TW-12 (HK)	24°03.659	88°21.479	9.1	717	337	8.66	225	475	440	3.3
TW-13 (HB)	24°03.157	88°21.206	33.5	982	448	8.52	335	250	195	2.8
TW-14 (HB)	24°03.145	88°21.225	21.3	1108	515	8.52	340	280	155	4.6
TW-15 (HB)	24°03.128	88°21.215	33.5	1013	472	8.45	510	375	235	2.8
TW-16 (HB)	24°03.069	88°21.200	18.3	608	283	8.68	255			
TW-17 (HB)	24°03.182	88°21.199	30.5	794	368	7.59	290			0.6
TW-18 (HK)	24°03.559	88°21.531	18.3	782	361	8.25	360			1
TW-19 (HK)	24°03.569	88°21.528	15.2	757	353	8.17	330			2.8
TW-20 (JB)	24°12.668	88°41.345	21.3	854	398	4.64	330	190	120	4.5
TW-21 (JB)	24°12.658	88°41.369	21.3	933	411	5.88	325	584	404	2.5
TW-22 (JB)	24°12.686	88°41.338	42.7	852	388	8.5	325			2.3
TW-23 (JB)	--	--	0.0	1066	494	7.62	360			0.2
TW-24 (JB)	24°12.561	88°41.188	21.3	916	427	8.17	330	105	85	
TW-26 (JB)	24°12.575	88°41.289	64.0	1017	425	8.6	400			0.1
TW-27 (JB)	--	--	0.0	1000	430	8.69	440			
TW-27 (NR)	23°55.413	88°23.297	30.5	965	430	8.16	405	20	12	
TW-28 (NRJ)	23°54.153	88°28.084	21.3	1326	605	7.33	455	505	495	4.6
TW-29 (NRJ)	23°54.109	88°28.062	21.3	733	357	8.83	300			
TW-29 (NRJ) Dup	23°54.109	88°28.062	21.3	1457	710	7.91	455			

Continued from pevious page.

Sample ID	Latitude (N)	Longitude (E)	Well Depth (m)	Conductivity (µS/cm)	TDS (mg/l)	Dissolved Oxygen (mg/l)	HCO_3^- (mg/l)	As_T (µg/l)	As(III) (µg/l)	PO_4^{3-} (mg/l)
TW-30 (NRJ)	23°54.048	88°28.061	36.6	793	367	7.06	330			
TW-31 (NRJ)	23°54.062	88°28.048	27.4	791	367	6.28	325			
TW-32 (NB)	24°11.863	88°13.540	24.4	454	218	8.74	120	1	0.36	
TW-33 (NB)	24°11.881	88°13.534	21.3	740	347	8.4	125			
TW-34 (NB)	24°11.845	88°13.439	21.3	1153	561	8.56	110			
TW-35 (NB)	24°12.075	88°13.385	21.3	868	423	8.55	140			
GAP (JB)	24°12.619	88°41.256	64.0	999	436	8.31	525			0.2
IRW-60' (JB)	24°12.699	88°41.400	18.3	785	383	5.51	330	579	317	1.9
IRW-I (NRJ)	23°54.293	88°29.691	91.4	741	361	7.94	345			
IRW-II (NRJ)	23°54.286	88°30.032	137.2	934	450	8.6	360			0.2
M. Rahaman (JB)	--	--		897	436	9.02	410			
PW-2 (HK)	24°03.566	88°21.508		198	96.5	7.73	60			0
PW-3 (JB)	24°12.661	88°41.338		909	443	2.27	170			
PW-4 (JB)	24°12.678	88°41.397		709	345	3.21	210			
RW-1	24°11.637	88°15.764		211	103.1	8.97	120			
RW-2	24°13.509	88°16.050		224	108.1	8.76	80			
RW-3	24°14.441	88°15.402		831	103.1	9.35	95			0
RW-4	24°24.882	88°06.028		230	110.7	8.8	50			
RW-5	24°26.888	88°09.981		235	114.6	8.98	65			

General data for water samples collected during January 2010 (continued on next page).

Sample ID	Latitude (N)	Longitude (E)	Well Depth (m)	Temp. (°C)	pH	Conductivity (µS/cm)	Dissolved Oxygen (mg/l)	Redox Potential (mV)	HCO_3^- (mg/l)	NH_4^+ (mg/l)	PO_4^{3-} (mg/l)	As_T* (µg/l)
TW-36 (BM)	23°56.360	88°16.176	33.5	27.5	6.97	810.4	2.8	239	405	0.65	1	>500
TW-37 (BM)	23°56.377	88°16.189	33.5	27.3	7.05	763.7	3.5	320	370	0.2	0.7	0
TW-38 (BM)	23°56.276	88°16.178	33.5	27.1	7.05	787	4	170	370	0.25	1.2	50-70
TW-39 (BM)	23°56.392	88°16.129	33.5	27.2	7.04	746.3	2.96	85	290	2	2.6	70
TW-40 (BM)	23°56.329	88°16.131	33.5	27.4	7.01	787.7	2.38	118	375	0.8	1.8	>500
TW-43 (HK)	24°03.570	88°21.532	15.2	26.8	7.01	784.6	3.61	70	405	0.65	4.1	>500
TW-45 (HK)	24°03.511	88°21.531	15.2	26.9	6.95	849.5	3.22	70	365	1.35	3.7	70-300
TW-46 (HK)	24°03.557	88°21.533	18.3	27.2	6.94	785.4	3.73	71	390	1.5	2.9	70
TW-47 (HK)	24°03.580	88°21.523	15.2	26.9	6.92	765	4.71	67	350	1.25	3.9	
TW-48 (HK)	24°03.671	88°21.470	9.1	26.7	6.87	823.5	4.35	83	340	1.15	2.4	
TW-49 (HK)	24°03.697	88°21.477	15.2	26.7	6.96	805.2	3.1	57	390	1.25	3.5	
TW-50 (HK)	24°03.701	88°21.373	36.6	27.0	7.04	868.2	4.64	69	450	1.25	3.1	
TW-51 (HK)	24°03.729	88°21.389	21.3	26.4	6.91	824.5	3.24	76	425	1	3.3	
TW-56 (NB)	24°11.896	88°13.466	21.9	26.8	6.5	682	4.15	407	150	0	0.5	0
TW-57 (NB)	24°11.882	88°13.432	21.3	26.6	7	458.9	3.3	269	190	0	0.6	0
TW-58 (NB)	24°11.865	88°13.383	24.4	27.4	6.6	626	3	260	150	0	0.6	0
TW-59 (NB)	24°11.866	88°13.464	22.9	27.0	6.77	760	3.02	326	275	0	0.5	
TW-60 (NB)	24°11.877	88°13.528	30.5	26.8	6.71	447	2.4	308	110	0	0.2	
TW-61 (NB)	24°11.866	88°13.538	30.5	26.7	6.41	482.4	3.32	238	110	0	0.5	
TW-62 (NBK)	24°12.124	88°13.464	24.4	27.4	6.75	597	2.69	321	200	0	0.8	
TW-63 (NBK)	24°12.068	88°13.477	30.5	27.0	6.74	591	4.1	166	190	0	0.3	
TW-64 (KHN)	23°58.524	88°06.824	33.5	27.5	7.36	1358	2.62	125	470	0	0.6	~10
TW-65 (KHN)	23°58.585	88°06.815	33.5	27.8	7.6	1400	4.35	123	460	0	0.8	~10
TW-66 (KHN)	23°58.633	88°06.825	30.5	27.1	7.59	1442	2.6	32	500	0	0.6	~10
TW-67 (KHN)	23°58.585	88°06.736	30.5	27.4	7.53	1391	4.21	130	470	0	0.5	<10

*As_T measured by HACH® Arsenic Test Kit.

General data for water samples collected during January 2010 (continued from previous page).

Sample ID	Latitude (N)	Longitude (E)	Well Depth (m)	Temp. (°C)	pH	Conductivity (µS/cm)	Dissolved Oxygen (mg/l)	Redox Potential (mV)	HCO_3^- (mg/l)	NH_4^+ (mg/l)	PO_4^{3-} (mg/l)	As_T* (µg/l)
TW-68 (KHM)	23°58.364	88°07.235	33.5	27.5	7.66	1383	4.9	71	495	0	1.1	0
TW-69 (KHM)	23°58.317	88°07.193	33.5	27.9	7.46	1389	3.3	110	425	0	0.8	~10
TW-70 (KHM)	23°58.373	88°07.343	33.5	27.8	7.69	1373	3.88	37	400	0	1.2	0
TW-71 (BM)	23°56.390	88°16.203	36.6	27.2	7.10	724	3.8	388	360	0	0.2	
TW-72 (BM)	23°56.391	88°16.170		27.2	7.04	788	3.05	310	380	0.25	0.7	
TW-73 (BM)	23°56.399	88°16.146	24.4	27.0	7.06	761	3.7	131	365	0.85	0.7	
TW-74 (BM)	23°56.284	88°16.244	39.6	26.9	7.10	756	4.02	115	380	0.65	1.3	
TW-75 (BM)	23°56.353	88°16.117	33.5	27.2	7.05	795	2.3	67	400	2	3	

*As_T measured by HACH® Arsenic Test Kit.

Anions

Sample ID	NO_3^- (mg/l)	SO_4^{2-} (mg/l)
TW-2 (BM)	1.79	n.d.
TW-3 (BM)	n.d.	n.d.
TW-5 (BM)	n.d.	n.d.
TW-10 (HK)	n.d.	5.00
TW-11 (HK)	1.36	4.88
TW-12 (HK)	n.d.	9.89
TW-18 (HK)	n.d.	n.d.
TW-19 (HK)	n.d.	n.d.
TW-20 (JB)	5.72	n.d.
TW-23 (JB)	1.37	8.27
TW-24 (JB)	n.d.	1.46
TW-26 (JB)	n.d.	2.87
TW-27 (JB)	n.d.	47.67
TW-28 (NRJ)	n.d.	35.80
TW-29 (NRJ)	n.d.	4.31
TW-29 (NRJ) Dup	50.62	47.93
TW-30 (NRJ)	n.d.	7.34
TW-31 (NRJ)	n.d.	5.81
TW-32 (NB)	n.d.	10.80
TW-33 (NB)	3.67	27.0
TW-34 (NB)	31.22	48.1
TW-35 (NB)	n.d.	38.2
GAP (JB)	1.37	3.3
IRW-I (NRJ)	n.d.	2.7
IRW-II (NRJ)	n.d.	1.8
PW-2 (HK)	5.04	20.7
PW-3 (JB)	n.d.	3.9
PW-4 (JB)	5.19	3.6
RW-1	1.27	10.2
RW-2	1.30	10.0
RW-3	1.26	10.1
RW-4	1.34	10.1
RW-5	1.29	10.3

n.d. = non-detectable

Anions (continued)

Sample ID	Cl^- (mg/l)	HCO_3^- (mg/l)
TW-1 (BM)	7.67	440
TW-2 (BM)	9.89	385
TW-3 (BM)	10.56	335
TW-4 (BM)	6.27	290
TW-5 (BM)	6.08	330
TW-6 (BM)	10.36	360
TW-7 (BM)	29.53	310
TW-8 (BM)	66.91	335
TW-9 (BM)	6.63	360
TW-10 (HK)	21.09	360
TW-11 (HK)	8.08	250
TW-12 (HK)	19.19	225
TW-13 (HB)	61.04	335
TW-14 (HB)	70.75	340
TW-15 (HB)	30.40	510
TW-16 (HB)	4.04	255
TW-17 (HB)	12.53	290
TW-18 (HK)	0.88	360
TW-19 (HK)	0.92	330
TW-20 (JB)	11.34	330
TW-21 (JB)	27.43	325
TW-22 (JB)	3.26	325
TW-23 (JB)	49.43	360
TW-24 (JB)	26.88	330

Sample ID	Cl^- (mg/l)	HCO_3^- (mg/l)
TW-26 (JB)	5.86	400
TW-27 (JB)	2.33	440
TW-27 (NRJ)	2.17	405
TW-28 (NRJ)	84.00	455
TW-29 (NRJ)	3.13	300
TW-29 (NRJ) Dup	79.72	455
TW-30 (NRJ)	14.97	330
TW-31 (NRJ)	12.76	325
TW-32 (NB)	41.30	120
TW-33 (NB)	78.20	125
TW-34 (NB)	199.51	110
TW-35 (NB)	114.37	140
GAP (JB)	9.45	50
IRW-60 (JB)	10.04	525
IRW-I (NRJ)	8.72	330
IRW-II (NRJ)	41.62	345
PW-2 (HK)	3.25	360
PW-3 (JB)	132.53	410
PW-4 (JB)	78.58	60
RW-1	5.34	170
RW-2	5.41	210
RW-3	5.46	120
RW-4	5.47	80
RW-5	5.44	95

Cations

Sample ID	Fe (mg/l)	Mg (mg/l)	Ca (mg/l)	K (mg/l)
TW-1 (BM)	n.d.	25.5	100.0	0.5
TW-2 (BM)	n.d.	29.0	110.5	1.1
TW-3 (BM)	2.6	24.0	91.7	2.1
TW-5 (BM)	1.2	26.9	106.4	1.6
TW-6 (BM)	n.d.	28.2	109.4	0.9
TW-8 (BM)	n.d.	24.3	101.8	0.5
TW-10 (HK)	9.3	32.7	117.8	3.7
TW-11 (HK)	6.3	22.3	100.0	2.3
TW-12 (HK)	4.0	24.1	102.6	1.9
TW-15 (HB)	6.4	38.6	139.9	1.8
TW-20 (JB)	22.3	31.8	136.6	3.2
TW-21 (JB)	8.7	30.7	117.9	2.8
TW-26 (JB)	n.d.	26.0	145.9	2.0
TW-29 (NRJ)	3.1	28.8	109.9	2.3
TW-34 (NB)	4.1	23.5	159.4	0.0
GAP (JB)	n.d.	35.0	160.1	2.9
IRW-60 (JB)	9.7	30.6	111.9	2.6
IRW-2 (JB)	0.5	25.8	130.1	2.6
PW-2 (HK)	2.1	3.5	26.2	2.3
RW-3	n.d.	6.2	23.8	2.4

n.d. = non-detectable

Total Arsenic

Sample ID	As_T (µg/l)	Sample ID	As_T (µg/l)
TW-1 (BM)	4394	TW-32 (KB)	1
TW-10 (HK)	344	TW-33 (NB)	2
TW-11 (HK)	504	TW-34 (NB)	0
TW-12 (HK)	476	TW-35 (NB)	1
TW-13 (HB)	250	TW-38 (BM)	81
TW-14 (HB)	281	TW-4 (BM)	60
TW-15 (HB)	375	TW-49 (HK)	102
TW-16 (HB)	43	TW-5 (BM)	1299
TW-17 (HB)	417	TW-50 (HK)	19
TW-18 (HK)	582	TW-6 (BM)	14
TW-19 (HK)	695	TW-62 (NBK)	3
TW-2 (BM)	4036	TW-64 (KHN)	11
TW-2 (BM)	4622	TW-65 (KHN)	10
TW-20 (JB)	193	TW-7 (BM)	226
TW-21 (JB)	649	TW-71 (BM)	3
TW-22 (JB)	112	TW-8 (BM)	3
TW-23 (JB)	638	TW-8 (BM)	1
TW-24 (JB)	107	TW-9 (BM)	72
TW-26 (JB)	6	GAP (JB)	37
TW-27 (JB)	52	IRW-60' (JB)	579
TW-27 (NR)	18	IRW-I (NRJ)	24
TW-28 (NRJ)	508	IRW-II (NRJ)	52
TW-29 (NRJ)	3	IW-2 (NBK)	3
TW-29 (NRJ)	89	M. Rahaman (JB)	37
TW-2a (BM)	95	PW-2 (HK)	2
TW-3 (BM)	310	PW-3 (JB)	4
TW-30 (NRJ)	43	PW-4 (JB)	3
TW-31 (NRJ)	641	RW-3	2

Stable Isotopes

δ^2H & $\delta^{18}O$

Sample ID	δ^2H (‰ V-SMOW)	δ^{18}O (‰ V-SMOW)	Sample ID	δ^2H (‰ V-SMOW)	δ^{18}O (‰ V-SMOW)
TW-1 (BM)	-25.21	-5.10	TW-63 (NBK)	-22.43	-3.88
TW-10 (HK)	-23.64	-4.57	TW-64 (NBK)	-24.54	-4.36
TW-11 (HK)	-31.53	-4.88	TW-65 (KHN)	-25.51	-4.70
TW-12 (HK)	-24.94	-4.34	TW-66 (KHN)	-25.21	-4.81
TW-13 (HB)	-21.11	-4.36	TW-67 (KHN)	-24.14	-4.61
TW-14 (HB)	-22.60	-4.55	TW-69 (KHN)	-25.86	-4.81
TW-16 (HB)	-20.86	-4.20	TW-7 (BM)	-28.69	-4.62
TW-17 (HB)	-26.17	-4.87	TW-71 (BM)	-23.82	-4.53
TW-19 (HK)	-23.83	-4.58	TW-73 (BM)	-22.69	-4.48
TW-21 (JB)	-33.44	-5.40	TW-74 (BM)	-21.75	-4.19
TW-33 (NB)	-24.98	-4.08	TW-8 (BM)	-27.24	-5.02
TW-34 (NB)	-20.35	-3.12	TW-9 (BM)	-28.21	-4.12
TW-36 (BM)	-29.30	-4.82	TW-9 (BM)	-21.45	-3.88
TW-37 (BM)	-30.94	-5.13	M. Rahaman (JB)	-42.12	-6.75
TW-38 (BM)	-19.13	-3.72	GAP (JB)	-34.35	-6.04
TW-40 (BM)	-19.80	-3.89	IRW-1 (NRJ)	-35.95	-6.08
TW-41 (BM)	-24.47	-4.70	IRW-2 (NRJ)	-35.76	-5.91
TW-43 (HK)	-28.66	-4.92	IRW-60 (JB)	-31.71	-5.28
TW-44 (HK)	-27.87	-4.67	IW-1 (HK)	-28.12	-4.82
TW-45 (HK)	-27.27	-4.77	IW-2 (NBK)	-21.61	-3.73
TW-46 (HK)	-28.40	-4.92	IW-3 (NBK)	-27.02	-4.04
TW-47 (HK)	-20.71	-4.40	IW-4 (NB)	-25.78	-3.77
TW-48 (HK)	-29.85	-4.70	PW-2 (HK)	-55.45	-8.41
TW-49 (HK)	-19.77	-3.97	PW-3 (JB)	0.32	0.96
TW-5 (BM)	-22.58	-4.45	PW-4 (JB)	3.69	2.19
TW-50 (HK)	-28.44	-4.93	PW-6 (BM)	-13.28	-0.33
TW-51 (HK)	-30.38	-5.22	PW-7 (HK)	-31.35	-3.56
TW-52 (HK)	-19.82	-4.27	PW-8 (NB)	-22.06	-1.48
TW-53 (HK)	-27.89	-4.76	PW-10 (BM)	-18.00	-1.76
TW-54 (HB)	-17.69	-3.73	PW-11 (BM)	-14.75	-0.84
TW-56 (NB)	-14.17	-2.52	SW-1 (HK)	-23.79	-3.26
TW-57 (NB)	-18.63	-3.72	RW-1	-53.26	-7.94
TW-58 (NB)	-19.38	-3.38	RW-2	-52.53	-8.22
TW-59 (NB)	-9.27	-1.48	RW-3	-53.30	-8.09
TW-6 (BM)	-24.28	-4.49	RW-4	-53.11	-8.04
TW-60 (NB)	-18.84	-3.28	RW-5	-51.83	-8.10
TW-61 (NB)	-18.45	-2.70	RW-6 (KHN)	-13.87	-1.89
TW-62 (NBK)	-21.90	-4.01			

$\delta^{13}C$-DIC

Sample ID	$\delta^{13}C$ (‰ V-PDB)	Std. Dev. (‰ V-PDB)
TW-36 (BM)	-10.57	0.05
TW-37 (BM)	-9.70	0.04
TW-38 (BM)	-9.55	0.04
TW-39 (BM)	-7.45	0.03
TW-40 (BM)	-8.47	0.03
TW-43 (HK)	-5.77	0.03
TW-45 (HK)	-5.93	0.04
TW-47 (HK)	-6.64	0.03
TW-48 (HK)	-12.64	0.03
TW-49 (HK)	-14.33	0.04
TW-50 (HK)	-7.58	0.04
TW-56 (NB)	-12.13	0.05
TW-57 (NB)	-10.79	0.04
TW-59 (NB)	-8.76	0.02
TW-60 (NB)	-12.86	0.07
TW-61 (NB)	-12.33	0.05
TW-62 (NBK)	-11.56	0.04
TW-64 (KHN)	-8.54	0.03
TW-65 (KHN)	-8.56	0.05
TW-66 (KHN)	-8.28	0.02
TW-69 (KHM)	-9.43	0.04
IW-2 (NBK)	-12.78	0.05
IW-3 (NBK)	-12.53	0.03
IW-4 (NBK)	-11.71	0.06

Appendix B - Sediment Analyses

This section contains general sediment descriptions, in addition to results from lab analyses.

General Sediment Characteristics

Samples were named according to location and depth in feet (e.g. BM-10), but are referred to in meters in the text. This table displays results from visual analysis of the sediments.

Beldanga-Makrampur (BM) -- Core #2			**Location:**	23°56.360'N	88°16.176'E
Sample ID	**Depth (ft)**	**Depth (m)**	**Color**	**Texture**	**Condition**
BM-10	10	3	Light Brown	Silty clay	wet
BM-20	20	6	Grey	Silty clay	semi dry
BM-30	30	9	Grey	Sandy clay	wet
BM-40	40	12	Grey	Sand	semi dry
BM-50	50	15	Grey	Clay	wet
BM-60	60	18	Grey	Silty clay	semi dry
BM-70	70	21	Grey	Silty clay	wet
BM-80	80	24	Dark Grey	Clay	wet
BM-90	90	27	Dark Grey	Sandy clay w/ gravel	wet
BM-100	100	30	Light Brown	Fine sand	semi dry
BM-110	110	34	Brown-Grey	Medium sand	semi dry
BM-120	120	37	Grey-Brown	Medium sand	semi dry
BM-130	130	40	Grey	Medium sand	wet

Hariharpara-Koshalpur (HK) -- Core #2			**Location:**	24°03.570'N	88°21.532'E
Sample ID	**Depth (ft)**	**Depth (m)**	**Color**	**Texture**	**Condition**
HK-10	10	3	Light Brown	Silty Clay	wet
HK-20	20	6	Brown	Silty Clay	wet
HK-30	30	9	Grey	Silty Clay	wet
HK-40	40	12	Dark Grey	Silty Clay	wet
HK-50	50	15	Dark Grey	Silty Clay	wet
HK-60	60	18	Dark Grey	Medium sand	wet
HK-70	70	21	Grey	Medium sand	wet
HK-80	80	24	Grey	Medium sand	wet
HK-90	90	27	Light Grey	Medium sand	wet
HK-100	100	30	Light Grey	Medium sand	semi dry
HK-110	110	34	Grey	Medium sand	wet
HK-120	120	37	Grey	Medium sand	wet
HK-130	130	40	Grey	Medium sand	wet
HK-140	140	43	Grey	Medium sand	wet

Nabagram-Binodpur (NB) – Core #2 **Location:** 24°11.896'N 88°13.466'E

Sample ID	Depth (ft)	Depth (m)	Color	Texture	Condition
NB-10	10	3	Orange-Brown	Silty Clay	Semi dry
NB-20	20	6	Orange-Brown	Fine Sand	Wet
NB-30	30	9	Orange-Brown	Fine Sand	Wet
NB-40	40	12	Dark Orange-Brown	Fine Sand	Wet
NB-50	50	15	Orange-Brown	Fine Sand	Wet
NB-60	60	18	Brown-Orange	Medium Sand	Wet
NB-70	70	21	Brown-Orange	Medium Sand	Wet
NB-80	80	24	Brown-Orange	Medium Sand	Wet
NB-90	90	27	Brown	Medium Sand	Wet
NB-100	100	30	Orange-Brown	Medium Sand	Semi dry
NB-110	110	34	Brown	Medium Sand	Wet

List of Sediment Core Samples – June 2009

Beldanga-Makrampur (BM) -- Core #1

23°56.423' N 88°16.158' E

Sample ID	Depth (ft)	Depth (m)
BM-10	10	3.0
BM-22	22	6.7
BM-42	42	12.8
BM-43	43	13.1
BM-44	44	13.4
BM-45	45	13.7
BM-52	52	15.8
BM-53	53	16.2
BM-54	54	16.5
BM-55	55	16.8
BM-60	60	18.3
BM-62	62	18.9
BM-64	64	19.5
BM-66	66	20.1
BM-68	68	20.7
BM-80	80	24.4
BM-88	88	26.8
BM-95	95	29.0
BM-97	97	29.6
BM-99	99	30.2
BM-108	108	32.9
BM-112	112	34.1
BM-115	115	35.1

Hariharpara-Koshalpur (HK) -- Core #1

24°03.771' N 88°21.568' E

Sample ID	Depth (ft)	Depth (m)
HK-8	8	2.4
HK-14	14	4.3
HK-20	20	6.1
HK-28	28	8.5
HK-35	35	10.7
HK-45	45	13.7
HK-58	58	17.7
HK-63	63	19.2
HK-70	70	21.3
HK-80	80	24.4
HK-105	105	32.0

Jalangi-Baramasia (JB) -- Core #1

24°12.654' N 88°41.385' E

Sample ID	Depth (ft)	Depth (m)
JB-12	12	3.7
JB-15	15	4.6
JB-24	24	7.3
JB-30	30	9.1
JB-35	35	10.7
JB-39	39	11.9
JB-55	55	16.8
JB-60	60	18.3
JB-65	65	19.8
JB-70	70	21.3
JB-75	75	22.9
JB-77	77	23.5
JB-80	80	24.4
JB-85	85	25.9
JB-98	98	29.9
JB-105	105	32.0
JB-115	115	35.1
JB-120	120	36.6
JB-125	125	38.1

Naoda-Rejlapara (NRJ) -- Core #1

23°53.093' N 88°28.068' E

Sample ID	Depth (ft)	Depth (m)
NRJ-20	20	6.1
NRJ-25	25	7.6
NRJ-35	35	10.7
NRJ-40	40	12.2
NRJ-42	42	12.8
NRJ-47	47	14.3
NRJ-52	52	15.8
NRJ-57	57	17.4
NRJ-62	62	18.9
NRJ-68	68	20.7
NRJ-72	72	21.9
NRJ-77	77	23.5
NRJ-83	83	25.3
NRJ-88	88	26.8
NRJ-93	93	28.3
NRJ-105	105	32.0
NRJ-110	110	33.5
NRJ-115	115	35.1
NRJ-120	120	36.6
NRJ-128	128	39.0
NRJ-138	138	42.1

List of Sediment Core Samples – January 2010

Nabagram-Binodpur (NB) -- Core #1

24°11.849' N 88°13.569' E

Sample ID	Depth (ft)	Depth (m)
NB-8	8	2.4
NB-15	15	4.6
NB-20	20	6.1
NB-28	28	8.5
NB-35	35	10.7
NB-37	37	11.3
NB-40	40	12.2
NB-45	45	13.7
NB-50	50	15.2
NB-58	58	17.7
NB-67	67	20.4
NB-72	72	21.9
NB-79	79	24.1
NB-89	89	27.1
NB-100	100	30.5
NB-107	107	32.6
NB-116	116	35.4
NB-117	117	35.7

Beldanga-Makrampur (BM) -- Core #3

23°56.377' N 88°16.189' E

Sample ID	Depth (ft)	Depth (m)
BM-10	10	3
BM-20	20	6
BM-30	30	9
BM-40	40	12
BM-50	50	15
BM-60	60	18
BM-70	70	21
BM-80	80	24
BM-90	90	27
BM-100	100	30
BM-110	110	34
BM-120	120	37
BM-130	130	40
BM-140	140	43

Kandi-Hizole (KHN) -- Core #1

23°58.524' N 88°06.824' E

Sample ID	Depth (ft)	Depth (m)
KHN-10	10	3
KHN-20	20	6
KHN-30	30	9
KHN-40	40	12
KHN-50	50	15
KHN-60	60	18
KHN-70	70	21
KHN-80	80	24
KHN-90	90	27
KHN-100	100	30

X-Ray Fluorescence

Values for elemental concentrations in sediments measured by hand-held XRF are reported in ppm (mg/kg) with ±2σ standard deviation. Values represent an average of six scans per sample.

Beldanga - Makrampur (BM) -- Core #2

Sample ID	Depth (m)	As	± 2σ	Fe	± 2σ	Mn	± 2σ	Ca	± 2σ	K	± 2σ	Cr	± 2σ	U	± 2σ	Cu	± 2σ	Zn	± 2σ
BM-10	**3**	9	7	29717	400	465	83	5337	295	10362	564	52	26	12	10	33	21	49	14
BM-20	**6**	15	7	43683	500	308	75	3552	320	15817	783	90	37	19	11	52	20	89	16
BM-30	**9**	5	6	25150	400	494	79	22717	600	15550	700	68	29	14	10	27	18	58	13
BM-40	**12**	2	5	11450	219	279	59	11113	378	10390	504	35	24	10	8	0	0	36	11
BM-50	**15**	5	7	32950	400	678	89	16667	600	20067	833	63	34	17	10	38	18	71	14
BM-60	**18**	8	6	29817	400	648	88	25283	667	18483	800	75	33	15	10	33	19	50	13
BM-70	**21**	8	6	32467	400	369	74	14017	500	19733	817	75	34	20	11	34	18	59	14
BM-80	**24**	13	7	30700	400	278	69	3038	267	13850	650	95	32	17	10	31	18	53	13
BM-90	**27**	18	7	34000	400	339	76	7959	382	14400	683	85	31	17	10	36	20	55	14
BM-100	**30**	10	6	27650	400	392	74	3576	283	15233	683	71	30	18	10	32	18	48	12
BM-110	**34**	7	5	9236	205	296	60	16100	417	9549	486	0	0	0	0	0	0	20	9
BM-120	**37**	8	5	9885	206	183	54	9901	368	8891	465	0	0	0	0	0	0	27	10
BM-130	**40**	18	6	7168	186	146	51	3115	211	8565	444	41	21	11	8	0	0	24	10

Hariharpara - Koshalpur (HK)-- Core #2

Sample ID	Depth (m)	As	± 2σ	Fe	± 2σ	Mn	± 2σ	Ca	± 2σ	K	± 2σ	Cr	± 2σ	U	± 2σ	Cu	± 2σ	Zn	± 2σ
HK-10	**3**	13	7	28800	400	458	84	23450	567	11933	600	64	27	11	10	36	21	55	14
HK-20	**6**	7	6	24700	400	418	77	30150	667	14193	664	40	28	11	10	28	19	44	13
HK-30	**9**	10	7	38733	500	559	94	17350	517	13050	667	67	30	16	11	36	22	56	15
HK-40	**12**	12	7	38617	500	526	89	9564	433	16483	717	72	32	15	11	39	21	54	15
HK-50	**15**	12	7	36783	467	517	88	11950	483	17567	783	77	32	22	11	31	20	64	15
HK-60	**18**	2	5	11143	205	202	57	8710	342	9514	473	32	22	10	8	3	16	20	10
HK-70	**21**	2	5	6791	175	140	50	4636	244	7821	423	16	20	21	8	14	17	13	9
HK-80	**24**	1	5	5954	168	124	48	5131	252	6979	402	27	20	6	7	1	15	11	9
HK-90	**27**	2	5	8693	191	128	47	6261	293	11900	517	29	23	10	8	7	15	14	9
HK-100	**30**	1	5	6185	162	114	44	5071	263	10548	498	23	21	9	8	7	14	22	9
HK-110	**34**	4	5	9339	195	233	54	10271	371	10961	503	25	23	3	7	8	15	20	9
HK-120	**37**	1	5	7068	175	124	47	8195	345	9168	483	29	22	9	7	5	15	16	9
HK-130	**40**	2	5	7326	174	138	46	6902	301	10514	504	18	22	7	7	10	14	16	8
HK-140	**43**	0	5	6798	168	97	43	8430	332	11567	500	27	22	9	7	7	13	17	9

Nabagram - Binopur (NB) -- Core #2

Sample ID	Depth (m)	As	± 2σ	Fe	± 2σ	Mn	± 2σ	Ca	± 2σ	K	± 2σ	Cr	± 2σ	U	± 2σ	Cu	± 2σ	Zn	± 2σ
NB-10	**3**	0	0	24497	342	306	67	1986	223	10852	569	88	30	14	9	32	18	28	11
NB-20	**6**	0	0	10832	222	194	54	1402	172	7637	435	41	23	13	7	0	0	37	11
NB-30	**9**	0	0	14489	257	241	57	1689	194	10033	506	65	26	0	0	29	18	34	11
NB-40	**12**	0	0	9574	205	234	55	1767	186	8310	452	41	23	12	7	0	0	38	10
NB-50	**15**	0	0	8454	191	164	49	1717	180	7761	432	45	23	13	7	0	0	21	9
NB-60	**18**	0	0	10707	212	277	57	2092	205	10811	517	48	24	15	8	0	0	30	10
NB-70	**21**	0	0	8330	183	223	51	2250	204	9558	482	50	24	15	7	0	0	18	8
NB-80	**24**	0	0	9232	199	141	48	1961	198	11200	517	47	23	14	8	0	0	40	10
NB-90	**27**	0	0	12935	235	296	59	2431	221	12525	560	44	24	15	8	0	0	44	11
NB-100	**30**	0	0	11387	225	279	59	2247	204	9950	492	48	24	13	8	0	0	45	11
NB-110	**34**	0	0	12244	228	299	59	2555	212	10421	512	45	25	14	8	0	0	58	11

Fe(II), Total Fe, Phosphate

Beldanga - Makrumpur (BM) -- Core #1

Depth (ft)	Depth (m)	Fe(II)	Std. Dev.	Fe_T	Std. Dev	$Fe(II)/Fe_T$	PO_4
10	3.0	848	396	990	12	0.86	475
22	6.7	2384	98	2351	110	1.01	959
42	12.8	1700	18	1907	184	0.89	1015
43	13.1	1639	52	2405	35	0.68	1101
44	13.4	2065	778	2868	1229	0.72	889
45	13.7	1741	43	2544	270	0.68	971
52	15.8	1370	45	1476	17	0.93	1044
53	16.2	2252	673	1834	503	1.23	1366
54	16.5	2596	96	3059	64	0.85	711
55	16.8	1452	14	1603	110	0.91	1104
60	18.3	1869	564	2077	925	0.90	817
62	18.9	1626	413	1100	485	1.48	981
66	20.1	1040	35	1214	108	0.86	1079
67	20.4	1620	422	1648	430	0.98	991
68	20.7	1456	552	1539	1539	0.95	489
80	24.4	1030	537	1416	164	0.73	294
88	26.8	4426	1008	4571	1050	0.97	221
97	29.6	808	227	920	91	0.88	576
99	30.2	385	52	588	86	0.65	704
108	32.9	260	22	658	6	0.40	753
112	34.1	848	50	1154	26	0.73	368
115	35.1	723	54	861	141	0.84	556

Total Digestions

Values presented here (mg/kg) are from total digestions of select sediment samples by aqua regia, measured by ICP-MS.

Beldanga – Makrampur (BM) -- Core #2

Sample ID	Depth (m)	As	Fe	Mn	Al	Mg	Ca	K	Cu	Pb	Zn
NB-10	3	4	3777	38	5521	531	318	469	15	5	31
NB-30	9	4	4822	75	4007	671	302	544	9	7	44
NB-60	18	1	3180	85	2498	612	346	395	3	3	23
NB-60 (Dup)	18	1	3301	88	2566	633	372	408	4	3	29
NB-90	27	1	3764	101	2688	858	353	586	3	4	43
NB-110	34	1	3723	110	2676	725	471	533	5	4	63

Nabagram - Binodpur -- Core #2

Sample ID	Depth (m)	As	Fe	Mn	Al	Mg	Ca	K	Cu	Pb	Zn
BM-20	6	10	4352	28	5248	1060	582	444	40	12	93
BM-80	24	9	4893	68	5836	760	735	610	28	10	49
BM-90	27	44	5240	115	5115	1275	5521	671	31	17	196
BM-90 (Dup)	27	18	5160	121	5082	1263	5609	662	25	14	103
BM-100	30	7	5143	74	4671	1353	559	643	23	9	58
BM-130	40	17	2958	43	2150	918	1706	492	3	3	37
BM-130 (Dup)	40	17	3094	43	2149	922	1252	556	3	3	24

Sequential Extractions

Values presented here (mg/kg) are from sequential extractions, measured by ICP-OES.

Arsenic

	BM-10	BM-20	BM-30	BM-40	BM-50	BM-60	BM-70	BM-80	BM-90	BM-100	BM-110	BM-120	BM-130
Step 1	0.0	0.4	0.0	0.0	0.0	0.0	0.0	0.0	0.0	0.0	0.0	0.0	0.7
Step 2	1.8	6.3	2.0	1.7	0.6	1.8	1.9	3.9	6.7	2.3	1.5	2.9	8.7
Step 3	2.1	3.4	2.1	2.3	2.4	3.6	2.3	3.7	6.9	3.0	2.7	3.2	8.7
Step 4	2.3	2.6	1.8	2.0	1.1	2.0	1.1	2.0	2.9	1.5	1.7	2.1	2.9
Step 5	4.8	0	4.7	2.8	5.0	4.4	3.5	6.7	1.2	3.9	2.7	3.9	0
Total	11.0	12.7	10.6	8.8	9.0	11.7	8.7	16.3	17.7	10.7	8.6	12.2	20.9

Manganese

	BM-10	BM-20	BM-30	BM-40	BM-50	BM-60	BM-70	BM-80	BM-90	BM-100	BM-110	BM-120	BM-130
Step 1	61	2	11	8	38	11	9	1	1	19	19	9	10
Step 2	54	14	15	8	29	13	11	2	9	34	32	10	13
Step 3	3	33	138	62	94	311	45	69	84	35	40	12	12
Step 4	38	47	17	8	15	37	13	16	39	17	10	6	10
Step 5	190	2	193	104	168	221	132	268	350	170	147	66	49
Total	347	98	373	190	343	592	209	356	483	274	248	103	93

Iron

	BM-10	BM-20	BM-30	BM-40	BM-50	BM-60	BM-70	BM-80	BM-90	BM-100	BM-110	BM-120	BM-130
Step 1	0	0	0	0	0	0	0	0	0	0	0	0	0
Step 2	21	0	13	14	1	13	13	10	0	80	14	14	0
Step 3	0	2620	3752	1890	5040	5175	3940	7914	6535	271	820	641	745
Step 4	4281	7242	1647	592	1790	2874	2186	2419	4736	2722	1036	928	823
Step 5	12573	6	9659	5420	11157	10119	10820	11636	9621	12284	4637	4913	4025
Total	16875	9868	15071	7916	17987	18181	16959	21979	20891	15357	6507	6495	5593